[AMERICAN JOURNAL OF SCIENCE, VOL. 292, OCTOBER, 1992, P. 565–636]

TECTONIC EVOLUTION OF THE CENOZOIC OLYMPIC SUBDUCTION COMPLEX, WASHINGTON STATE, AS DEDUCED FROM FISSION TRACK AGES FOR DETRITAL ZIRCONS

MARK T. BRANDON* and JOSEPH A. VANCE**

ABSTRACT. The Olympic subduction complex (OSC), exposed in the Olympic Mountains of northwest Washington State, consists of an imbricated assemblage of Cenozoic sandstone, mudstone, and minor pillow basalt. The tectonic evolution of the OSC has been difficult to resolve because of poor age control, especially for the more easterly parts of the complex. The fission track (FT) method is used here to date detrital zircons from sandstones of the OSC in order to define better the timing of deposition, subduction accretion, and metamorphism.

The external detector method was used to determine grain ages for individual detrital zircons. For unreset samples, the detrital zircons retain pre-depositional FT ages, which are related to the thermal history of the source region from which the zircons were derived. The samples are inferred never to have seen temperatures in excess of about 175° to 185°C. For these samples, determination of the FT age of the youngest population of grain ages is especially useful because it represents the maximum age for deposition of the sediment. For reset samples, maximum temperatures are inferred to have exceeded 240° to 245°C, so that the zircons were annealed after deposition. Zircon grain ages from these samples show a restricted range of ages which can be used to define a cooling age for the rock following metamorphism.

We report FT results for 19 sandstone samples with a total of 928 grain ages. Of the 15 samples from the OSC, 11 are unreset, and 4 are reset. The remaining 4 samples are from unmetamorphosed Eocene basin sequences to the east and southeast of the OSC and are included here for purposes of comparison. The statistical methods outlined in Brandon (this issue) are used to interpret each of the unreset grain-age distributions. The χ^2 age method estimates the FT age of the youngest population of "plausibly related" grains, defined as the χ^2 age. The peak-fitting method is used to decompose an entire grain-age distribution into a set of component grain-age populations, each of which is distinguished by a peak age, defined as the average FT age of the component population.

The unreset Eocene basin samples have χ^2 ages of 51 to 39 Ma. Comparisons between χ^2 ages and independently determined depositional ages indicate a lag time of less than ~5 my between the cooling age of the youngest zircons and deposition. Thus, the χ^2 age is assumed to be a reasonable proxy for the depositional age of the sandstone. The χ^2 age usually coincides with the youngest peak age as determined by the peak-fitting method. Thus, these ages correspond to a specific population of young zircon grains. We refer to this young population as a *moving peak* because the age of the population appears to shift with

*Department of Geology and Geophysics, Yale University, P.O. Box 6666, New Haven, Connecticut 06511

** Department of Geological Sciences, AJ-20, University of Washington, Seattle, Washington 98195.

but lag slightly behind the depositional age of the sandstone. A likely source for these zircons is the Cascade volcanic arc, which has been active continuously from ~36 Ma to present.

All the unreset samples from the OSC and the Eocene basin localities contain a common set of older peaks, which we call *static peaks* because they remain relatively constant in age regardless of the depositional age of the sample. The peak-fitting method indicates three static peaks with ages of 43, 57, and 74 Ma. Possible source areas for the static peaks include unreset Late Cretaceous plutons and Eocene reset terrains located on the eastern side of the Omineca belt and in the North Cascade Mountains. The relatively constant age of the static peaks from sample to sample provides further evidence that samples designated as unreset have not been affected to any significant degree by partially resetting after deposition.

The FT results for the OSC samples define a concentric pattern with reset samples (cooling age = 14 Ma) restricted to the central part of the OSC, unreset Upper Oligocene and Lower Miocene clastic rocks (χ^2 = 27 to 19 Ma) lying around the perimeter of the reset area, and unreset Middle Eocene to Lower Oligocene clastic rocks (χ^2 = 48 to 32 Ma) at a still greater distance. This pattern is interpreted as part of a domal structure that formed during emergence and uplift of the modern Olympic Mountains, starting at ~12 Ma. The reset region in the central OSC represents the youngest and most deeply exhumed part of the OSC. It lies in the center of the Olympic Mountains and coincides with the area of highest topographic relief. Rocks in this area are interpreted to have been accreted to the base of the accretionary wedge at about 17 Ma and to have been metamorphosed at temperatures greater than about 240° to 245°C and at a depth of about 12 km. At about 14 Ma, these rocks cooled below the closure temperature ~239°C at a rate of about 16.5°C/my. Erosion of the surface of the wedge began at about 12 Ma when the wedge first became subaerially exposed. Erosional unroofing of the wedge was apparently driven by continued underplating and ductile thickening within the wedge. About 12 km of rocks were removed in ~12 my, indicating an average erosion rate of ~1 km/my. At present, the central reset area is underlain by another 30 km of accreted sedimentary materials, which indicates an average rate of wedge thickening of 1.75 km/my over the last 17 my.

INTRODUCTION

The Olympic Mountains of northwestern Washington State mark the only place along the modern Cascadia subduction zone where the Cascadia accretionary wedge has been uplifted and exposed (fig. 1). The Olympics are a young mountain range which became emergent at about 12 Ma due to the development of a large arch in the subducting Juan de Fuca plate (Brandon and Calderwood, 1990). Prior to that time, the Cascadia forearc high was below sealevel. Brandon and Calderwood (1990) argue that the mountainous topography in the Olympics has been sustained by continued subduction accretion and within-wedge deformation. At the position of the central part of the Olympics, the accretionary wedge has a current thickness of about 30 km. Gravity and seismic refraction data, reviewed in Brandon and Calderwood (1990), indicate

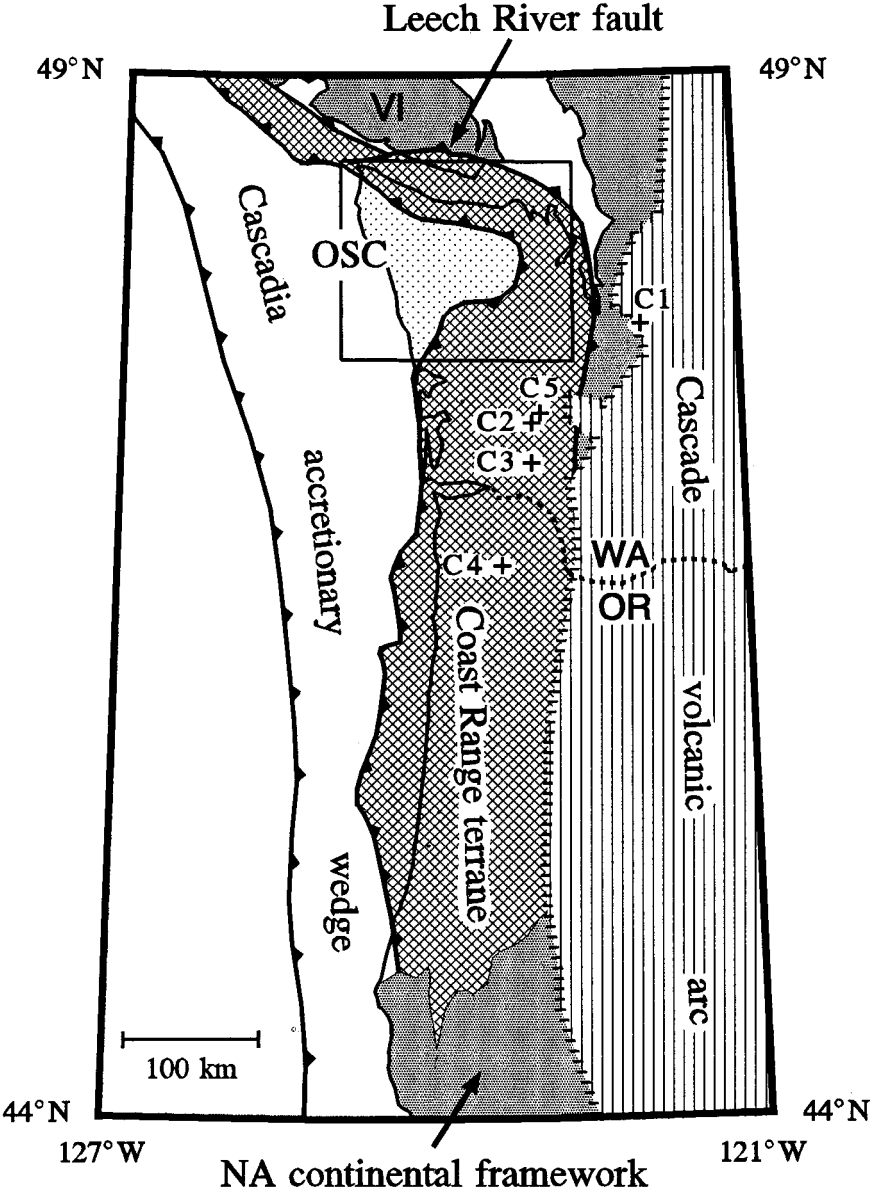

Fig. 1. Geologic map showing the regional setting of the Olympic subduction complex (OSC). The North American continental framework is shown in a dark gray pattern. The Coast Range terrane, in a cross-hatched pattern. The Cascade volcanic arc and its basement are shown in a vertical ruled pattern. The Cascadia accretionary wedge has no pattern in the offshore area, and where it is exposed as the OSC in the Olympic Mountains, it is marked by a screened pattern. The box shows the location of the map in figure 2. The locations of our Eocene basin samples (table 3) are marked C1 through C5. Abbreviations: VI = Vancouver Island, WA = Washington, OR = Oregon.

that most, if not all, of the wedge in that area is composed of sedimentary materials. It is inferred that these sedimentary materials originated on the Juan de Fuca plate and were transferred to the base of the accretionary wedge by the process of subduction underplating.

Following the development of mountainous relief in the Olympics, erosion has steadily denuded the forearc high in this area. Various estimates indicate that about 10 to 12 km of overburden has been removed from the central part of the Olympics (Brandon and Calderwood, 1990; also data presented here). Thus, the Olympics are of particular interest in that they provide a unique view of the deep interior of an active accretionary wedge.

A major goal of our work has been to resolve better the age of clastic sedimentary rocks within the Olympic subduction complex (OSC), the name used here for the outcrops of the Cascadia accretionary wedge in the Olympic Mountains.[1] A common problem that besets many studies of onland subduction complexes is a paucity of age-diagnostic fossils. Furthermore, those few fossils that are found typically come from unusual rock units, such as isolated blocks of limestone, chert, or pillow basalt. Deep marine clastic sedimentary rocks, which comprise the bulk of many subduction complexes, commonly lack fossils and therefore are difficult to date. These rocks are particularly important because they include trench-basin turbidites which represent the youngest part of the incoming sedimentary section (Underwood, Bachman, and Schweller, 1980). In most modern trenches, there is a marked difference between the age of the subducting oceanic plate and the time of subduction, on the order of 8 my for the Cascadia subduction zone to 155 my for the Mariana subduction zone (Jarrard, 1986). Thus, in geologic studies of uplifted accretionary wedges, it is necessary to determine the age of trench-basin turbidites in order to constrain reasonably the timing of subduction and accretion.

Our approach to this problem is to use the fission-track (FT) method to date individual detrital zircons from sandstones of the OSC. The relatively low thermal gradient associated with most subduction zones suggests that temperatures throughout much of a typical accretionary wedge are less than those needed to cause significant annealing of fission tracks in zircon ($<185°$–$200°C$, as determined below). If a sandstone sample has remained at fairly low temperatures since deposition, then the detrital zircons would remain unreset, and their FT ages would reflect the thermal history of the source region from which the dated zircons were eroded. The external detector method of FT dating (Naeser, Naeser, and McCulloh, 1989) is a single-grain dating method. When it is used to date an igneous or metamorphic rock, the individual FT grain ages reflect a common thermal history and thus can be combined to

[1] In the past, the OSC has been informally called the "Olympic core rocks" (Tabor and Cady, 1978a, b), with the name based on the fact that these rocks are mainly exposed in the geographic core of the Olympic Mountains. Unfortunately, this name is commonly confused with the term "metamorphic core complex." Thus, we adopt the name "Olympic subduction complex" to avoid further confusion.

calculate a more precise average age. For an unreset sandstone, the dated grains do not have a common thermal history, so it becomes necessary to identify specific grain-age populations within the overall FT grain-age distribution.

We use two statistical methods from Brandon (this issue) to identify component grain-age populations in our unreset samples. For the OSC sandstones, we are particularly interested in determining the age of the youngest component population, because it provides a maximum limit for the depositional age of the sample. The older component populations have also proven useful for resolving the provenance of the sandstones and as an indicator of partial resetting. If the source region for the zircons was tectonically or magmatically active, as was the case for the Pacific Northwest during the Cenozoic, then the time lag between the FT age of the youngest zircons and deposition of the sandstone should be relatively short (< 5 my, as estimated below). In this case, the FT age of the youngest zircons could actually serve as a reasonable proxy for the depositional age of the sample.

In this paper, we report FT data for 19 sandstone samples with a total of 928 grain ages. Of the 15 samples from the OSC, 11 are unreset and retain detrital FT ages, and 4 are reset and provide information about the cooling history of the OSC. For purposes of comparison, we include 4 additional unreset sandstone samples and 1 volcanic tuff from unmetamorphosed Eocene strata to the east and southeast of the Olympics (C1–C5 in fig. 1). These samples provide information about the time lag between the age of the youngest fraction of FT grain ages and the depositional age of the rock. They are also used in the interpretation of some distinctive older component populations found in many of the unreset OSC samples.

The OSC FT data are used to examine the following questions: (1) What are the depositional ages of the poorly fossiliferous clastic rocks of the central and eastern OSC? (2) What is the timing of metamorphism and cooling for reset rocks of the central OSC? (3) What was the source region for accreted sediments in the OSC? (4) What implications do these age data have for the tectonic evolution of the OSC?

Note on reference time scales.—In this paper, we use the global geologic time scale of Harland and others (1990). Every attempt has been made to ensure that previously published isotopic ages have been calculated with respect to modern standardized isotopic constants (Harland and others, 1990, p. 190–196). For correlation between the global time scale and the local Pacific Northwest biostratigraphic zones, we use Armentrout (1981) and Rau (1981), as modified by the results of Prothero and Armentrout (1985).

GEOLOGICAL OVERVIEW

Regional Tectonic Setting

From a Cenozoic perspective, the Cascadia margin can be viewed as being composed of four major tectonic elements (fig. 1). The first and most inboard element is the *North American continental framework* (gray

screened pattern in fig. 1) which marks the relatively rigid part of the overriding continental plate during Cenozoic subduction. In the areas depicted in figure 1, the continental framework consists of a complex assemblage of Paleozoic and Mesozoic terranes. These terranes were sutured to continental North America during the Jurassic and Cretaceous (Monger, Price, and Tempelman-Kluit, 1982; Brandon, Cowan, and Vance, 1988). By Cenozoic time, they were an integral part of the North American plate.

The next tectonic element is the *Cascade volcanic arc* (vertically ruled pattern in fig. 1), which includes the modern stratovolcanoes of the Cascade Range, such as Mount Saint Helens and Mount Rainier, as well as older arc volcanic flows, pyroclastic deposits, and subvolcanic plutons (Smith, 1989; Sherrod and Smith, 1989). This arc is a direct manifestation of the current subduction regime. Stratigraphic relationships and isotopic ages indicate that the arc was initiated at about 36 Ma and has been continuously active until the present, but with diminished activity from 17 to 7 Ma (Robinson, Brem, and McKee, 1984; Vance, Walker, and Mattinson, 1986; Smith, 1989; Sherrod and Smith, 1989; Priest, 1990; J.A. Vance, unpublished isotopic ages). The arc was built mainly on the continental framework, but volcanic deposits in the forearc region do overlap to the west onto the Coast Range terrane, a more outboard tectonic element (fig. 1).

Armstrong (1978), Ewing (1980), and Heller, Tabor, and Suczek (1987), among others, have argued that the Cascade volcanic arc was preceded by the "Challis arc," which corresponds to a widespread and shortlived volcanic event that covered broad regions of northwestern United States and western Canada. This event was mainly focused between 52 and 42 Ma (Armstrong, 1988; Armstrong and Ward, 1992; J.A. Vance, unpublished data). There remains much debate about whether or not Challis volcanism was subduction related (Moye and Johnson, 1989; Norman and Mertzman, 1991). For instance, Moye and Johnson (1989) attribute volcanism to widespread Eocene crustal extension in Montana, Washington, Idaho, and British Columbia, an interpretation that may be more compatible with the broad extent and short duration of the Challis event. If this alternative is correct, then there would be no identifiable Cenozoic volcanic arc prior to about 36 Ma.

Parts of the continental framework and the Cascade arc have been subjected to extension, transcurrent faulting, and vertical-axis rotation during the Cenozoic (Heller, Tabor, and Suczek, 1987; Wells and Heller, 1988; England and Wells, 1991). This deformation is considered to be within-plate because the magnitude of the deformation is minor when compared with the total relative displacement between North America and the offshore Pacific basin (Engebretson, Gordon, and Cox, 1985). In contrast, the Coast Range terrane and the Cascadia accretionary wedge, which lie outboard of the Cascade arc and the continental framework, were formed and/or accreted within the western North American plate boundary and bear a more pronounced record of Cenozoic tectonism.

The *Coast Range terrane* (cross-hatched pattern in fig. 1) is a coherent allochthonous terrane distinguished by a regionally extensive section of Paleocene to Middle Eocene basalts, consisting of pillowed and massive flows with a stratigraphic thickness of at least 4 km, and perhaps more (Snavely and MacLeod, 1974; Cady, 1975; Tabor and Cady, 1978b; Duncan, 1982; Wells and others, 1984; Massey, 1986). Related gabbros and sheeted dikes are also locally present (Massey, 1986). K-Ar and Ar-Ar ages from Duncan (1982) indicate that basaltic volcanism was mainly focused between 62 and 53 Ma, with some younger flows at about 48 Ma. Although there are many local stratigraphic names for this unit (Metchosin, Crescent, Black Hills, Siletz River, and Roseburg; see Wells and others, 1984), in regional syntheses, it is commonly referred to as the Coast Range basalts. Some authors have divided the Coast Range basalts into two separate terranes (Siletz and Crescent terranes; Siberling and others, 1987), based on differences in the amount of vertical-axis rotation, but this distinction does not seem significant. As used here, the Coast Range terrane consists of the Coast Range basalts as a basement unit and overlying Eocene and younger sandstones and shales, dominantly marine in origin. Minor amounts of continent-derived clastic sedimentary rocks are found as interbeds in the Coast Range basalts and, in some places, stratigraphically underlie the basalts (Blue Mountain unit of the Olympic Mountains; Cady, 1975; Tabor and Cady, 1978b; Einarsen, 1987). This relationship suggests that the basalts formed close to the continental margin (Wells and others, 1984; Einarsen, 1987; Heller and others, 1992).

There are two general types of interpretations for the Coast Range basalts (Snavely and MacLeod, 1974; Duncan, 1982; Wells and others, 1984; Snavely, 1987; Clowes and others, 1987; Einarsen, 1987). The *seamount interpretation* (option 1 in fig. 2) considers the basalts to have formed on the Kula and/or Farallon plates, as either a hotspot-generated seamount chain or anomalously thick oceanic crust. This intra-oceanic feature was then accreted to the North American margin after it collided at the subduction zone, sometime during the Eocene.

The *marginal basin interpretation* (option 2 in fig. 2) views the Coast Range basalts as representing oceanic crust that formed by rifting and spreading within a small marginal basin landward of the North American subduction zone, perhaps in a fashion similar to the opening of the Andaman Sea at the Sumatran convergent margin (Curray and others, 1979). Oblique opening of the marginal basin would have involved both continental rifting and also transform faulting. Figure 2 shows the marginal basin forming in a back-arc position. Others (Wells and others, 1984; Snavely, 1987; Einarsen, 1987) favor a forearc position. The critical question is the location of the volcanic arc at the time of rifting. Did it correspond to the Challis volcanic province or was it located elsewhere? These differences aside, both variants of the marginal basin interpretation postulate that a large part of the original convergent margin, including the forearc and maybe the arc as well, was displaced northward leaving behind a truncated continental margin with little indication of the

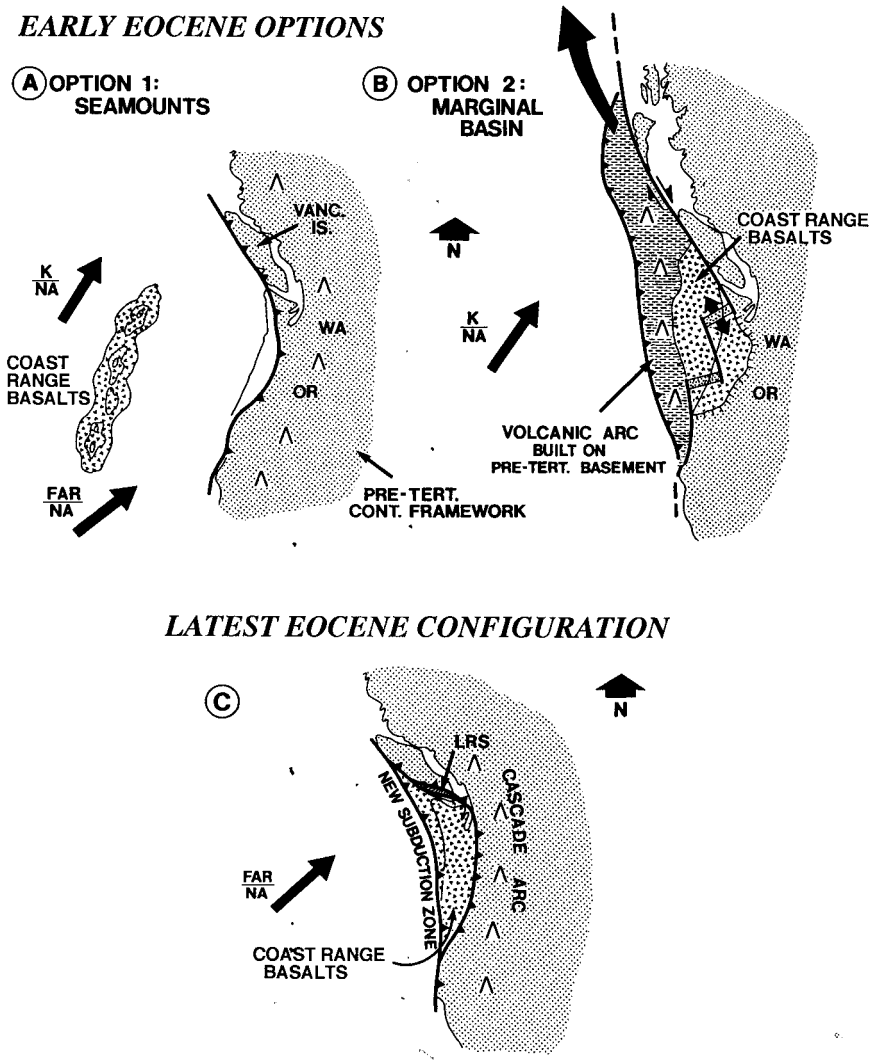

Fig. 2. Alternative interpretations for the early Cenozoic tectonic evolution of the Pacific Northwest (modified from Clowes and others, 1987). Two options are shown for the formation and accretion of the Coast Range basalts. (A) Option 1 shows the Coast Range basalts as a seamount chain, which subsequently collided with the margin. The Challis volcanic province is inferred to be the volcanic arc at that time. The front of this arc is marked by inverted V's. (B) Option 2 shows the basalts forming within an obliquely spreading marginal basin. Oblique rifting in the backarc area caused the arc and forearc to be translated northward, leaving behind the Coast Range basalts and a truncated continental margin. (C) Terrane accretion, whether by option 1 or 2, was completed by the end of the Late Eocene. This time marks the inception of the modern Cascadia margin, with the zone of plate subduction and active sediment accretion now located outboard of the Coast Range terrane. The arrows in each figure mark the relative plate motion of Kula (K) and Farallon (FAR) with respect to a fixed North America (NA), as reported in Wells and others (1984). Abbreviations: WA = Washington, OR = Oregon, and LRS = Leech River schist.

former subduction zone. Other observations relevant to this interpretation include geologic evidence for early Cenozoic continental truncation of the western side of Vancouver Island and Washington (Johnson, 1984; Brandon, 1989a, b), and paleomagnetic and geologic evidence suggesting that the offset arc/forearc fragment may be presently located in Alaska (Cowan, 1982; Moore and others, 1983; Davis and Plafker, 1986; Irving and Wynne, 1990).

While it is generally agreed that the Coast Range terrane was accreted some time during the Eocene, a more precise determination depends on which of the above interpretations is correct. For instance, it has been argued that the onset of voluminous continent-derived clastic sedimentation in the Coast Range terrane at about 50 Ma indicates that terrane accretion was largely completed by that time (Heller and Ryberg, 1983; Wells and others, 1984; Heller, Tabor, and Suczek, 1987; Snavely, 1987). This interpretation, however, assumes that the Coast Range basalts formed as an intra-oceanic seamount terrane, at a significant distance seaward of the North American continental margin. If the Coast Range basalts formed at the continental margin (option 2 in fig. 2), then this sedimentological evidence is not particularly diagnostic. Snavely (1987) has called attention to some local unconformities and faults as evidence of final "docking" at ~52 Ma of the Coast Range terrane with North America. However, the features noted by Snavely (1987) are found only within the Coast Range terrane and thus do not provide a direct link between the terrane and the more inboard continental framework.

We prefer a younger age for terrane accretion, based, in part, on the movement history of the Leech River fault on southern Vancouver Island (fig. 1). The Leech River fault represents the only segment of the tectonic boundary between the Coast Range terrane and the continental framework where structural relationships have been clearly resolved. Elsewhere, the boundary is hidden beneath a thick cover of younger forearc deposits and can be only roughly delimited by geophysical data (Clowes and others, 1987; Finn, 1990). At present, the Leech River fault dips at about 40° to the northeast and has at least 15 km of dip separation (fig. 8 in Clowes and others, 1987). It places Middle Eocene greenschist- and amphibolite-facies metamorphic rocks of the Leech River schist over low-grade Coast Range basalts (Fairchild and Cowan, 1982; Rusmore and Cowan, 1985). K-Ar ages for biotite, muscovite, and hornblende from the schist and from related synkinematic intrusions are concordant within analytical uncertainties and indicate rapid cooling at 42 Ma (Fairchild and Cowan, 1982; this average age was calculated using the original data from Wanless and others, 1978, after conversion to modern isotope constants). Motion on the Leech River fault entirely postdated metamorphism of the Leech River schist (Fairchild and Cowan, 1982), as indicated by truncated metamorphic isograds and imbrication of rocks with contrasting metamorphic grade. The fault itself is overlaid by Upper Oligocene strata of the Caramanah Group (Fairchild and Cowan, 1982). Sediments in that area have yielded fossils assignable to the Upper Zemorrian (B. Cameron, 1981, personal communication), which corre-

lates with the interval 30 to 24 Ma (Prothero and Armentrout, 1985). Based on this evidence, the accretion of the Coast Range terrane with North America would be bracketed between 42 and 24 Ma. We note that the inception of the modern Cascade volcanic arc at ~36 Ma lies within this interval.

The fourth and last tectonic element is the *Cascadia accretionary wedge,* which includes the OSC of the Olympic Mountains (fig. 1; the wedge has no pattern in the offshore area and a screened pattern for the exposed OSC). The Cascadia wedge is inferred to have been initiated after accretion of the Coast Range terrane. For the seamount option (fig. 2), the new subduction zone would have coincided with the thrust fault that detached the seamount terrane from the subducting oceanic plate. For the marginal basin option (fig. 2), the new subduction zone would have been initiated along the transform boundary that separated the offset arc/forearc fragment from the Coast Range terrane.

Clowes and others (1987) have argued that when the Cascadia subduction zone was initiated, the lithospheric base of the Coast Range terrane was stripped away and subducted, and the Cascadia accretionary wedge accumulated in its place through a combination of subduction underplating and frontal subduction accretion. At present, all that is left of the Coast Range terrane is a relatively thin thrust sheet which forms an arcward-dipping structural lid to the underlying Cascadia accretionary wedge. This relationship is best demonstrated in the Olympic Mountains where Late Miocene to recent uplift has exposed the underlying accretionary wedge (fig. 3). In that area, the Coast Range terrane is folded into a broad, dome-like anticline (Tabor and Cady, 1978a, b). In the eastern half of this anticline, the Coast Range terrane is commonly steeply dipping and locally overturned. The base of the terrane is clearly truncated by a series of faults, the most prominent of which is called the Hurricane Ridge fault (Tabor and Cady, 1978b). These are older-over-younger faults in that they place Lower Eocene Crescent Formation (local name of the Coast Range basalts) over OSC sedimentary rocks of Late Eocene and Early Oligocene age, as determined by our FT dating (Needles-Gray Wolf assemblage of Tabor and Cady, 1978b). The overlying Coast Range terrane contains a widespread and generally conformable marine sequence, Eocene through Early Miocene in age. Unconformities are locally present, but they usually display no more than a gentle angular discordance. This relationship indicates that the Coast Range terrane remained generally flat-lying prior to the Late Miocene (Brandon and Calderwood, 1990). Thus, we infer that the Hurricane Ridge and related faults originated as arcward-dipping thrust faults that formed when the Cascadia subduction zone was first initiated. The present steep dip of these faults is attributed to the Late Miocene and younger uplift of the Olympic Mountains.

Using seismic reflection data, Clowes and others (1987) have identified a similar structural configuration beneath southern Vancouver Island for the contact between the Coast Range terrane and the Cascadia

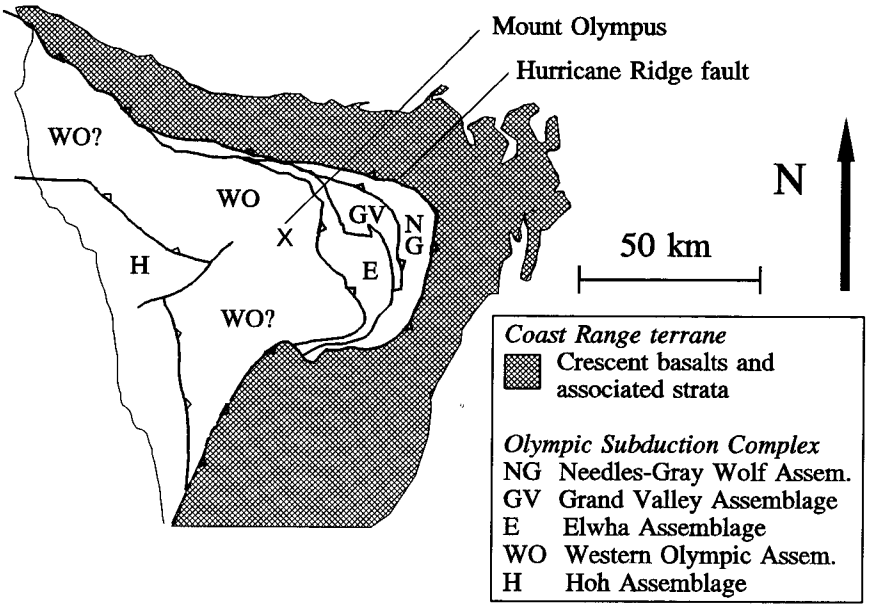

Fig. 3. Geologic map of the Olympic Mountains after Tabor and Cady (1978b). The highest point in the Olympic Mountains is Mount Olympus (2427 m). The Hurricane Ridge fault separates the relatively coherent Coast Range terrane from highly deformed rocks of the Olympic subduction complex.

accretionary wedge. Their interpretation could also be applied to the COCORP reflection profile across the northern Oregon Coast Range (Keach and others, 1989), although in that case, Keach and others (1989) considered the observed mid-crustal reflectivity to be a feature internal to the Coast Range terrane.

Plate tectonic reconstructions indicate that the Cascadia accretionary wedge has evolved in a fairly uniform and simple fashion. Lonsdale (1988) has shown that after about 43 Ma, subduction at the Cascadia margin only involved the Farallon plate and its younger derivative, the Juan de Fuca plate. Since then, relative convergence along the Washington segment of the Cascadia subduction zone has been fairly steady with rates of 45 to 80 km/my and directions within 30° of orthogonal to the margin (K. Kelly and D. Engebretson, written communication, 1991). We estimate that 1550 km of Farallon plate has been consumed since 36 Ma, when the subduction zone was assumed to have been initiated (see Engebretson, Gordon, and Cox, 1985; Clowes and others, 1987, for data and calculation). Over that time interval, the dominant tectonic process has been subduction accretion; there is no evidence for collision of terranes or seamounts. In fact, Davis and Karsten (1986), among others, have noted that seamounts are relatively rare on the present-day Juan de Fuca plate.

Geology of the Olympic subduction complex

Our present understanding of the geology of the Olympic Mountains is based mainly on a regional study by the United States Geological Survey which culminated in a comprehensive geologic map and tectonic synthesis by Tarbor and Cady (1978a, b), They identified five lithic assemblages within the OSC (fig. 3), distinguished mainly on the basis of lithology and sandstone petrology, and to a lesser extent, on deformational style, structural position, and age. From east to west, these units are the Needles-Gray Wolf, Grand Valley, Elwha, Western Olympic, and Hoh lithic assemblages.

The age of the Hoh assemblage, exposed in the western OSC, is well established on the basis of numerous collections of benthic foraminifera, most of which are Early Miocene and possibly early Middle Miocene in age (Saucesian, and possibly Relizian; Rau, 1975, 1979; Tabor and Cady, 1978b). To the east, however, fossils are rare. Most of the identified fossils are from red limestones which occur as thin interbeds in lenses of pillow basalt. The age of the limestones appears to be confined to the Early and Middle(?) Eocene (Rau, 1975; Snavely and others, 1986; Snavely, Rau, and Hafley, 1986; P. Snavely, 1989, written communication; W. Rau, 1989, 1990, written communication). Pillow basalts are widespread in the eastern OSC, but they constitute only a small fraction of the rocks exposed there (Tabor and Cady, 1978b). They are very similar to the Crescent basalts in the overlying Coast Range terrane and appear to be tectonic slices derived from the upper plate (Tabor and Cady, 1978a, b; Applegate and Brandon, 1989). The main point here is that the fossils in these basalts do not provide any direct information about the age of the surrounding turbidite sandstones and mudstones, which make up the bulk of the OSC. The clastic units of the central and eastern OSC have yielded only poorly preserved megafossils from 5 localities (Tabor and Cady, 1978b). These fossils have been tentatively assigned to the interval Paleocene to Oligocene (Cady, MacLeod, and Addicott, 1963; Tabor and Cady, 1978b) and thus provide only a crude estimate of age.

Tabor and Cady (1978a, b) argued that the stratigraphic age of the OSC becomes younger from east to west as one moved structurally downward from the Hurricane Ridge fault. Their inference was based mainly on widespread evidence of thrust imbrication together with the predominance of sedimentary younging directions with tops in a generally eastward direction. Tabor and Cady (1978a, b) also noted evidence that indicated that the OSC was arched into a broad domal structure with the deepest structural levels exposed in the central part of the OSC. Our subsequent work supports this interpretation. For instance, Brandon and Calderwood (1990) have shown that the distribution of metamorphic assemblages in the OSC outlines a broad metamorphic culmination with the highest metamorphic grade, corresponding to the occurrence of prehnite in sandstones, localized in the central OSC. Tabor (1972) noted that the degree of cleavage development and metamorphic recrystallization increases as one moves across the eastern flank of this culmination,

from the eastern OSC and into the central OSC. The domal structure of the OSC is considered in more detail below in the light of our FT data.

It is important to note that further microprobe work on the metamorphic assemblages reported by Brandon and Calderwood (1990) has shown that the identification of lawsonite was in error. The reported metamorphic assemblages can be corrected by simply deleting lawsonite as a phase. Further work has shown that the general conclusions of Brandon and Calderwood (1990) are not substantially changed by this error. The lawsonite occurrence was mainly used to help constrain metamorphic pressure. The reset zircon FT data presented here indicate a nearly identical depth of burial, as discussed below.

Previous Isotopic Dating

In an attempt to obtain better age control, Tabor (1972) dated a number of sedimentary rocks from the eastern OSC using the whole rock K-Ar method. For each sample, he analyzed two different size fractions derived by sieving the pulverized sample. He argued that the coarse fraction was representative of the detrital mineral grains in the rock, and the fine fraction was representative of the matrix, much of which is composed of newly crystallized metamorphic minerals. The results of Tabor's study are difficult to interpret. First, the basic assumption—that the size distribution of the pulverized sample is representative of the size distribution of the original mineral grains—is difficult to accept. Second, the fact that each size fraction consists of an unknown mixture of different minerals means that the resulting isotopic data consist of a combination of three different isotopic systems: (1) highly retentive detrital minerals which should give unreset detrital ages, (2) poorly retentive detrital minerals which should give a range of partially or completely reset "ages," and (3) newly crystallized minerals which should give metamorphic ages. Tabor (1972) attempted to resolve these problems by plotting the age of the fine fraction against "metamorphic rank," which was a petrographically determined index used to represent the degree of recrystallization of the sample. This plot showed that with increasing recrystallization, the K-Ar ages appeared to converge with an age of 30 Ma (corrected for modern isotopic constants), which Tabor (1972) interpreted to be the age of metamorphism. Tabor (1972) also called attention to 4 highly recrystallized fine-grained mica phyllite samples that gave very consistent young K-Ar ages between 17 and 20 Ma with an average of 17.9 Ma (corrected for modern isotopic constants). These ages were interpreted as recording late-stage metamorphic recrystallization which Tabor (1972) attributed to local zones of intense shearing. Our FT data indicate that Tabor's 18 Ma age is probably related to regional metamorphism, whereas the 30 Ma appears to be a composite isotopic age with no clear geologic significance.

FT DATING OF DETRITAL ZIRCONS

A unique feature of the external-detector method of FT dating is that it yields ages for individual mineral grains (Naeser, Naeser, and McCul-

loh, 1989). Thus, for a single sandstone sample, this method can be used to discriminate multiple grain-age populations among detrital zircons derived from mixed sources. Such dating is time consuming because a large number of grains must be counted, preferably 50 or more (Brandon, this issue). As a consequence, there have been relatively few serious FT studies of detrital zircon (Hurford, Fitch, and Clarke, 1984; Baldwin, Harrison, and Burke, 1986; Kowallis, Heaton, and Bringhurst, 1986; Naeser and others, 1987; Cerveny and others, 1988; Naeser, Naeser, and McCulloh, 1989). This method, however, has great potential for resolving fundamental problems of age, provenance, and correlation for zircon-bearing sandstones. Furthermore, with only a few samples, it is possible to characterize broadly the cooling history of the source regions from which the zircons were derived, thus providing quick insight into regional-scale tectonic problems.

This section examines the FT method as applied to the dating of detrital zircons. First, we review the current literature on annealing of fission tracks in zircon and use these data to estimate the thermal stability zone and closure temperature for the zircon FT system. Next, we report our laboratory procedures for FT dating. Last, we summarize the methods used to identify component populations in FT grain-age distributions.

Annealing of Fission Tracks in Zircon

A fission track marks the escape path of two highly charged nuclei formed during fission of a ^{238}U atom. The rate of annealing of the damage zone around the track is a function of both time and temperature. The earliest laboratory studies of FT annealing in zircon (Fleischer, Price, and Walker, 1965; Krishnaswami, Lal, and Prabhu, 1974) suggested anomalously high stability temperatures (295° and 355°C, respectively, to produce 50 percent annealing in 10 my). These results are clearly at variance with estimated closure temperatures determined from field studies using several isotope chronometers (Zeitler and others, 1985). One problem with the early laboratory studies was that the degree of annealing was only qualitatively estimated, resulting in poor resolution of the "50 percent annealing" isopleth.

We use the results of two new quantitative studies (Zaun and Wagner, 1985; Tagami, Ito, and Nishimura, 1990) to estimate the annealing behavior of zircon fission tracks for some simple and geologically relevant situations (tables 1 and 2). Tagami, Ito, and Nishimura (1990) report the degree of annealing as a function of temperature as determined in a series of 1 hr annealing experiments. Zaun and Wagner (1985) use naturally annealed samples from a deep borehole with a well constrained thermal history to determine the thermal stability of tracks over a 100 my period.

Stepwise heating.—First, consider the case of an idealized stepwise thermal event where the sample is held at a constant elevated temperature for a time interval of Δt. Table 1 shows the temperatures required to

TABLE 1

Stepwise heating needed to produce 10 and 90 percent annealing of fission tracks in zircon

Time duration Δt (my)	10% annealing $Tz_{10\%}$ (°C)	90% annealing $Tz_{90\%}$ (°C)
1	199	262
5	186	246
10	181	239
25	174	230
100	164	217

Note: Estimated using an Arrhenius equation, $\Delta t(my) = \exp[-A_0 + A_1/T(°K)]$, and annealing data from Zaun and Wagner (1985) and Tagami, Ito, and Nishimura (1990) for zircon. Constants used: $A_0(10\%) = 57.37$, $A_1(10\%) = 27089$, $A_0(90\%) = 49.72$, and $A_1(90\%) = 26617$.

produce 10 percent ($Tz_{10\%}$) and 90 percent ($Tz_{90\%}$) annealing of zircon fission tracks during this stepwise event. $Tz_{10\%}$ and $Tz_{90\%}$ are chosen to approximate the lower and upper limits, respectively, of the zone of partial track stability (Wagner, 1981). In other words, for a specified Δt, fission tracks are considered to be effectively stable at temperatures less than $Tz_{10\%}$ and effectively unstable at temperatures greater than $Tz_{90\%}$. This idealized stepwise model can be used to interpret the thermal history of samples that either have remained unreset or have been completely annealed.

For example, the preservation of unreset detrital FT ages in a sandstone can be interpreted as indicating that temperatures never exceeded about 185° to 200°C (Δt = 1 and 5 my in table 1), based on the assumption that a real thermal event would usually have Δt > 1 to 5 my. Using this temperature limit, we estimate that in a typical continental setting, the thermal stability zone for zircon fission tracks will extend to no deeper than about 6 km, assuming a typical continental thermal gradient of 30°C/km and an average surface temperature of 8°C. Thermal gradients are generally much smaller for subduction zone setting, about 10° to 20°C/km, which would indicate a greater maximum depth range for the thermal stability zone, 9 to 19 km, assuming a similar surface temperature.

Monotonic cooling.—Consider another case of considerable geologic relevance. An initially annealed sample at a temperature in excess of $Tz_{90\%}$ cools monotonically across the partial stability zone to temperatures less than $Tz_{10\%}$. Clearly, there is no single closure temperature because the FT system closes gradually as the sample moves through the partial stability zone. Nonetheless, we can identify an effective closure temperature Tz_c, which corresponds to the temperature of the rock at the time recorded by the FT age (Dodson, 1976, 1979). The method of Dodson (1976, 1979) and the zircon annealing data of Zaun and Wagner (1985) and Tagami, Ito, and Nishimura (1990) are used to calculate Tz_c for the case of monotonic cooling at a constant rate of cooling (table 2).

TABLE 2

Zircon closure temperatures

Cooling Rate (°C/my)	Tz_c (°C)
1	212
10	234
15	238
30	245
100	258

Note: Estimated using eqs 10 and 11 in Dodson (1979) and annealing data from Zaun and Wagner (1985) and Tagami, Ito, and Nishimura (1990). Constants used: $E_{50\%} = 49.77$ kcal/mole, $B = 3.160 \times 10^{-22}$ my.

Hurford (1986) provides an independent estimate of Tz_c based on a variety of isotopic data he used to produce a detailed cooling history for rapidly cooled orthogneisses from the Lepontine Alps. His estimate of $Tz_c = 240° \pm 50°C$ for a cooling rate of 15°C/my is in good agreement with our prediction of 238°C (table 2).

The low closure temperature for the zircon FT system makes it ideal for dating of detrital grains. The reason is that, relative to higher temperature isotope chronometers, the amount of time between closure of the zircon FT system in rocks of the source region and deposition of those zircons in a sedimentary basin should be relatively short. For instance, we might expect a closure temperature of about 235° to 245°C, given typical cooling rates of 10° to 30°C/my. These temperatures would correspond to a depth of about 8 km, assuming that the source region had a typical continental thermal gradient of 30°C/km and a surface temperature of 8°C. Obviously, volcanism and associated subvolcanic plutonism would greatly reduce the depth at which closure occurred.

Laboratory Procedures

About 2 to 12 kg of fine- to medium-grained sandstone were collected at each sample locality. Samples were crushed, washed, and sieved. Zircon was isolated using hydraulic separation, heavy liquids, and magnetic separation. Sieving and handpicking were used to isolate a final fraction of 400 to 800 grains in the 100 to 170 mesh-size range. We usually selected only the well formed euhedral grains, but some rounded grains were also intentionally included. The selected zircons were mounted in heat-softened teflon discs and then polished. The mount was then etched in a eutectic mixture of KOH and NaOH at 220°C for 6 to 12 hrs as necessary, to obtain a high quality etch (Gleadow, 1981, p. 10). In many cases, samples were dated using two mounts per sample, each with different etch times in order to avoid biases between old and young grains (Naeser and others, 1987). Our experience, however, did not reveal any systematic age differences between paired mounts.

Reset samples usually required the greatest amount of etch time which suggests a lower density of α-radiation damage in those zircons (Gleadow, 1981). For zircon, the partial stability zones for α-radiation damage and for fission tracks appear to overlap, with fission tracks having slightly greater thermal stability than α-damage (Kasuya and Naeser, 1988; Tagami, Ito, and Nishimura, 1990). Thus, we infer that the thermal event responsible for annealing fission tracks in our reset samples is also responsible for annealing the α-radiation damage.

The mounts were covered with a flake of low U muscovite and irradiated in a nuclear reactor, either at University of Washington (UW) (reactor decommissioned in 1988) or at Oregon State University (OSU). The measured cadmium ratios (relative to an Au monitor) at the irradiation positions used in these reactors was ~ 100 for the UW reactor and 14 for the OSU reactor, indicating that the neutron fluence was well thermalized. Green and Hurford (1984) argue that for FT dating, the cadmium ratio relative to an Au monitor should be significantly greater than 3.

The neutron fluence was determined by reference to the track density produced in a muscovite flake mounted on either a glass standard of known U content (SRM 962; Carpenter and Reimer, 1974) or zircons of a known age (Fish Canyon tuff; Hurford and Green, 1983, p. 299). Glass standards were used in 5 out of the 7 irradiations. In all cases, the fluence monitors were placed at both ends of the irradiation package to determine fluence gradients. Mounts of Fish Canyon zircon were included as secondary standards in all packages that used a fluence monitor with a glass standard.

All tracks were counted using the same microscope setup (Zeiss microscope, 1250× magnification using oil). Systematic traverses were made, and all suitable grains were counted. Care was taken to count only properly etched grains where the section was parallel to the c crystallographic axis, polishing scratches were sharply defined, and all tracks were clearly resolved. An effort was made to count grains with both low and high track densities to avoid systematic biases between young and old grains.

Ages were calculated using standard formulas and constants (Hurford and Green, 1983, p. 285–286), with the exception of the ^{238}U spontaneous fission decay constant for which we adopt 7.03×10^{-17} yr^{-1} (Roberts, Gold, and Armani, 1968; Naeser, Naeser, and McCulloh, 1989, p. 166). The internally calibrated zeta method is superior to the externally calibrated method used here (Hurford and Green, 1983). Nonetheless, the secondary standards show that our ages are not systematically biased. The mean age of 72 grains of Fish Canyon zircon from internal standards used in 6 irradiations is 28.6 ± 1.9 Ma (F1 in table 3; note that one internal standard is from another study), which compares favorably with the accepted K-Ar age of 27.9 Ma (Hurford and Green, 1983).

When assigning an age and uncertainty to a group of grain ages, there should be a reasonable assurance that the grain ages have experienced a common thermal history. The χ^2 test of Galbraith (1981) and Green (1981) provides one method for checking this assumption. A

group of grain ages is judged to be completely reset when the distribution passes the χ^2 test at a probability $P(\chi^2) > 5$ percent (Galbraith, 1981; Green, 1981). This result indicates that there is a reasonable probability that Poisson variability in the radioactive decay process is the sole source of variability among the grain ages. In this case, a *pooled age* is calculated by combining track data for all dated grains (Green, 1981, eq 3). The assignment of an age is more difficult when the χ^2 test is failed ($P(\chi^2) < 5$ percent). The most common approach is to calculate a *mean age* directly from the grain ages (Green, 1981, eq 10). This approach is not suitable for mixed distributions of grain ages, as might be found in an unreset or partially reset sandstone. In these cases, it is necessary to use decomposition methods, like the χ^2 age and Gaussian peak-fitting methods of Brandon (this issue) or the peak fitting methods of Galbraith and Green (1990).

The estimated total uncertainty for a FT age includes two sources of error, called grain error and group error (Brandon, this issue). Grain error corresponds to the uncertainties associated with measuring the spontaneous and induced track densities in each of the grains. For a single grain age or for a pooled age, the grain error is estimated assuming Poisson errors for the measured spontaneous and induced track densities (Green, 1981, eq 4). For a mean age, the grain error is estimated using the standard error calculated from the grain age distribution (Green, 1981, eq 11; note typographical error in equation). Group error corresponds to those uncertainties that are common to all grains in the group, such as uncertainties associated with laboratory calibration constants or the measured track density in the mica detector of a fluence monitor. The total uncertainty of a cited FT age should include both the grain and group errors (Green, 1981, eq 5). In this paper, unless otherwise noted, all uncertainties represent total uncertainties and are cited at two times the standard error ($\pm 2s$), approximately equal to a 95 percent confidence interval around the estimated age.

The uranium content of each grain was calculated using the method of Pott (1987, p. 448) and is reported in Brandon and Vance (1992). This information was used to see if there was any obvious correlation between grain age and U content for our unreset and reset grain age distributions; none was found. The U content of the grain is equal to the U content of the glass standard times the induced track density for the grain divided by the induced track density for the glass standard. The SRM 962 glass standard has an effective U content of 12.3 ppm (Green, 1985, p. 3; note that the SRM 612 glass is an older version of SRM 962). For fluence monitors using Fish Canyon zircons as a standard, the measured neutron fluence was used to calculate the induced track density expected for a mica detector against an SRM 962 glass standard.

Decomposition of FT Grain-age Distributions

A substantial challenge in FT dating of unreset detrital zircons is the interpretation of the resulting grain-age distributions. The grain ages,

themselves are not sufficiently precise to be used individually. In our study, the average total uncertainty (±2s) for the FT age of a single zircon grain is about ±26 percent of the estimated age. Therefore, it is necessary to gather grain ages into related groups in order to improve the precision of the age estimates and also to reduce the grain-age data to a more meaningful and compact form.

One approach to this problem is to view a grain-age distribution as a mixture of several component grain-age populations, with each component derived from a specific *FT source terrain* (Brandon, this issue). A FT source terrain is defined as a discrete area in the general source region that yields zircons of a characteristic FT age. In reality, a given source region is probably capable of delivering a wide range of FT grain ages, but it is anticipated that a few dominant component populations will account for the bulk of the grain ages. In our study, component populations were identified using two methods from Brandon (this issue).

The first method, called the χ^2 *age method,* is designed to isolate a group of young grain ages that with statistical confidence might plausibly have been derived from a single-age FT source terrain. This method is based on the χ^2 test of Galbraith (1981) and Green (1981). To calculate the χ^2 age of a grain-age distribution, the grain ages are first arranged in order of increasing age. Moving down the list, a *sum age* and $P(\chi^2)$, the probability for the χ^2 test, are calculated at each grain age. The sum age is the pooled age for all grain ages equal to or younger than the current grain age. The χ^2 test compares a distribution of grain ages with their sum age, which is the expected age of the grains if they were derived from a single-age source. $P(\chi^2)$ is the probability that deviations from the expected age might be due solely to Poisson variations associated with the process of radioactive decay. Brandon (this issue) defines the χ^2 age as the pooled age of the largest group of young grains that still retains $P(\chi^2)$ greater than 1 percent. The critical probability of 1 percent is used to ensure that if any bias exists it will be toward a slightly older age. This choice is in keeping with the main use of the χ^2 age as a maximum limit for the depositional age of the sample. The advantage of the χ^2 age method is that it is relatively simple to calculate and carries the statistical assurance that the age is representative of the youngest fraction of "plausibly related" grain ages.

The second method, called the *Gaussian peak-fitting method,* decomposes the full grain-age distribution into a series of component grain-age populations. In statistics, this type of distribution is called a finite-mixture distribution (McLachlan and Basford, 1988). The Gaussian peak-fitting method utilizes the composite probability density plot of Hurford, Fitch, and Clarke (1984), which portrays the grain-age distribution as a continuous probability density plot. The basic assumption is that each of the component grain-age populations in the composite probability density plot can be represented by a unique Gaussian function, defined by a mean μ_{fj}, a relative standard deviation W_{fj}, and the number of grains N_{fj}, where $j = 1, \ldots, g$, with g equal to the total number of component

populations. Each of the component Gaussian distributions can be considered to correspond to specific peaks in the composite probability density plot. As used here, the term "peak" refers to any component Gaussian distribution, even those for which there is no visible peak in the composite probability density plot. This situation can occur when two component populations are closely spaced in age so that their respective Gaussian distributions overlap.

The parameters for the component Gaussian functions are determined using a nonlinear least-squares program developed by Brandon (this issue). The reader is referred there for specific details. That paper outlines a procedure and some criteria for judging the overall suitability of a best-fit solution. It also presents some test examples using simulated and real data that show how the method performs, what its limitations are, and how it compares with the binomial peak-fitting method of Galbraith and Green (1990).

The relative standard deviation, W_{fj}, is equal to σ_{fj}/μ_{fj}, where σ_{fj} is the absolute standard deviation of the jth Gaussian peak as represented in the composite probability density plot. Both W_{fj} and σ_{fj} provide a useful measure of the width of the peak, which, in turn, is related to the degree of variation among those grain ages that make up the peak. We prefer to use the relative standard deviation, W_{fj}, because it does not vary significantly as a function of FT age. Analysis of zircons from volcanic rocks indicates that for a single-age source, W_{fj} should be about 16.3 percent (C5 and F1 in table 3). We use the following general guidelines. When a best-fit peak has W_{fj} between 12 to 20 percent, this is taken as evidence that the peak corresponds to a component population derived from a single-age FT source. A peak with W_{fj} greater than about 20 percent has a high probability of being a composite peak, defined as a peak composed of two or more single-age populations. A peak with W_{fj} significant less than about 12 percent suggests that the underlying component population was incompletely sampled, which tends to occur when the number of grains in a peak, N_{fj}, is less than about 8 to 10. This reflects the downward bias of the estimated standard deviation associated with a small sample size.

The Gaussian peak-fitting method is best viewed as a technique for decomposing a grain-age distribution into a form that is more compact but still faithfully represents the original observations. In this sense, the best-fit peaks can be viewed as a proxy for the sample distribution. It is important to remember that the grain-age distribution represents a small sample drawn from a much large parent population. This limits our ability to make statistical inferences about the characteristics of the FT source terrains from which the zircons were eroded (see discussion in Brandon, this issue). In our analysis, we use the Gaussian peak-fitting method mainly as a means to identify older component populations in the grain-age distributions from our unreset samples. It also provides an estimate of the age of the youngest component population which can be used as an independent check of the χ^2 age. Our experience indicates

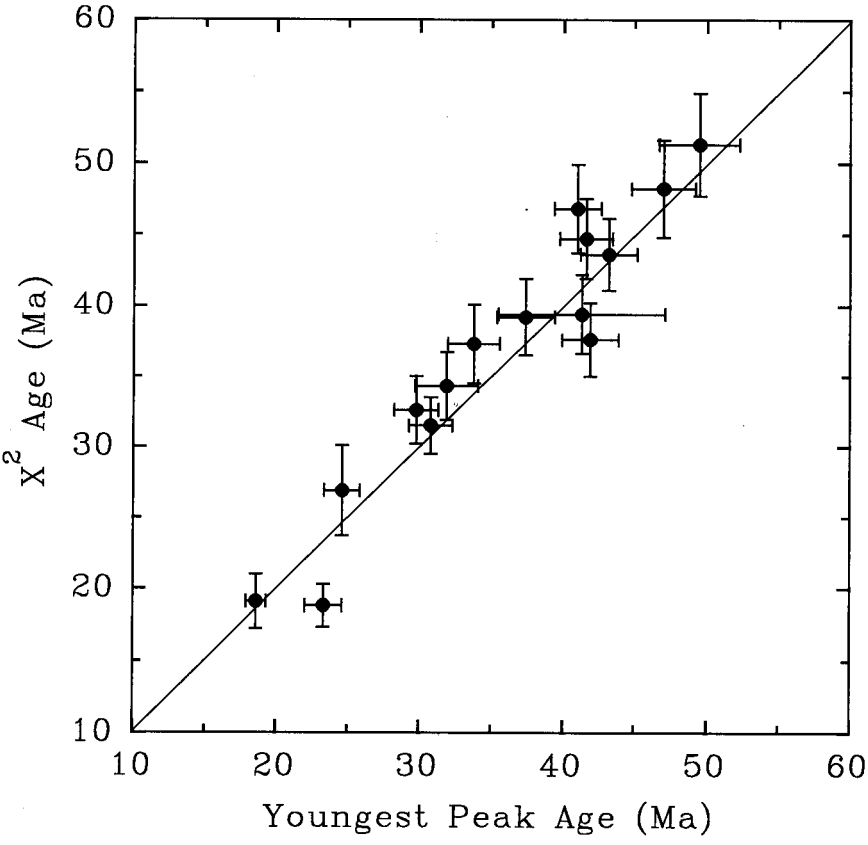

Fig. 4. Comparison of χ^2 ages and youngest peak ages for each of the unreset samples in this study. The diagonal line marks the locus of points where the χ^2 age would be equal to the youngest peak age. The error bars show the 95 percent confidence intervals (±2 standard error) for the estimated ages. Note that the ages estimated by the two methods appear to be in good agreement in that their error bars generally overlap the diagonal line. Nonetheless, the old-side bias of the χ^2 age method is apparent in that the majority (12 out of 15) of the points plot slightly above the diagonal line.

that there is good agreement between the youngest peak age and the χ^2 age (fig. 4). Note that the conservative bias of the χ^2 age method is apparent in that the χ^2 age for a sample is commonly slightly older than the age of the youngest Gaussian peak.

FT RESULTS

This section reports zircon FT ages for 19 sandstone samples, 15 of which are from the OSC. The samples are divided into 4 groups. The first group, which is included for the purposes of comparison, consists of unreset samples from Eocene basins located to the east and southeast of

the Olympic Mountains (table 3, fig. 1). The next 2 groups comprise the unreset OSC samples which are divided on the basis of location into a western group and an eastern group (tables 4 and 5, fig. 5). The last group consists of reset samples from the central part of the OSC (table 7, fig. 5). Figure 6 summarizes the χ^2 ages and peaks ages determined for all of the unreset samples. Sample locations and local geologic setting are described in app. I. The primary data, including FT measurements, grain ages, and other related calculations, are reported in Brandon and Vance (1992).

The OSC samples were selected to include all the major units of Tabor and Cady (1979a, b), except for the Miocene Hoh assemblage of the western OSC which is already well dated. Most OSC samples were collected along an east-west transect through the middle of the Olympic Mountains, with some supplementary samples to the north and south

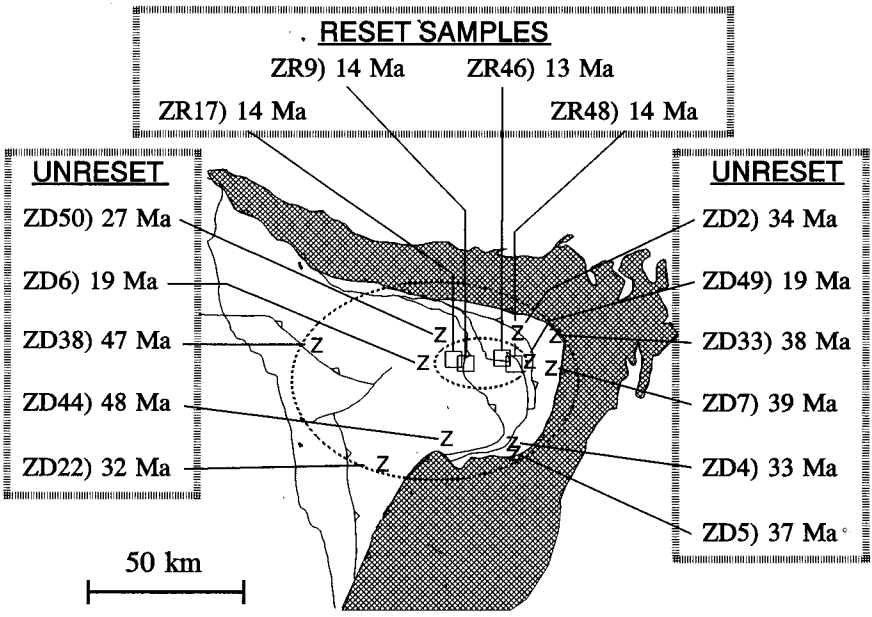

Fig. 5. Summary map of zircon FT ages from the OSC. χ^2 ages are reported for unreset samples (tables 3–5). Youngest peak ages are reported for reset samples (table 7). The prefixes "ZD" and "ZR" in the laboratory sample numbers indicate unreset and reset samples, respectively. On the map, unreset samples are plotted with a "Z," and reset samples with a box. The inner dashed line encloses the reset zircon localities. The outer dashed line encloses an area where apatite FT ages for OSC sandstones are total reset and yield cooling ages less than 12 Ma (Roden, Brandon, and Miller, 1990). This area cooled through the apatite closure temperature (~115°C) while the Olympic Mountains were being uplifted and denuded.

TABLE 3

Zircon FT results for Eocene basins samples and other miscellaneous samples

Lab#	Geologic unit, location	Age range, number of grains	Youngest fraction		Older peaks			Oldest fraction
			χ^2 Age	Youngest peak	(~43 Ma)	(~57 Ma)	(~74 Ma)	(> ~100 Ma)
Unreset sandstones from Eocene basins								
C1)	Upper part of Puget Group, Ravensdale, Washington (EA ≥ ~38.2 Ma)	24 - 259 Ma N_t = 50	39.4 ± 2.8 Ma N_f = 18	41.3 Ma* N_f = 19 W = 23%	41 Ma*	56 Ma N_f = 10 W = 19%	79 Ma N_f = 12 W = 24%	106 - 259 Ma N_f = 7
C2)	Skookumchuck Fm., S of Centralia, Washington (EA ~39.2 Ma)	32 - 143 Ma N_t = 60	44.7 ± 2.8 Ma N_f = 24	41.6 Ma* N_f = 11 W = 16%	42 Ma*	57 Ma N_f = 21 W = 21%	97 Ma N_f = 27 W = 33%	101 - 143 Ma N_f = 14
C3)	Stillwater Member of the Cowlitz Fm., N of Ryderwood, Washington (EA ~48 to 37.5 Ma)	35 - 248 Ma N_t = 60	51.3 ± 3.6 Ma N_f = 26	49.5 Ma* N_f = 17 W = 17%	50 Ma*	- n.d. -	75 Ma N_f = 35 W = 24%	100 - 248 Ma N_f = 8
C4)	Cowlitz Fm., W of Timber, Oregon (EA ~48 to 37.5 Ma)	28 - 169 Ma N_t = 60	43.6 ± 2.5 Ma N_f = 26	43.2 Ma* N_f = 21 W = 18%	43 Ma*	59 Ma N_f = 18 W = 16%	75 Ma N_f = 18 W = 28%	108 - 169 Ma N_f = 4
Unreset volcanic tuff								
C5)	Skookumchuck Fm., Centralia coal mine, Washington	33 - 51 Ma N_t = 20	(same as pooled age)	39.4 ± 1.8 Ma N_f = 19.6 W = 15.3%	Pooled age = 39.2 ± 2.7 Ma $P(\chi^2)$ = 57%			
Reference sample of unreset volcanic zircon								
F1)	Fish Canyon tuff, (internal standards for 6 irradiations)	21 - 40 Ma N_t = 72	26.3 ± 1.6 Ma N_f = 52	28.6 ± 1.6 Ma N_f = 68.4 W = 17.3%	Mean age = 28.6 ± 1.9 Ma [accepted K-Ar age = 27.9 Ma]			

Notes: EA = expected depositional age. N_t = total number of grains analyzed. N_f = estimated number of grains in a specific peak or fraction. All uncertainties are cited at ±2 standard error and include group error. W = estimated relative standard deviation for a peak, expressed in percentage of the peak age. * = youngest peak coincides with the ~43 Ma P_1 peaks. n.d. = not detected.

TABLE 4

Zircon FT results for the western group of unreset samples from the Olympic subduction complex

Lab#	Geologic unit, location	Age range, number of grains	Youngest fraction		Older peaks			Oldest fraction
			χ^2 Age	Youngest peak	(~43 Ma)	(~57 Ma)	(~74 Ma)	(> ~100 Ma)
ZD38)	Western Olympic Assemblage, SE of Forks	31 - 279 Ma N_t = 61	46.8 ± 3.1 Ma N_f = 23	41.0 Ma* N_f = 12 W = 18%	41 Ma*	65 Ma N_f = 27 W = 23%	81 Ma N_f = 15 W = 23%	110 - 279 Ma N_f = 7
ZD22)	?Western Olympic Assem., North Fork Ranger Station	23 - 84 Ma N_t = 50	31.5 ± 2.0 Ma N_f = 28	30.8 Ma N_f = 23 W = 17%	44 Ma N_f = 20 W = 17%	62 Ma N_f = 3 W = 11%	78 Ma N_f = 4 W = 14%	- n.d. -
ZD44)	?Western Olympic Assemblage, NW of Quinault Lk.	37 - 180 Ma N_t = 25	48.2 ± 3.4 Ma N_f = 16	47.0 Ma* N_f = 13 W = 17%	47 Ma*	- n.d. -	69 Ma N_f = 10 W = 21%	125 - 180 Ma N_f = 2
ZD50)	Western Olympic Assemblage, Glacier Creek	24 - 101 Ma N_t = 25	26.9 ± 3.2 Ma N_f = 4	24.6 Ma N_f = 3 W = 11%	45 Ma N_f = 11 W = 18%	- n.d. -	73 Ma N_f = 9 W = 15%	97 - 101 Ma N_f = 2
ZD6)	Western Olympic Assemblage, Mount Tom	14 - 195 Ma N_t = 50	19.1 ± 1.9 Ma N_f = 15	18.6 Ma N_f = 14 W = 24%	42 Ma N_f = 12 W = 18%	58 Ma N_f = 19 W = 24%	86 Ma N_f = 3 W = 16%	153 - 195 Ma N_f = 2

Notes: N_t = total number of grains analyzed. N_f = estimated number of grains in a specific peak or fraction. All uncertainties are cited at ±2 standard error and include group error. W = estimated relative standard deviation for a peak, expressed in percentage of the peak age. * = youngest peak coincides with the ~43 Ma P_1 peaks. n.d. = not detected.

TABLE 5

Zircon FT results for the eastern group of unreset samples from the Olympic subduction complex

Lab#	Geologic unit, location	Age range, number of grains	Youngest fraction		Older peaks			Oldest fraction
			χ^2 Age	Youngest peak	(~43 Ma)	(~57 Ma)	(~74 Ma)	(> ~100 Ma)
ZD49)	Grand Valley Assemblage, Wellesley Peak	14 - 229 Ma N_t = 55	18.8 ± 1.5 Ma N_f = 18	23.3 Ma N_f = 32 W = 24%	46 Ma N_f = 15 W = 28%	- n.d. -	76 Ma N_f = 4 W = 22%	125 - 229 Ma N_f = 2
ZD2)	Possibly Needles-Gray Wolf Assem., Hurricane Ridge	22 - 195 Ma N_t = 55	34.3 ± 2.4 Ma N_f = 18	31.9 Ma N_f = 10 W = 21%	49 Ma N_f = 32 W = 20%	69 Ma N_f = 2 W = 9%	94 Ma N_f = 9 W = 29%	110 - 195 Ma N_f = 4
ZD7)	Needles-Gray Wolf Assemblage, Sunnybrook Meadows	28 - 389 Ma N_t = 60	39.2 ± 2.7 Ma N_f = 19	37.4 Ma* N_f = 11 W = 16%	37 Ma*	53 Ma N_f = 36 W = 18%	78 Ma N_f = 6 W = 21%	119 - 389 Ma N_f = 5
ZD33)	Needles-Gray Wolf Assemblage, Tyler Peak	26 - 184 Ma N_t = 50	37.6 ± 2.6 Ma N_f = 13	41.9 Ma N_f = 21 W = 18%	42 Ma*	64 Ma N_f = 15 W = 15%	83 Ma N_f = 9 W = 14%	108 - 184 Ma N_f = 4
ZD4)	Probably Needles-Gray Wolf Assem., Skokomish River	28 - 126 Ma N_t = 48	32.6 ± 2.4 Ma N_f = 16	29.8 Ma N_f = 8 W = 10%	41 Ma N_f = 19 W = 15%	61 Ma N_f = 16 W = 24%	- n.d. -	108 - 126 Ma N_f = 4
ZD5)	Possibly Needles-Gray Wolf Assem., W of Staircase Station	29 - 83 Ma N_t = 49	37.3 ± 2.8 Ma N_f = 18	33.8 Ma N_f = 9 W = 15%	- n.d. -	56 Ma N_f = 40 W = 23%	- n.d. -	- n.d. -

Notes: N_t = total number of grains analyzed. N_f = estimated number of grains in a specific peak or fraction. All uncertainties are cited at ±2 standard error and include group error. W = estimated relative standard deviation for a peak, expressed in percentage of the peak age. * = youngest peak coincides with the ~43 Ma P_1 peaks. n.d. = not detected.

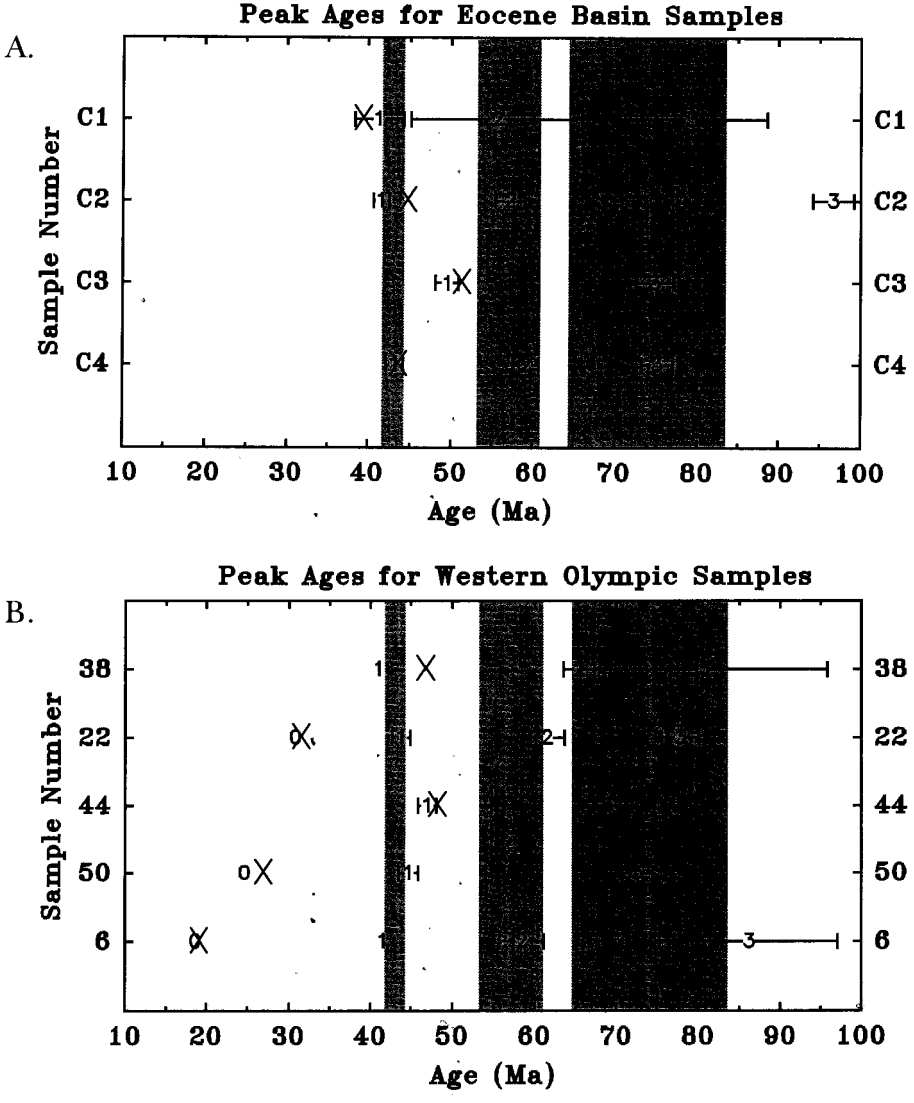

Fig. 6. Summary diagrams showing χ^2 ages and best-fit peak ages for unreset samples from (A) the Eocene basin localities, (B) the western OSC group, and (C) the eastern OSC group. Data are from tables 3 to 5 as referenced by the sample numbers. χ^2 ages are indicated with an "X." Peak ages are indicated with a "0" for the youngest peak, and "1," "2," and "3" for the older peaks (P_1, P_2, and P_3). The error bars show the estimated uncertainty (±1 standard error) for the peak ages. The vertical dotted lines and associated gray bands mark the average ages and uncertainties (±1 standard error) for the P_1, P_2, and P_3 peaks (see result C in table 6).

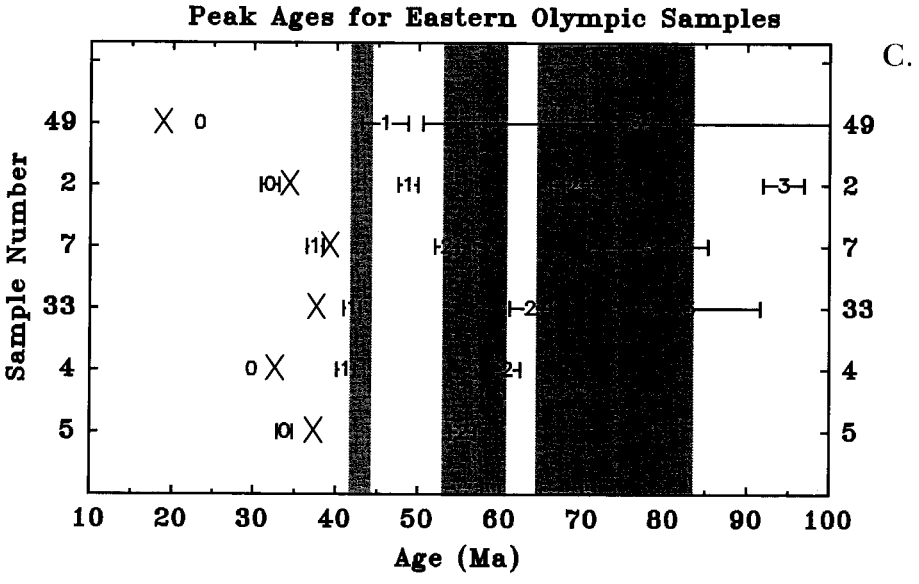

Fig. 6 (continued)

(fig. 5). All the OSC samples come from turbidite sequences, indicating marine deposition below storm wave base, presumably in a deep marine setting, such as a trench basin.

Our discussion of these data is divided into three parts. The first part focuses on the youngest populations of FT grain ages in the unreset OSC and Eocene basin samples. The second part considers the older component populations in these unreset samples. The third part examines FT ages for the reset OSC samples.

An important problem in interpreting out FT data is the distinction between unreset and reset samples. One crude indicator is the total range of FT grain ages in a sample distribution. On this basis, there appears to be a clear distinction between samples that have a wide distribution in grain ages that we designate as "unreset" (tables 3–5; distribution widths from 54-361 my) and those that have a very narrow distribution which we designate as "reset" (table 7; distribution widths from 13-27 my). One difficulty with this classification is that it ignores the possibility that the "unreset" samples might have been only partially reset or the "reset" samples might not have been totally reset. We consider these problems in detail below, following the presentation of the FT data. Our conclusions are that the "unreset" samples have not been significantly affected by partial resetting (<10 percent reduction in age), and that the "reset" samples retain a significant fraction of incompletely reset grains.

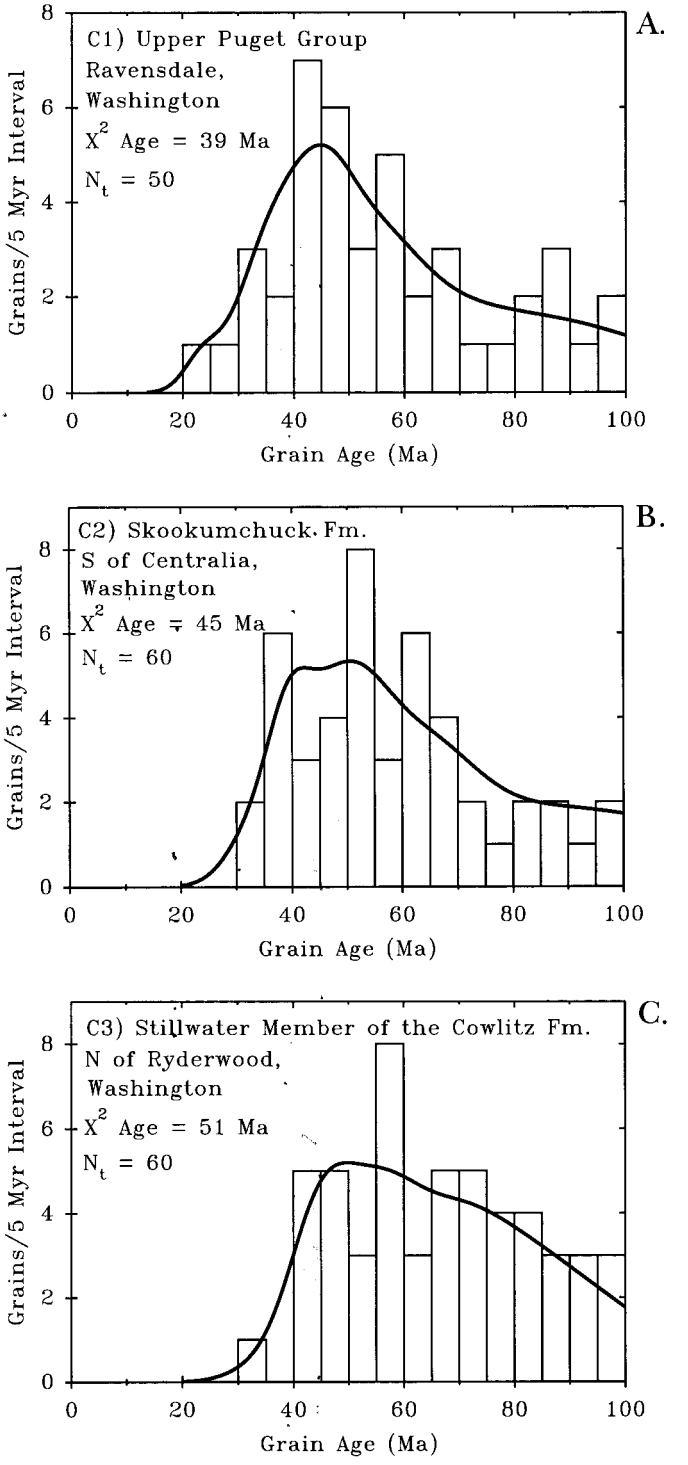

Fig. 7 (A–E) Composite probability density plots and grain-age histograms for the Eocene basin samples. Results are summarized in table 3. Note that the density plot and histogram are plotted using the same vertical scale with units of "number of grains per 5 my interval."

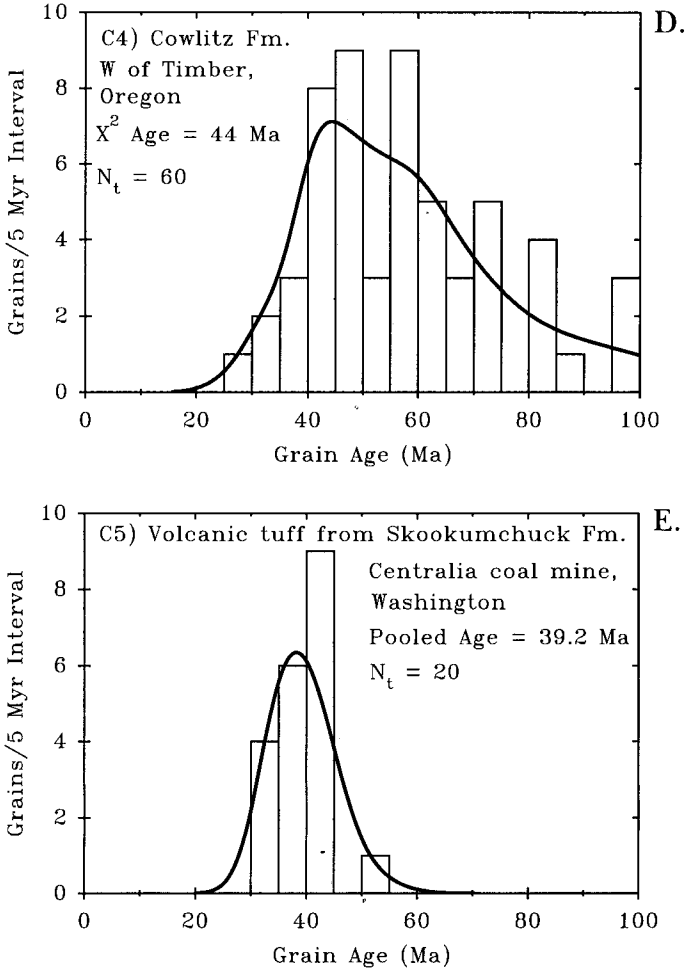

Fig. 7 (continued)

Youngest Populations in the Unreset Samples

Eocene basin samples.—Samples C1 to C4 (table 3, fig. 7) were collected from Eocene basin sequences located to the east and southeast of the Olympics (fig. 1). They are used here to examine the relationship between depositional age and the FT age of the youngest grain-age population. The samples are friable arkosic sandstones lacking any indication of low grade metamorphism. All 4 samples come from reasonably well dated stratigraphic sections with depositional ages of Middle and Late Eocene (48–37.5 Ma; see app. I). There is generally good

agreement between the χ^2 ages and youngest peak ages (table 3). The widths of the youngest peaks are consistent with their derivation from a single-age FT source terrain, with the possible exception of C1. Expected depositional ages are listed in the first column of table 3. A quick comparison shows that the χ^2 ages and the youngest peak ages provide reasonable approximations of the expected depositional ages. This relationship is examined in more detail below.

Sample C1, collected from the Puget Group at Ravensdale, Washington, lies about 6 km north of the Green River section of the Puget Group, which was dated by Turner and others (1983) using plagioclase K-Ar and apatite FT methods. The exact stratigraphic relationship between these two parts of the Puget Group is poorly resolved due to sparse outcrop in the surrounding area. The Ravensdale locality is considered to lie near the top of the Puget Group, whereas the good K-Ar ages of Turner and others (1983) are from the middle of the Puget Group, at about 1025 to 1540 m below the top of the unit (fig. 2 in Turner and others, 1983). The 6 good K-Ar ages from this interval are tightly clustered and show no evidence of younging upsection. When combined, they indicate a mean K-Ar age of 43.3 ± 1.65 Ma (±95 percent uncertainty). Turner and others (1983) estimate that the Green River gorge section was accumulated at rates in excess of >250 m/my. High accumulation rates seem to be a general feature of Eocene basins in western Washington (Johnson, 1985). Based on this minimum accumulation rate, we estimate that the Ravensdale locality is less than 5.1 my younger than the Green River locality (5.1 my = 1280 m/250 m/my), which would give a depositional age of 38.2 Ma or older. Our FT data from the Ravensdale locality indicate a χ^2 age of 39.4 ± 2.8 Ma. The estimated lag time would be less than 1.2 ± 3.3 my (±95 percent uncertainty; note that the estimated uncertainty does not include uncertainties for the accumulation rate calculation).

Locality C2 from the Skookumchuck Formation lies near a well dated locality in the Centralia coal mine. An interbed of tuff in the coal beds has yielded a zircon FT age of 39.2 ± 2.7 Ma (C5 in table 3). Tuffs from this locality have yielded K-Ar plagioclase ages that average at 40 Ma (Triplehorn, Turner, and Frizzell, 1980). Sample C2 has a χ^2 age of 44.7 ± 2.8 Ma and a youngest peak age of 41.6 Ma, both of which are slightly older than the expected depositional age. Estimates of the lag time range from 5.5 ± 3.9 my (±95 percent uncertainty) using the χ^2 age and the zircon FT age for the C5 tuff to 1.6 my using the youngest peak age and the K-Ar ages from Triplehorn, Turner, and Frizzell (1980).

Sample C3 was collected from the Stillwater Member of the Cowlitz Formation which has a depositional age somewhere within the interval 48 to 37.5 Ma (see app. I). The χ^2 age of 51.3 Ma and the youngest peak age of 49.5 Ma for this sample are consistent with its expected depositional age. Stratigraphic position provides another test. The Skookumchuck Formation (C2) stratigraphically overlies the Stillwater Member (C3) of the Cowlitz Formation (Walsh and others, 1987). Thus, sample C2

should be younger than sample C3, which is consistent with their χ^2 ages, 44.7 and 51.3 Ma, respectively.

Sample C4 is from the Cowlitz Formation of northwestern Oregon. In southwest Washington, the Cowlitz is considered to have a depositional age somewhere in the range 48 to 37.5 Ma (see app. I). C4 has a χ^2 age of 43.6 Ma and a youngest peak age of 43.2 Ma, both of which are consistent with the expected depositional age.

These results support our interpretation that the FT age of the youngest grain-age population closely tracks the depositional age of the sandstone. Our estimates indicate that the lag time is probably less than about 5 my. A short lag time is compatible with geologic evidence that indicates widespread igneous and tectonic activity in Washington, Idaho, Montana, and British Columbia throughout much of the Eocene (Armstrong and Ward, 1991). Tectonic activity diminished during the Oligocene and Miocene, but igneous activity in the Cascade volcanic arc, from Oligocene to present, probably provided another source of young zircons. This point is important because χ^2 ages for our unreset OSC samples range from Eocene to Miocene, with 6 out of 11 samples having ages significantly younger than the Eocene basin samples.

Based on the evidence above, we have chosen to adopt the assumption that for the unreset OSC samples, their χ^2 ages are within about 5 my of their true depositional ages. The time interval of 5 my is not much greater than the uncertainties associated with our age estimates. Therefore, in our discussion below, the χ^2 age is used as a proxy for the depositional age of the rock, but the reader should remain mindful that this is only an approximation.

Western group of OSC samples.—Of the 5 samples in this group (table 4, fig. 5), 3 come from well-mapped parts of the Western Olympic assemblage of Tabor and Cady (1978b). The remaining 2 are from an undifferentiated unit (Tur of Tabor and Cady, 1978b), which may represent a western continuation of the Western Olympic assemblage (see fig. 3 in Heller and others, 1992). The composite probability density plots for these samples (fig. 8) show clear evidence of mixed grain-age populations. There is generally close agreement between the χ^2 age and the youngest peak age, with the exception of sample ZD38 for which the χ^2 age is about 6 my older than the youngest peak age. The widths of the youngest peaks are consistent with their derivation from a single-age FT source terrain, with the possible exception of ZD6.

The χ^2 ages suggest that the samples were deposited over a broad interval of time, about 30 my (~48 to 19 Ma). The younger χ^2 ages (19 and 27 Ma) come from locations near Mount Olympus, whereas the older χ^2 ages are from the westernmost part of the Western Olympic assemblage and its presumed extensions. The 30 my span in ages and their separation on the map into two age groups suggest that the Western Olympic assemblage may include more than one stratigraphic unit.

Eastern group of OSC samples.—This group consists of 6 samples collected from the Grand Valley and Needles-Gray Wolf assemblages of

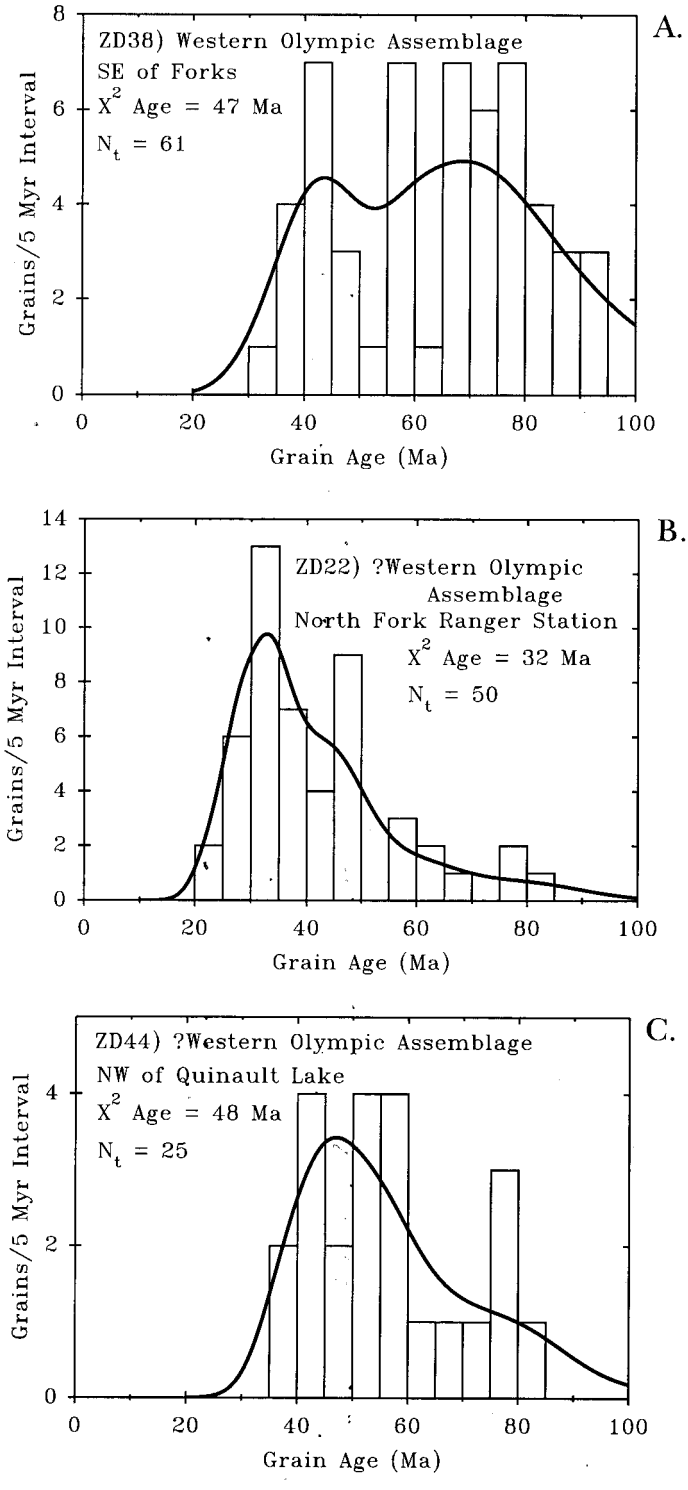

Fig. 8 (A–E) Composite probability density plots and grain-age histograms for the western group of unreset OSC samples. Results are summarized in table 4. Note that the density plot and histogram are plotted using the same vertical scale with units of "number of grains per 5 my interval."

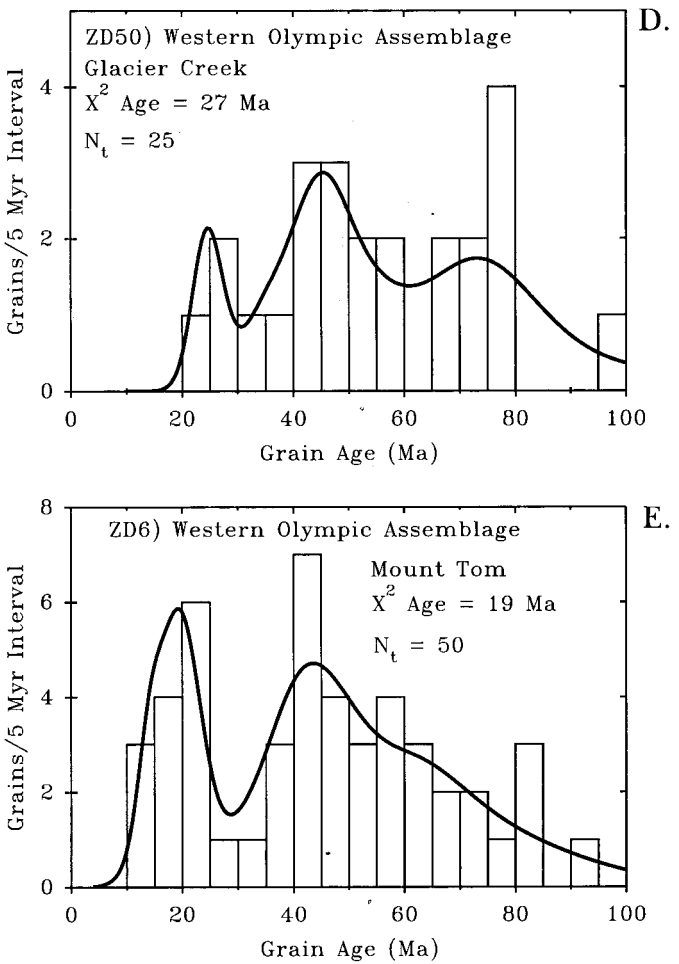

Fig. 8 (continued)

Tabor and Cady (1978b), exposed along the eastern perimeter of the OSC (table 5, fig. 5). Composite probability density plots (fig. 9) show that the grain-age distributions are polymodal. In general, there is good agreement between the χ^2 ages and youngest peak ages (table 5), with the exception of sample ZD49 (discussed below). Once again, peak widths for most of the youngest peaks suggest derivation from a single-age FT source.

Two samples were collected from the Grand Valley assemblage of Tabor and Cady (1978b). Sample ZD49 from Wellesley Peak has a χ^2 age of 19 Ma, which is significantly younger than the age of its youngest best-fit peak at 23 Ma. The width of this youngest peak is large (W = 24

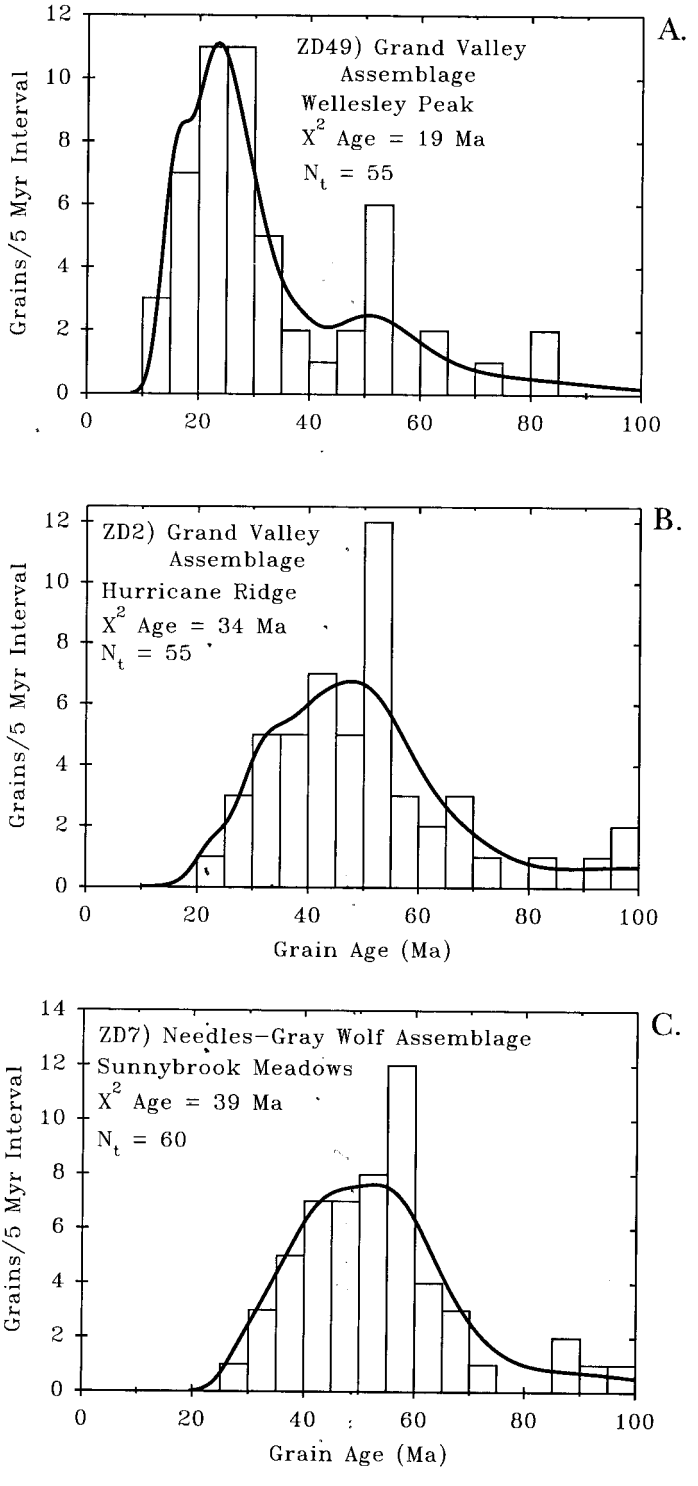

Fig. 9 (A–F) Composite probability density plots and grain-age histograms for the eastern group of unreset OSC samples. Results are summarized in table 5. Note that the density plot and histogram are plotted using the same vertical scale with units of "number of grains per 5 my interval."

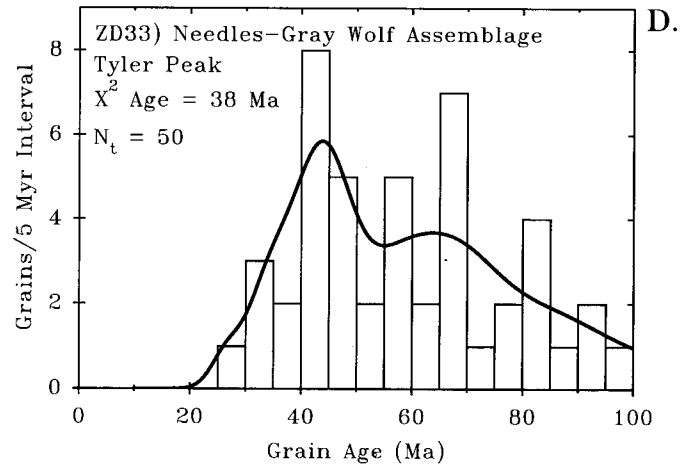

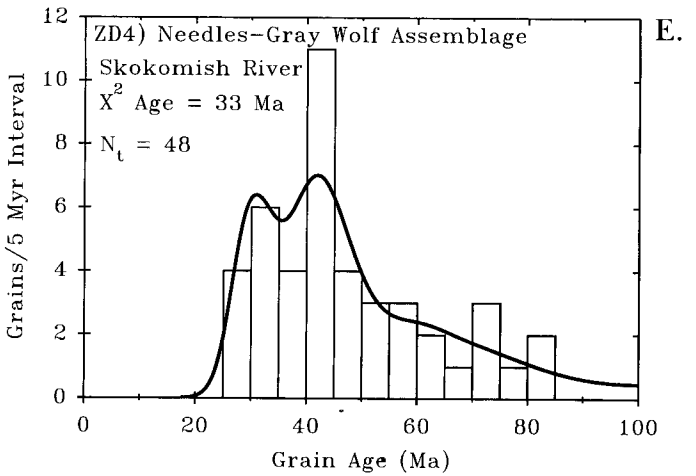

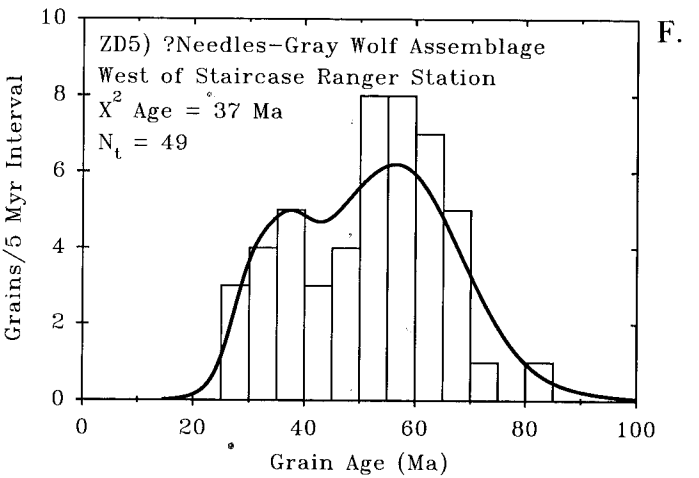

Fig. 9 (continued)

percent) indicating that the peak contains zircons derived from a composite FT source. In this case, the χ^2 age provides a better estimate of the FT age of the youngest grain-age population in this sample.

Sample ZD2 from Hurricane Ridge was also collected from outcrops mapped as Grand Valley assemblage, but it gives a much older χ^2 age of 34 Ma. We doubt that both these samples are from the same stratigraphic unit because of the significant contrast in their apparent ages (15 my = 34 Ma − 19 Ma). The younger of the two "Grand Valley" samples, ZD49 from Wellesley Peak (χ^2 age = 19 Ma; table 5), appears to be the same age as one of the samples from the western group of unreset OSC samples, ZD6 from Mount Tom (χ^2 age = 19 Ma; table 4). This similarity in age suggests that parts of the Western Olympic assemblage may be equivalent to parts of the Grand Valley assemblage.

The older of the two "Grand Valley" samples, ZD2 from Hurricane Ridge (χ^2 age = 34 Ma, table 5), was collected immediately west of a mapped contact separating the Grand Valley assemblage from the Needles-Gray Wolf assemblage lying to the east. It has a χ^2 age similar to those obtained for unreset samples from the Needles-Gray Wolf assemblage (discussed below; see fig. 5). We suggest that ZD2 from Hurricane Ridge actually belongs to the Needles-Gray Wolf assemblage. This interpretation would only require a small westward shift (~100 m) in the mapped position of the contact, which is not particularly well defined at our sample locality (Tabor, Yeats, and Sorensen, 1972). Alternatively, the Grand Valley assemblage may include a larger range of stratigraphic ages or sample ZD2 may simply lack young zircon.

Two sandstones (ZD7, ZD33) were collected from well mapped parts of the Needles-Gray Wolf assemblage in the northeastern part of the OSC. Another sample (ZD4) was collected from unit Tsc of Tabor and Cady (1978b), which is probably a southern continuation of the Needles-Gray Wolf. All 3 samples show a tight cluster of χ^2 ages in the range 39 to 33 Ma. Furthermore, the χ^2 ages and youngest peak ages agree well, and the widths of the youngest peaks are consistent with a single-age source.

A fourth sample (ZD5) was collected from an area mapped as the "basaltic facies" of the Blue Mountain unit (Tbmb of Tabor and Cady, 1978b; also see Tabor, 1982), but we suspect that the rocks we sampled are part of the Needles-Gray Wolf assemblage. Mapping in the northeast part of the Olympics (Tabor and Cady, 1978b; Einarsen, 1987) has shown that the Blue Mountain unit stratigraphically underlies and is interbedded with the Lower Eocene basalts of the Crescent Formation. Relationships are not as clear in the southeast where sample ZD5 was collected. We were unable to find a stratigraphic relationship between the sandstone unit that we sampled and nearby exposures of lower Crescent Formation (red limestone and pillow basalt). Furthermore, the dated sandstone is not basaltic but instead is composed mainly of quartz and plagioclase with minor plutonic and volcanic lithic clasts, biotite, and muscovite. The heavy mineral fraction yielded abundant epidote and garnet. The χ^2 age for sample ZD5 is 37 Ma, which is about 17 my

younger than the age of the Crescent Formation (~54 Ma for the upper Crescent; Duncan, 1982). Map patterns (Tabor, 1982) suggest that the dated sandstone is structurally interleaved with lower Crescent basalts. Thus, it is possible that the dated locality lies within a tectonic slice of the Needles-Gray Wolf assemblage. Tabor (1982) has identified rocks equivalent to the Needles-Gray Wolf assemblage (unit Tsc of Tabor, 1982) as lying just 2 km to the north of our locality ZD5.

Older Peaks in the Unreset Samples

Using the Gaussian peak-fitting method of Brandon (this issue), we have found that the unreset grain-age distributions commonly contain about 4 to 6 resolvable peaks (ZD5 and C2 are exceptions with only 2 and 3 resolvable peaks, respectively). This result indicates that there are older component populations, that is, grain-age populations that predate the youngest peak in a grain-age distribution. Peak ages for these older populations are typically younger than 100 Ma. In fact, our unreset distributions generally contain only a few grains older than 100 Ma (see column labeled "oldest fraction" in tables 3–5). As a result, our summary tables and figures focus almost exclusively on the time interval 0 to 100 Ma. We examine here the set of older peaks lying within this age range.

Our analysis suggests that the older peaks are clustered into three age groups, located at about 43, 57, and 74 Ma, respectively (fig. 6). These groups are designated as P_1, P_2, and P_3, in order of increasing age. The label P_0 is used to refer to the youngest peak in the grain-age distribution.

The assignment of an older peak to a specific group is usually straightforward, because most (9 out of 15) of the unreset grain-age distributions contain three resolvable older peaks in the range 0 to 100 Ma. For distributions with fewer than 3 older peaks, the peaks are assigned to the nearest group. In a number of cases (8 out of 15), the youngest peak, P_0, overlaps with the P_1 group and thus is considered to be a member of that group. These cases are labeled with asterisks in tables 3 to 5. This circumstance is expected for older samples that have depositional ages that coincide with the age of the P_1 group.

Figure 10 summarizes the estimated peak widths, W, for all the best-fit peaks. Note that those P_0 peaks that overlap with the P_1 group are labeled with a composite symbol composed of a "0" and an overstruck "1." Most of the P_0, P_1, and P_2 peaks appear to have been derived from single-age FT source terrains, as indicated by W values that plot close to the dashed reference line ($W \approx 16.3$ percent). W values for the P_3 peaks show a much larger range (14–33 percent), suggesting that most of these peaks were derived from composite FT source terrains.

The feature we consider to be most important about the P_1, P_2, and P_3 peaks is that peak ages within each group do not appear to vary as a function of depositional age. In figure 11, the age of each of the older peaks is plotted as a function of the χ^2 age of the sample, which is assumed to be a reasonable proxy for depositional age. Note that the P_1 group

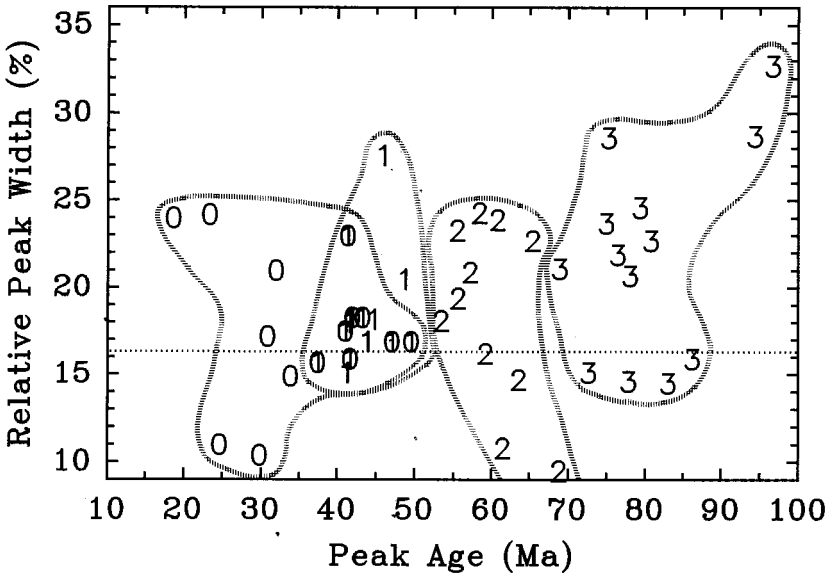

Fig. 10. Peak width as a function of peak age for the best-fit peaks identified in the unreset OSC and Eocene basin samples (tables 3–5). Peak width corresponds to the relative standard deviation of the best-fit peak. The horizontal dashed line marks the approximate relative peak width for a population of zircons derived from a single-age source ($W \approx 16.5$ percent). The broken lines outline the various groups of peaks ages, P_0, P_1, P_2, and P_3. In those cases where an "older" P_0 peak overlaps in age with the group of P_1 peaks, the peak age is plotted using a "0" and an overstruck "1" (see text for details). Note that P_0, P_1, and P_2 peaks commonly have widths similar to that expected for a single-age source, whereas P_3 peaks are much more variable in width suggesting a composite source.

includes those "older" P_0 peaks (labeled with a "0") that overlap with the P_1 group. Within each group, the peak ages vary significantly around the average age for their group; however, there is no indication that the older peak ages are correlated with their χ^2 ages. To illustrate this point, we have fit regression lines to peak ages in each of the P_1, P_2, and P_3 groups. The lines, which are shown in figure 11, were determined by weighted least squares using peak age as the dependent variable and χ^2 age as the dependent variable. The slopes of the regression lines are nearly horizontal. Over the 32 my range of observed χ^2 ages (51–19 Ma), systematic changes in peak age within each of the groups of older peaks were calculated to be ≤ 1.5 my.

This result suggests that the ages of the FT source terrains from which the older peaks were derived did not vary significantly with time. As a further test of this interpretation, we have collected all the P_1, P_2, and P_3 peaks from tables 3 to 5 into an OSC group and an Eocene basin group and then constructed two synoptic plots (fig. 12) representing the composite probability density distributions for these two groups of old peaks. The plots were constructed in the usual way (eqs 1, 2 in Brandon, this

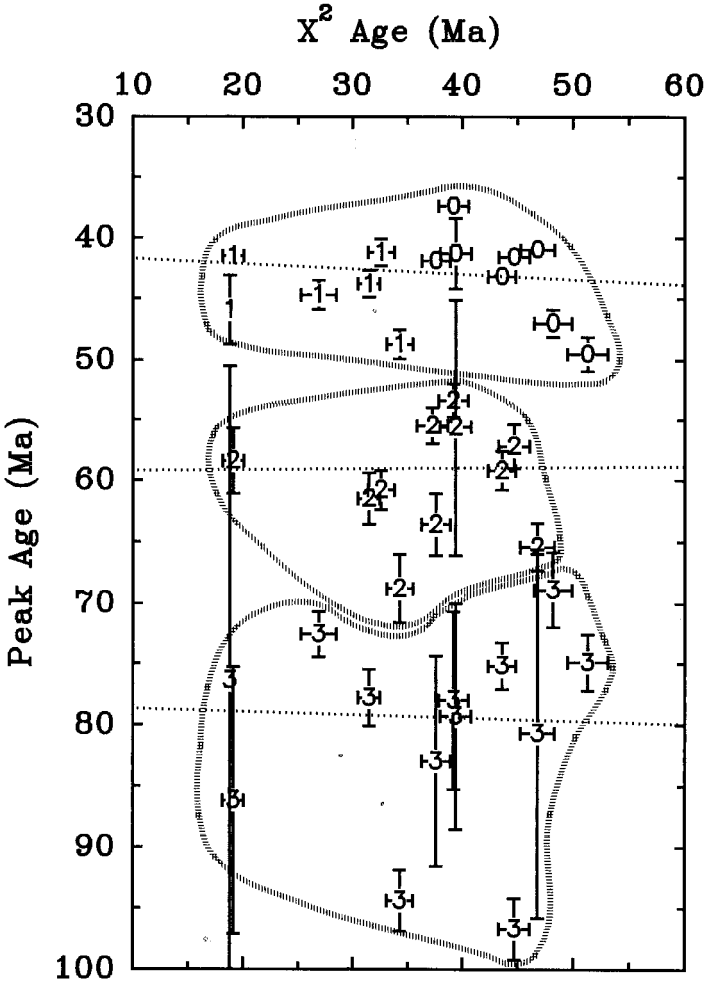

Fig. 11. Ages of the older peaks (P_1, P_2, and P_3) as a function of their χ^2 age, used here as a proxy for depositional age. The objective is to see if ages of the older peaks vary systematically as a function of depositional age. The broken lines outline the various groups of peak ages, P_1, P_2, and P_3. Note that the P_1 group includes those "older" P_0 peaks that overlap with this group (see text for details). The error bars indicate uncertainties for the peak age and the χ^2 age (± 1 standard error). The dashed lines represent regression lines fit to each of the three groups of peak ages with χ^2 age as the independent variable and peak age as the dependent variable. The fact that these lines are nearly horizontal indicates that the peak ages within each group do not vary significantly as a function of depositional age over the time span represented by our samples (19 to 51 Ma).

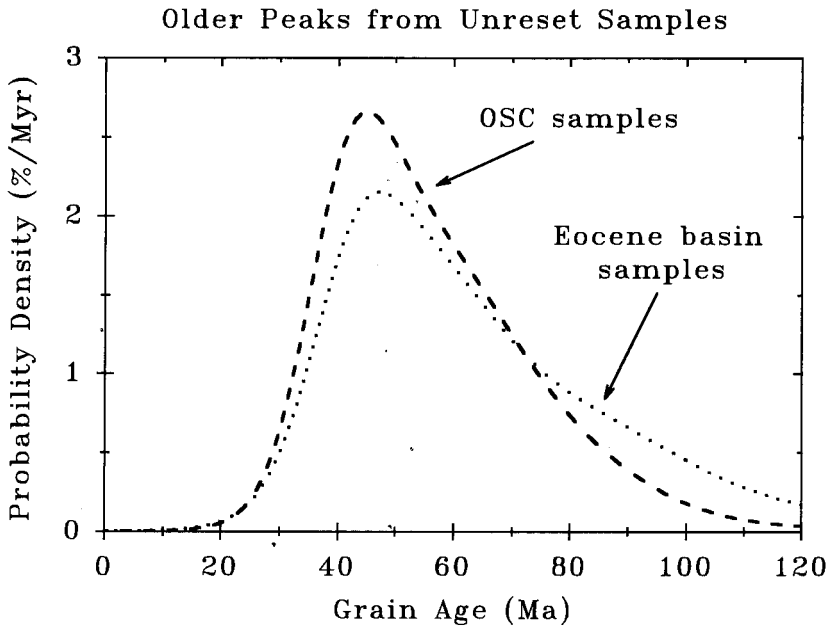

Fig. 12. Synoptic composite probability density plots representing all the older peaks found in the unreset OSC samples and the Eocene basin samples. The plots were constructed using the Gaussian parameters for the best-fit P_1, P_2, and P_3 peaks, as identified in tables 3 through 5 (see text for further details). The synoptic plots show that the OSC samples and the Eocene basin samples contain a similar set of older peaks. These plots were decomposed using the peak-fitting method in order to determine average ages for the P_1, P_2, and P_3 peaks. See table 6 for those results.

issue) except that the Gaussian parameters for each peak (μ_f, W_f, N_f) were substituted for the age and standard error of each grain (μ_i, s_i). The best-fit Gaussian peaks are considered to be useful proxies for the grain-age populations that make up the peaks. In this way, we are able to separate the P_1, P_2, and P_3 peaks from other peaks in their respective sample grain-age distributions and then recombine them to form a synoptic plot that represents the composite probability density distribution for all the older peaks identified in a group of related samples. In figure 12, these plots have been normalized to 100 percent to account for differences in the number of grain ages in the two groups.

As can be seen (fig. 12), there is little difference in the "older peaks" distributions for the OSC and Eocene basin groups. Furthermore, the Gaussian peak-fitting method yields a similar set of peak ages for both distributions (table 6). This result is remarkable, especially in light of the fact that OSC samples are on the average about 10 my younger than the Eocene basin samples. Table 6 also includes a set of best-fit peaks for a distribution where all the older peaks from both groups are combined.

TABLE 6

Best-fit peaks for composite probability density plots of all identified older peaks

Sample group	Best-fit peaks		
	(~43 Ma)	(~57 Ma)	(~74 Ma)
A. Unreset Olympic samples 11 samples, N_t = 394 grains	42.4 ± 2.0 Ma N_f/N_t = 31% W = 17.5%	56.1 ± 7.3 Ma N_f/N_t = 39% W = 22.4%	69.7 ± 18 Ma N_f/N_t = 30% W = 28.8%
B. Unreset Eocene basin samples 4 samples, N_t = 209 grains	43.3 ± 2.6 Ma N_f/N_t = 20% W = 17.0%	55.3 ± 23 Ma N_f/N_t = 30% W = 21.8%	73.8 ± 20 Ma N_f/N_t = 50% W = 35.8%
C. All unreset samples 15 samples, N_t = 603 grains	42.9 ± 2.1 Ma N_f/N_t = 29% W = 17.8%	56.9 ± 7.6 Ma N_f/N_t = 40% W = 23.1%	74.0 ± 19 Ma N_f/N_t = 31% W = 31.2%

Notes: N_t = total number of grains. N_f = estimated number of grains in a specific peak or fraction. All uncertainties are cited at ±2 standard error and include group error. W = estimated relative standard deviation for a peak, expressed in percentage of the peak age.

This result is considered to be the best estimate of the average ages of the P_1, P_2, and P_3 peaks, which are 42.9 ± 2.1 Ma, 56.9 ± 7.6 Ma, and 74.0 ± 19 Ma, respectively (±95 percent uncertainty). The reference lines and error limits shown in figure 6 are based on these estimates. It is important to note that the average peak ages shown in table 6 are analogous to weighted averages of the original peak ages (tables 3–5), where each peak is weighted relative to the number of grain ages it contains. This explains why some of the reference lines shown in figure 6 do not bisect their respective group of peak ages.

Summary.—These comparisons indicate that the P_1, P_2, and P_3 peaks are persistent features of our unreset grain-age distributions. Furthermore, they are present in both our OSC samples and also in our Eocene basin samples, which suggest that sediments in these two areas were derived from a common source region. Another interesting feature of the older peaks is that they appear to remain fairly constant in age, regardless of the depositional age of the sample. We refer to this kind of peak as a *static peak*. Apparently, the FT source terrains that supplied zircons for these peaks did not evolve significantly over the time interval represented by our samples, Middle Eocene through Early Miocene. In contrast, a *moving peak* refers to a grain-age population that changes with depositional age of the sample. A moving peak indicates that the FT source terrain did evolve significantly with time. In our study, the younger P_0 peaks are examples of moving peaks.

There is an apparent conflict in our interpretation as it pertains to the "older" P_0 peaks, that is, those that overlap with and are included in the P_1 group (labeled "0" in fig. 11). In the present section, we suggest that the peak ages in the P_1 group do not vary with depositional age,

whereas in the previous section, we argued that the P_0 peaks, including the older P_0 peaks, track the depositional age of the sediment. In one case, it may seem that we are arguing that the older P_0 peaks are static peaks, whereas in the other case we conclude that they are moving peaks. Our explanation for this apparent conflict is that the older P_0 peaks are from samples that were probably being deposited at the time that the FT source terrain for the P_1 group was being formed. We infer that this source terrain experienced a rapid cooling event at about 43 Ma resulting in an upper crustal section with a common zircon FT age. Thus, while this FT source terrain was forming, we might expect that zircons derived from it would show a progressively decreasing FT age. The source terrain would become truly static only after the cooling event was completed.

Reset OSC Samples

The four reset samples (table 7) are from the central part of the OSC (fig. 5) and coincide with the area of highest metamorphic grade (Brandon and Calderwood, 1990). These samples differ markedly from the unreset samples in that their grain ages are relatively young (6–36 Ma), and their grain age distributions span a fairly narrow age range (13–27 my). Furthermore, their composite probability density plots show a single narrow peak (fig. 13), rather than the broad polymodal distributions that characterize the unreset samples.

The interpretation of these data, however, in terms of specific cooling ages is difficult because all the samples fail the χ^2 test, indicating that, in addition to the radioactive decay process, there are other sources of variability affecting the grain ages in each distribution. Experiments,

TABLE 7

Zircon FT results for reset samples from the Olympic subduction complex

Lab#	Geologic unit, location	Age range, number of grains	Mean age	χ^2 Age	Best-fit peaks	
					Young peak	Old peak
ZR17)	Western Olympic Assemblage, Humes Glacier	10 - 36 Ma N_t = 50	19.1 ± 2.2 Ma	14.4 ± 1.0 Ma N_f = 32	14.3 ± 0.7 Ma N_f = 28 W = 21%	25.1 ± 1.7 Ma N_f = 22 W = 29%
ZR9)	Western Olympic Assemblage, Queets Glacier	6 - 33 Ma N_t = 50	17.1 ± 1.7 Ma	10.3 ± 1.0 Ma N_f = 9	14.4 ± 0.6 Ma N_f = 27 W = 24%	20.1 ± 1.2 Ma N_f = 23 W = 33%
ZR46)	Grand Valley Assemblage, W of Hayden Pass	10 - 23 Ma N_t = 20	14.9 ± 1.6 Ma	13.7 ± 1.0 Ma N_f = 16	13.1 ± 0.8 Ma N_f = 10 W = 19%	16.9 ± 3.9 Ma N_f = 10 W = 22%
ZR48)	Elwha Assemblage, Mount Fromme	12 - 26 Ma N_t = 50	17.1 ± 1.3 Ma	15.4 ± 0.9 Ma N_f = 36	14.5 ± 0.7 Ma N_f = 21 W = 15%	19.0 ± 1.2 Ma N_f = 29 W = 20%

Notes: N_t = total number of grains analyzed. N_f = estimated number of grains in a specific peak or fraction. All uncertainties are cited at ±2 standard error and include group error. W = estimated relative standard deviation for a peak, expressed in percentage of the peak age.

both in the laboratory (Tagami, Ito, and Nishimura, 1990) and under well controlled natural conditions (Green and others, 1989), have shown that FT data from partially annealed apatites and zircons commonly do not pass the χ^2 test. This result might be anticipated for a detrital population, because the population would have had an initially wide variation in FT grain ages, prior to annealing. However, Tagami, Ito, and Nishimura (1990) found the same result in their experiments where they partially annealed single-age populations of volcanic zircons that prior to annealing had passed the χ^2 test. Their experiments indicate that the rate of annealing and the associated reduction of apparent FT ages vary from grain to grain within a population that otherwise started with a common FT age.

We propose that the incoherent behavior of zircons during annealing, as indicated by low χ^2 probabilities, is mainly related to grain-to-grain variations in the amount of α-radiation damage. The experimental work of Kasuya and Naeser (1988) indicates that fission tracks in natural zircons have a much lower thermal stability than those in laboratory-annealed zircon, with the controlling factor being the presence of α-damage in the natural zircons. The physical and chemical properties of zircon are strongly affected by accumulated α-damage, with metamict zircons as an end result. This damage can be annealed by heating. Tagami, Ito, and Nishimura (1990) show that the zone of partial stability for α-damage overlaps with the low temperature side of the zone of partial stability for fission tracks. In the study of Kasuya and Naeser (1988), only the laboratory-annealed zircons exhibited unusual annealing properties. There was no detectable difference in annealing behavior among the natural zircons, despite the fact that they varied considerably in FT age (15–75 Ma) and average uranium content (100–250 ppm) (FT ages and uranium contents were estimated from data in Kasuya and Naeser, 1988). Apparently, the annealing behavior of zircon is transformed after the accumulation of a specific density of α-damage. Judging from Kasuya and Naeser (1988), this transformation is completed in a time scale of less than 15 my even for zircons with relatively low uranium content (their 15 Ma zircons had U $\approx$ 100 ppm).

Composition is another factor that can affect fission track annealing, as has been demonstrated for apatite and olivine (Green and others, 1985; James and Durrani, 1986). However, for zircon, composition is probably not an important factor because, relative to apatite and olivine, zircon has a more restricted compositional range. The main solid solution is the substitution of Hf for Zr; the amount of substitution is fairly limited in most natural zircons (Hf/Zr ratio $\approx$ 0.02 – 0.04; Deer, Howie, and Zussman, 1982). To our knowledge, there have been no studies of the annealing behavior of zircon as a function of composition. Krishnaswami, Lal, and Prabhu (1974) have shown that the etching properties of zircon are not significantly affected by Hf/Zr variations.

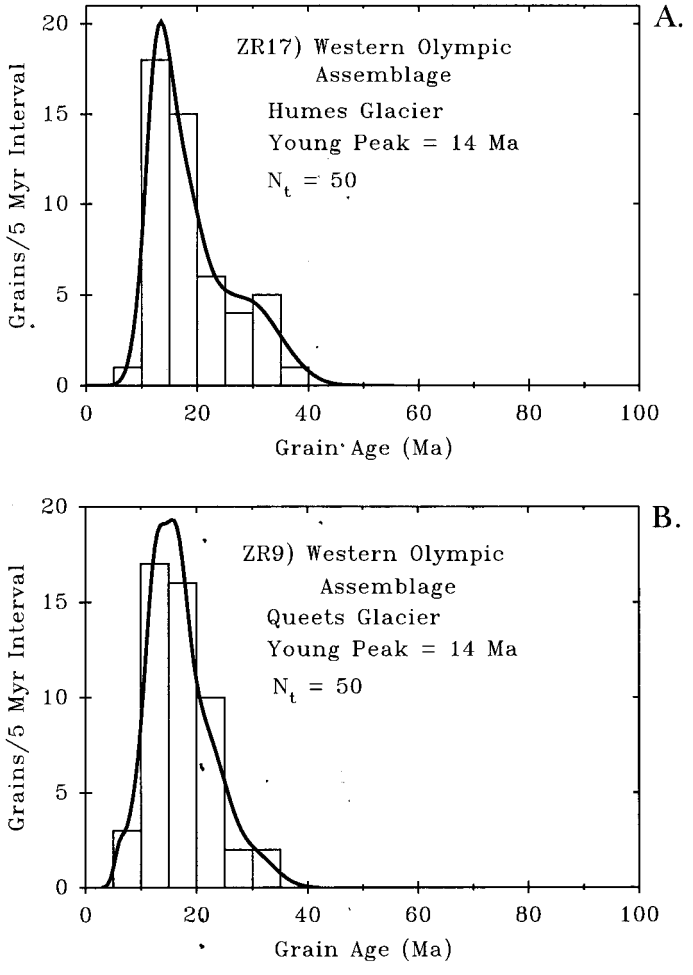

Fig. 13 (A–D) Composite probability density plots and grain-age histograms for reset samples from the OSC. Results are summarized in table 7. Note that the density plot and histogram are plotted using the same vertical scale with units of "number of grains per 5 my interval."

In light of these problems, how do we assign cooling ages to the reset samples? Green (1981) suggests that the mean age should be used for samples that fail the χ^2 test. This approach requires that there are no systematic biases among the grain ages, which does not appear to be the case for our reset samples. Our approach is to assume that the youngest FT grain ages in our reset samples are associated with the most completely annealed zircons, in which case the age of the youngest best-fit peak should provide a good estimate of the cooling age. Seward and

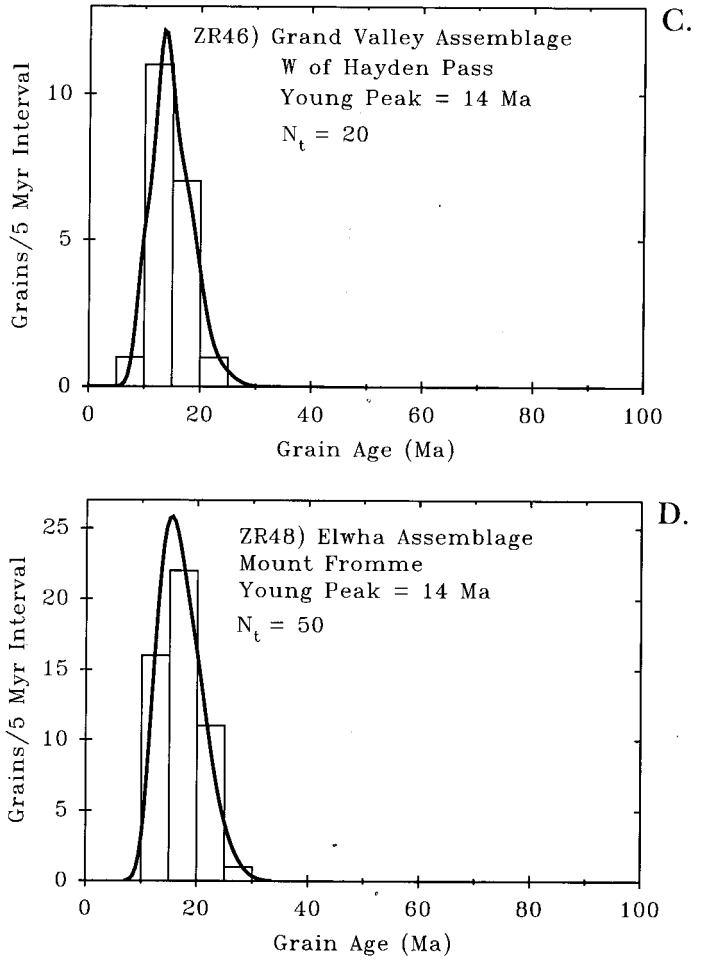

Fig. 13 (continued)

Rhoades (1986) use a similar argument for interpreting partially reset zircon FT ages from the Alpine fault of New Zealand. The youngest peak ages for our reset samples are tightly clustered about an average of 14 Ma (table 7), which we accept as the cooling age for these samples (fig. 5).

The χ^2 age might also provide a suitable estimate of the cooling age. But we prefer the peak-fitting method for reset samples because it lacks the old-side bias that is built into the χ^2 age method. Note that for 3 out of 4 of the reset samples, there is little difference in the ages determined by these two methods.

In our analysis using the peak-fitting method, we found that a two-peak model consistently produced the best fit (table 7), which implies

that, prior to resetting, the zircons were probably divided into two groups on the basis of their annealing properties. We suggest a possible explanation for this observation. If α-damage is the main factor influencing annealing behavior in zircon, then the results of Kasuya and Naeser (1988) suggest that during annealing of a detrital FT grain-age distribution, fission tracks in the youngest fraction of grains should have the greatest thermal stability and those in the older α-damaged fraction should have the lowest thermal stability. We propose that the older peak in our reset samples corresponds to the youngest zircon population in the original unreset distribution and the younger, more completely annealed peak corresponds to the older α-damaged grains in the original distribution.

At this point, we need to estimate the closure temperature for the reset samples. The closure temperature equation of Dodson (1979) as applied to the zircon FT system (table 2) assumes a population of zircons that was initially completely annealed at temperatures above $Tz_{90\%}$ (table 1) and then cooled through the FT partial stability zone at an approximately steady cooling rate. For our reset samples, we assume that the zircons associated with the youngest peaks were completely annealed prior to cooling. Geologic evidence suggests that the central part of the OSC was exhumed in a relatively simple and steady fashion (Brandon and Calderwood, 1990), so that a steady cooling rate should provide a reasonable approximation. The cooling rate must be specified in order to calculate the closure temperature. We use the average cooling rate after closure to approximate the cooling rate during closure, as specified by the following relationship,

$$\frac{dT}{dt} \approx \frac{Tz_c - T_s}{\Delta t}, \tag{1}$$

where Tz_c is the closure temperature, T_s is the average surface temperature, and Δt is time interval between closure at Tz_c and exposure at the surface. Δt is set equal to 14.1 Ma, the average zircon FT cooling age. T_s is approximated as 8°C, which is the present average annual temperature for the Olympics and surrounding shallow marine environments (Kincer, 1941, p. 690, 1170–1171; Lewis and others, 1988, p. 15214, 15222). Dodson's equation (see footnote in table 2) and eq (1) are solved simultaneously to find the two unknowns, Tz_c and dT/dt. The result is a cooling rate of 16.5°C/my and a closure temperature of 239°C.

Partial Resetting of the Unreset Samples

At this point, we examine a fundamental assumption of our study, that our unreset samples are not partially reset. Partial resetting reduces all ages in a grain-age spectrum. If undetected, a sample might be assigned an anomalously young depositional age. Three lines of evidence indicate that significant partial resetting has not occurred.

The first is the fact that the etch times for our unreset samples were significantly shorter than those for our reset samples, indicating that the unreset zircons possess, on the average, a greater density of α-damage (Krishnaswami, Lal, and Prabhu, 1974; Gleadow, 1981; Tagami, Ito, Nishimura, 1990). Our interpretation is that the unreset detrital zircons still retain α-damage that formed prior to deposition of the zircons. In other words, the unreset samples did not see metamorphic temperatures high enough to anneal the older α-damage. Fission tracks have greater thermal stability than α-damage (Tagami, Ito, and Nishimura, 1990). Therefore, we conclude that the older fission tracks in the unreset zircons have not been affected by partial resetting.

The second line of evidence is based on the P_1, P_2, and P_3 peaks. If these peaks are static peaks, as argued above, then they can be viewed as internal standards with known initial FT ages. The presence of the same older peaks in both the unreset OSC samples and in the unmetamorphosed Eocene basin sandstones indicates that the unreset OSC zircons have not suffered any significant partial resetting. If partial resetting had occurred, then we would expect to see a reduction in the ages of these peaks, as well as the ages of the P_0 peaks. A simple description of partial resetting is the *proportional model* where spontaneous track density is reduced by the same proportional amount for all zircons. In this case, each grain age would be shifted by an amount proportional to its FT age at the time of resetting. For example, consider a sample grain-age distribution composed of two component populations that would have present-day peak ages of P_0 = 19 Ma and P_1 = 43 Ma if the distribution had remained unreset. This sample is subjected to a thermal event at 15 Ma that causes 20 percent annealing in accord with the proportional model. The P_0 peak takes on a present-day age of 18.2 Ma, which is a 0.8 my shift from its expected unreset age of 19 Ma. The P_1 peak takes on a present-day age of 37.4 Ma, which is a 5.6 my shift from its expected unreset age of 43 Ma. This example shows that, if the proportional model is correct, the older peaks are much more sensitive to the effects of partial resetting. Given the precision of our peak-fitting method, we should be able to detect cases where the older peaks were reduced in age by more than about 10 percent. For one of our unreset samples, a 10 percent shift in the final FT ages of older peaks due to partial resetting would translate into an even smaller reduction (<2–5 percent) in the final FT age of the youngest grain-age population.

The third line of evidence stems from the study of Kasuya and Naeser (1988), which is reviewed at length in the previous section. Their annealing experiments indicate that the proportional model does not provide a valid description of the annealing process until all zircons have accumulated sufficient α-damage to transform their annealing properties to a common "natural" state. In other words, fission tracks in the youngest zircons in a grain-age distribution will enjoy a greater thermal stability during the first several million years after closure of their FT systems. For our reset samples, this phenomenon works in our favor

because it increases the relative sensitivity of the older peaks to partial resetting.

SOURCES FOR THE DETRITAL ZIRCONS

A viable FT source terrain for the detrital zircons in our unreset samples must meet three requirements. First, the source terrain must be able to provide a sufficient supply of zircons. Second, the area surrounding the source terrain must be able to supply detritus consistent with the overall composition of the dated sandstone. Third, the terrain must have a cooling history that is compatible with the FT ages of the zircons derived from it.

Petrologic Characteristics of the Source Region

Zircon occurs most commonly as an accessory mineral in intermediate and silicic igneous rock. It is stable over a wide range of metamorphic conditions and is resistant to abrasion and weathering in the sedimentary environment. Therefore, rock units that might serve as a significant source of detrital zircon include intermediate and silicic plutonic and volcanic rocks and their metamorphic and sedimentary derivatives. The FT method introduces some unavoidable biases as to the types of zircons that are dated. In order to ensure that a significant fraction of grains will be countable and correctly oriented, we generally select only those zircons that are clear and relatively free of cracks and retain a euhedral prismatic form. As a result, our FT grain-age distributions are biased toward first-cycle zircons from young plutonic and meta-plutonic source terrains. Older zircons, which are commonly cracked, abraded, or opaque and mostly uncountable, are therefore underrepresented.

Examination of thin sections and heavy mineral suites indicates that all our sandstone samples contain a prominent plutonic/metamorphic component and a subordinate volcanic component. Detrital phases that are diagnostic of the plutonic/metamorphic component include microcline, perthite, polycrystalline quartz, biotite, muscovite, and minor garnet. Petrologic data in Heller and others (1992) indicate that sandstones from the OSC generally have a subquartzose lithofeldspathic composition. Our Eocene basin samples appear to have a similar composition (Puget Group in Heller and others, 1992) but in some cases may be somewhat more feldspathic than the OSC sandstones.

Many of the sandstones in the OSC, and also those of the Eocene basin units to the east of the OSC, contain detrital muscovite. Heller and others (1992) have studied the chemical and isotopic composition of these muscovites and have shown that they were derived from a high-grade metamorphic source that had a high initial $^{87}Sr/^{86}Sr$ ratio > 0.710 and an average K–Ar age of ~68 Ma. Heller and others (1992) argue that these sandstones were probably derived from more radiogenic source terrains lying in the eastern part of the Cordillera. Armstrong, Taubeneck, and Hales (1977), Armstrong (1988), and many others have shown that the initial $^{87}Sr/^{86}Sr$ ratio for igneous rocks increases systematically to

the east across the Cordillera of northwestern United States and western Canada, coincident with the transition from oceanic and juvenile continental rocks to the west and older, more radiogenic continental craton to the east. This transition is usually represented by a $^{87}Sr/^{86}Sr$ line (fig. 14) which corresponds to a specific isopleth with a "transitional" initial $^{87}Sr/^{86}Sr$ value. In the western United States, the $^{87}Sr/^{86}Sr$ line is usually drawn at the 0.706 isopleth (Armstrong, Taubeneck, and Hales, 1977; Carlson and others, 1991), whereas in western Canada, Armstrong (1988) has used the 0.707 isopleth.

The above observations indicate that the source region for our unreset sandstones was dominated by intermediate to silicic plutonic and/or meta-plutonic rocks with subordinate volcanic rocks. Muscovite-bearing metamorphic rocks with high initial $^{87}Sr/^{86}Sr$ were also present, at least locally. The K-Ar ages of the muscovite (Heller and others, 1992) and the FT peak ages for detrital zircons from our unreset sandstones indicate that the source terrains for these detrital components were unroofed and cooled during the latest Cretaceous and early Cenozoic.

FT Source Terrains and Peak Ages

Our FT peak ages provide further information about the source region. The task of matching a peak age with a specific FT source terrain is complicated by the fact that a source terrain is, by definition, an area of active erosion. The actual rocks that supplied the sediment for our sandstone samples no longer exist, as they have long since been eroded away. Furthermore, the FT age of the source terrain can be modified by younger processes, such as deep erosion, tectonic denudation, or magmatic activity. The only thing certain is that the present-day age of a FT source terrain must be equal to or younger than the FT peak age of a population of detrital zircons derived from that terrain in the past. In some situations, it might be possible to deduce how the age of a FT source terrain has evolved with time. One approach is to use geologic observations and isotopic data from present-day outcrops of the source terrain to extrapolate back in time. The other approach is to date detrital zircons from sedimentary units of different ages that can be shown to have been derived from the same source terrain. The resulting FT grain-age distributions can then be used to determine how the source terrain has evolved through time. Both approaches are used in our analysis here.

The way that a FT source terrain evolves with time is clearly related to its local tectonic setting. We identify three idealized cases that serve to illustrate this relationship.

1. Steady uplift and erosion.—In this case, a FT source terrain is eroded at a steady rate so that the cooling age of rocks at the surface becomes progressively younger with time. Examples include active collision belts such as Taiwan and the Himalayas (Liu, 1982, 1988; Cerveny and others, 1988). FT dating of detrital zircons eroded from this type of terrain would show a *moving peak* that would lag closely behind the depositional age of the sediments. The lag time between peak age and

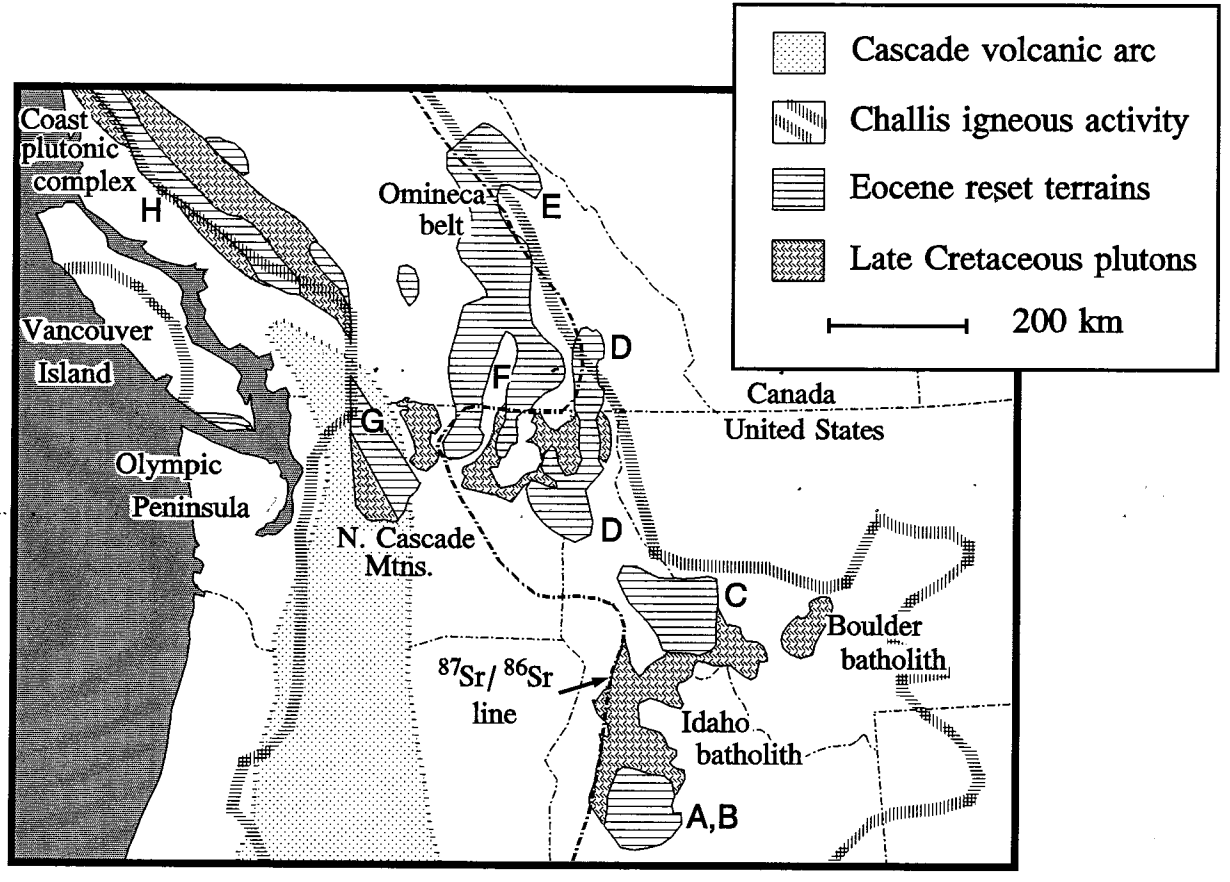

Fig. 14. Map showing potential source terrains for zircon populations found in the unreset samples. Letters (A) through (H) mark areas that are summarized in table 8. The Challis volcanic province (outlined by heavy broken lines) occupies a large area extending from British Columbia, eastern Washington, Idaho, Montana, and eastern Oregon and may include a smaller separate area on the west side of Vancouver Island. The $^{87}Sr/^{86}Sr$ line corresponds to a designated isopleth with a "transitional" initial $^{87}Sr/^{86}Sr$ value. The 0.706 isopleth is used in western United States, and the 0.707 isopleth is used in western Canada (see text for further details).

depositional age would be a function of the thermal gradient and the erosion rate. Present-day outcrops of the source terrain would be characterized by relatively young low-temperature isotopic ages (K-Ar biotite, and FT for zircon, sphene, and apatite). In particular, zircon FT ages for present-day outcrops would be significantly younger than the associated peak age for the sandstone. There is no evidence that a source terrain of this type was present in the Pacific Northwest at the time of deposition of our samples (Eocene to Miocene).

2. *Prolonged volcanic activity.*—Persistent intermediate or silicic volcanism, such as might be associated with an active volcanic arc, would introduce progressively younger zircons into the depositional system. Most of the transported sediment in this setting would probably be eroded from constructional volcanic forms associated with active volcanic vents because local topographic relief would be greatest in those areas. Silicic pyroclastic material erupted during explosive volcanic events might represent another sedimentary component. This type of source terrain would produce a *moving peak.* If most of the detrital zircons were derived from the youngest and most volcanically active part of the source terrain, then their FT grain ages might approximate a single-age population, as indicated by a peak with a narrow width. Furthermore, the age of that peak might be only slightly older than the depositional age of the sandstone. A local example of this type of source is the modern Cascade arc.

3. *Punctuated thermal event.*—In this case, a hot source terrain is rapidly cooled and then slowly eroded. Examples include tectonic denudation by extensional faulting, emplacement of a shallow-level pluton or dike swarm, widespread hydrothermal metamorphism, or eruption of a large volume of volcanic rock during a short-lived volcanic event. The expectation here is that a significant thickness of the upper crust would cool through the zircon FT closure temperature within a short time interval. Subsequent erosion of this "quenched" upper crust would yield detrital zircons with a narrow range of FT ages. This type of source terrain would produce a *static peak,* in that the peak age would not vary significantly with the depositional age of the sandstone. Present-day outcrops of the source terrain might still preserve evidence of rapid cooling at the time of the FT peak age. Local examples of this type of source terrain would include the Eocene reset terrains of Armstrong (1988) and Armstrong and Ward (1991) and the short-lived Challis volcanic province (Armstrong and Ward, 1991).

Potential FT Source Terrains

We have identified four distinctive zircon populations in our unreset sandstone samples. One of these populations corresponds to a young moving peak P_0 with a peak age ranging from 34 to 19 Ma. The remaining three correspond to our static peaks, with estimated average ages and associated 95 percent confidence intervals of P_1 = 43 Ma (41–45 Ma), P_2 = 57 Ma (49–64 Ma), and P_3 = 74 Ma (35–93 Ma) (result C in

table 6). In most cases, the peaks are relatively narrow (fig. 10), which suggests that they were derived from single-age sources. The P_3 peaks are an exception; they have a wide range of widths, 14 to 33 percent, suggesting a composite source terrain.

To facilitate our search for the sources of these zircon populations, we have compiled a map of potential FT source terrains (fig. 14). The general characteristics of some of these terrains are listed in table 8. The map highlights general geologic units that are considered to contain sufficient zircon to have served as a source and are known to have cooled through the zircon FT closure temperature (~240°C) sometime during the Late Cretaceous to Oligocene, coincident with the range of our peak ages (~100 to 19 Ma). We exclude Mesozoic and Paleozoic eugeoclinal rocks which comprise much of the accreted terranes within western British Columbia, western Washington, Oregon, and northern California. Locally, these terranes do include plutonic rocks, but isotopic ages and local geology (Armstrong, Taubeneck, and Hales, 1977; Heller and others, 1985; Armstrong, 1988; Renne, Becker, and Swapp, 1990) indicate that zircons from these rocks should have FT ages older than 100 Ma. The map (fig. 14) is restricted to areas west of the Rocky Mountains because this range of mountains has probably acted as a major continental drainage divide throughout the Cenozoic.

The potential source terrains shown in figure 14 can be categorized into 4 groups. The first group corresponds to the Cascade volcanic arc which has been active from ~36 Ma to present (table 8). Specific source rocks within this terrain include volcanic flows, pyroclastic deposits, epizonal plutons, and reset wall rocks. Granitic stocks and batholiths with ages between 35 to 3 Ma are widely exposed at the north end of the Cascade arc (Tabor and others, 1989, p. 17; Smith, 1989). The Cascade arc represents the only obvious source for the young moving peaks (34-19 Ma) in our samples. The narrow width of these peaks indicates a single-age source. Thus, we infer that most of the detrital zircons from this source were derived from the youngest and most volcanically active parts of the terrain.

The second group corresponds to the Challis volcanic event, which was a short-lived igneous event mostly focused during the interval 52 and 42 Ma (table 8). The event was characterized by voluminous, widespread volcanism and subordinate epizonal intrusions (Armstrong, 1979, 1988; Ewing, 1980). Volcanism was mainly concentrated in a 250 to 800 km-wide belt that extended from northwestern Canada to Oregon, Idaho, and Wyoming (area outlined by the heavy broken lines in fig. 14). Challis-age volcanism and plutonism have also been recognized on the western side of Vancouver Island (50 Ma Flores volcanics; Irving and Brandon, 1990). The age of the youngest parts of the Challis belt overlaps with the average age of our P_1 peak and may represent the source of that zircon population, a possibility that is considered in more detail below.

TABLE 8

Characteristics of some potential FT source terrains

Name and location*	Estimated zircon FT age of present-day outcrops†	Muscovite present?	Initial $^{87}Sr/^{86}Sr$	References
CENOZOIC VOLCANIC FIELDS				
Cascade volcanic arc	36 - 0 Ma	no	low	[2,3]
Challis volcanic province	52 - 42 Ma	no	variable	[1,3]
EOCENE RESET TERRAINS				
A. Epizonal plutons and reset wall rocks, S Idaho batholith	mean = 41 Ma (35 - 46 Ma, N_z = 6)	minor	high	[4]
B. Older reset rocks, S Idaho batholith	mean = 66 Ma (53 - 82 Ma, N_z = 8)	yes	high	[4]
C. Bitterroot lobe, N Idaho batholith	mean = 50 Ma (42 - 55 Ma, N_z = 15)	yes	high	[5]
D. Priest River metamorphic core complex, WA, ID, and BC	~45 Ma	yes	high	[6,7]
E. N Monashee Mtns., NE Omineca belt, BC	~48 Ma	yes	high	[8]
F. Okanagan and Kettle metamorphic core complexes, WA and BC	~49 Ma	minor	transitional	[9,7]
G. Chelan block, North Cascade Mtns., WA	mean = 44 Ma (36 - 57 Ma, N_z = 15)	yes	low	[10,3]
H. Coast Plutonic Complex, BC	mean = 51 Ma (19 - 100 Ma, N_z = 43)	rare	low	[11]

* Reference letters for the Eocene reset terrains are used to show their locations in figure 14.

† When available, zircon FT ages for the Eocene reset terranes are summarized by a mean age, the range of ages, and the number of age determinations (N_z). In the remaining cases, we have approximated the expected zircon FT age using K-Ar biotite and apatite FT ages. References: *Muscovite present:* Miller and Bradfish, 1980; Hyndman, 1983; plus other references cited below. *Initial $^{87}Sr/^{86}Sr$:* Armstrong, 1988; Carlson and others, 1991. *Isotopic ages and local geology:* [1] Armstrong, 1979; Ewing, 1980; Irving and Brandon, 1990; Armstrong and Ward, 1992. [2] Robinson, Brem, and McKee, 1984; Vance, Walker, and Mattinson, 1986; Smith, 1989; Sherrod and Smith, 1989; Priest, 1990. [3] J.A. Vance, unpublished isotopic ages. [4] Criss, Lanphere, and Taylor, 1982; Sweetkind and Blackwell, 1989; Lewis and Kiilsgaard, 1991. [5] Chase, Bickford, and Tripp, 1978; Desmarais, 1983. [6] Miller and Engels, 1975. [7] Parrish, Carr, and Parkinson, 1988. [8] Sevigny, Parrish, and Ghent, 1989; Sevigny and others, 1990. [9] Medford, 1975; Fox and others, 1976. [10] Tabor and others, 1987, 1989; Babcock and Misch, 1988; Miller and Bowring, 1990; Haugerud and others, 1991. [11] Parrish, 1983; Armstrong, 1988.

The third group consists of the "Eocene reset terrains" which, as defined in the literature (Miller and Engels, 1975; Armstrong, Taubeneck, and Hales, 1977; Ewing, 1980; Criss, Lanphere, and Taylor, 1982; Parrish, Carr, and Parkinson, 1988; Armstrong, 1988; Armstrong and Ward, 1991), correspond to large areas in the Pacific Northwest where rocks of all ages were isotopically reset and cooled during the Eocene. These areas are distinguished by pervasive resetting of K-Ar biotite ages to the interval 60 to 35 Ma. Resetting appears to have been caused by a variety of processes, including early Tertiary plutonism, hydrothermal metamorphism, and extensional faulting (Ewing, 1980; Criss, Lanphere, and Taylor, 1982; Parrish, Carr, and Parkinson, 1988; Armstrong, 1988; Armstrong and Ward, 1991). In most cases, the reset terrains are dominated by plutonic rocks and show evidence of rapid cooling, which makes them prime candidates for our Eocene static peaks, P_1 and P_2 at 43 and 57 Ma, respectively. At least one of the Eocene reset terrains, the Coast Plutonic Complex (H in table 8 and fig. 14), appears to have evolved in a more protracted fashion. Extensive FT dating by Parrish (1983) indicates that this terrain was unroofed and/or cooled slowly during the early Tertiary and thus is an unlikely source for our static peaks.

The fourth group corresponds to unreset Late Cretaceous plutonic rocks which are ubiquitous in this part of the Cordillera (Armstrong, Taubeneck, and Hales, 1977; Armstrong, 1988). We suspect that these rocks might have provided the detrital zircons that make up the P_3 peak. In the Canadian segment of the Cordillera, Armstrong (1988) identified a period of Cretaceous magmatism, extending from about 120 to 70 Ma, which is preceded and followed by well defined magmatic lulls. Intruded late during this interval in a belt along the eastern side of the Cordillera (east of the $^{87}Sr/^{86}Sr$ line in fig. 14) are a series of muscovite-bearing plutons with high initial $^{87}Sr/^{86}Sr$ values (Miller and Bradfish, 1980; Armstrong, 1988). These plutons and their metamorphic equivalents might have provided the detrital muscovite found in the OSC sandstones. The average K-Ar age of these muscovites ($\sim$68 Ma, Heller and others, 1992) is somewhat younger than the Late Cretaceous igneous age of the source, thus allowing time for metamorphism, cooling, and uplift of the source. In their interpretation, Heller and others (1992) emphasized some specific peraluminous granites (E in fig. 14) which lie at the northern end of the belt of eastern Cordilleran muscovite-bearing plutons (Armstrong, 1988). At present, there is no evidence that would restrict the muscovite source terrain to that specific part of the belt.

At this point, we examine more closely the sources for the P_1 and P_2 static peaks. Table 8 summarizes estimated zircon FT ages of present-day outcrops for some selected source terrains. For the Cenozoic volcanic terrains (Cascade and Challis), zircon FT ages are considered to be equivalent to the magmatic age of the terrains. For the Eocene reset terrains, the present-day zircon FT ages are from published FT data where available or estimated by interpolation between K-Ar biotite and apatite FT ages that have closure temperatures that closely bracket the closure temperature of the zircon FT system. For moderate cooling

rates ~ 15°C/my, closure temperatures for K-Ar biotite, zircon FT, and apatite FT are ~300°, ~240°, and ~115°C, respectively (table 2; Hurford, 1986).

Only three of the source terrains in table 8 appear to have present-day zircon FT ages that are compatible with the ~43 Ma zircons that make up the P_1 peak: (1) the Challis volcanic province, (2) epizonal plutons and reset wall rocks of the southern Idaho batholith, and (3) the Chelan block of the North Cascades Mountains. The remaining Eocene reset terrains are too old to have served as a source for this peak. Of these three options, the Challis volcanic province seems the most unlikely, because the zircons would have to be derived from the youngest part of the volcanic province. Given the presence of older volcanic rocks, it is difficult to envision how this terrain could have acted as a static, single-age source for a period of ~24 my (43–19 Ma).

The next option is the Eocene reset terrain in the southern Idaho batholith (A in table 8 and fig. 14). The Idaho batholith is cut by a number of Challis-age epizonal plutons with dimensions ranging up to 70 km across (Armstrong, 1974; Criss, Lanphere, and Taylor, 1982). The plutons have K-Ar biotite ages that cluster at 44 ± 6 Ma (Criss, Lanphere, and Taylor, 1982). They are thought to be comagmatic with nearby Challis volcanic rocks which have an average age of about 45 Ma (Armstrong, 1974; 16 K-Ar ages, recalculated using modern isotopic constants). Extensive isotopic dating (Criss, Lanphere, and Taylor, 1982) has shown that K-Ar biotite ages for Mesozoic rocks in the vicinity of these plutons have been reset to a mean age of 43 Ma with a range of 37 to 46 Ma. Criss, Lanphere, and Taylor (1982) have demonstrated that this resetting is related to hydrothermal metamorphism associated with the epizonal plutons. Zircon FT ages from the reset wallrocks have a mean of 41 Ma with a range of 35 to 46 Ma (A in table 8; Sweetkind and Blackwell, 1989). We note that Heller and others (1992) discount the Idaho batholith as a source for the OSC sandstones. Their argument is based primarily on significant differences in the isotopic composition of the OSC sandstones and sandstones of the Eocene Tyee Formation of southwest Oregon, which Heller and others (1985) concluded were derived from an Idaho batholith source.

The third and preferred option for the P_1 peak is the Eocene reset terrain in the Chelan block of the North Cascades Mountains of western Washington (Haugerud and others, 1991; G in table 8 and fig. 14). The Chelan block consists of a complex assemblage of high-grade granitoid gneisses, subordinate metamorphosed supracrustal rocks, and young lineated orthogneiss dikes. Haugerud and others (1991) have shown that magmatic activity, metamorphism, and ductile deformation extended from 75 to 45 Ma and was followed by rapid cooling. Zircon FT ages for the Chelan block give a mean of 44 Ma with a range of 57 to 36 Ma (table 8).

We have identified only two options for the source of the ~57 Ma zircons that make up the P_2 peak. The first option corresponds to an

older group of reset rocks found in and adjacent to the southern Idaho batholith (B in table 8). These rocks consist mainly of Mesozoic granites and subordinate metasedimentary country rock. In contrast to the younger reset rocks described above for this area (A in table 8), these older reset rocks are usually well removed from the Eocene epizonal plutons. Isotopic dating by Criss, Lanphere, and Taylor (1982) has shown that these rocks have an older range of reset K-Ar biotite ages, from 93 to 53 Ma, and that their ages are well separated from the K-Ar biotite ages that distinguish the younger reset rocks (A in table 8). Zircon FT ages from the older reset rocks have a mean of 66 Ma and a range of 53 to 82 Ma (B in table 8; Sweetkind and Blackwell, 1989). We infer that these cooling ages are related to unroofing of the Idaho batholith by extensional faulting during the latest Cretaceous or early Tertiary (Hyndman, Alt, and Sears, 1988, p. 349–352). Unroofing must postdate metamorphism of the high-grade metamorphic rocks that surround the batholith, dated at about 105 to 80 Ma (Hyndman, Alt, and Sears, 1988), and predate deposition of 50 Ma Challis volcanic rocks that unconformably overlie the exhumed metamorphic rocks. There are two problems that seem to discount these rocks as a source for our sandstones. First is the isotopic studies of Heller and others (1985, 1992) which seem to preclude the Idaho batholith as a source for the OSC sandstones. The second is the present-day zircon FT age of the terrain ($\sim$66 Ma), which is probably too old to be correlative with the $\sim$57 Ma P_2 peak.

The only other option for the source of the P_2 peak is one or more of the remaining Eocene reset terrains (C–F in table 8). The Bitterroot lobe of the northern Idaho batholith, the Priest River, Okanagan, and Kettle metamorphic core complexes, and metamorphic rocks of the northern Monashee Mountains were all rapidly cooled by tectonic denudation during the Paleocene to Middle Eocene (see Parrish, Carr, and Parkinson, 1988, for a review). After cooling, these reset terrains would be ideal candidates for the source of a static peak. Furthermore, they are dominated by granitoid rocks and thus could have served, at least in part, as the source of the arkosic detritus found in the OSC and Eocene basin samples. The more eastern source terrains, the Bitterroot lobe, Priest River complex, and northern Monashee Mountains (C, D, and E in table 8), would also have been able to supply radiogenic metamorphic muscovite. The principal problem with this option is that the present-day zircon FT age of these terrains is significantly younger than the $\sim$57 Ma age of the P_2 peak. It is possible that erosion of these terrains has removed that portion of the crust that was "quenched" during extension faulting and associated tectonic denudation. The thickness of the "quenched" crust is controlled by the cumulative throw on the extensional faults and can be no greater than the depth to the onset of the partial stability zone for fission tracks in zircon, which is estimated to lie at $\sim$6 km, assuming a normal continental thermal gradient (see section on "Annealing of Fission Tracks in Zircon" for further details). Therefore, we would have to attribute the young FT ages for present-day outcrops to limited throw on

the extensional faults and/or deep erosion following tectonic denudation.

Summary

In this brief analysis, we have attempted to identify the provenance of the OSC and Eocene basin sandstones, with special emphasis on the source of detrital zircons. While it is difficult to identify uniquely specific sources, it is quite clear that suitable source terrains do exist in the Pacific Northwest. The evidence outlined above suggests that the OSC and Eocene basin sandstones were derived from a river system that originated on the eastern side of the Omineca belt, either in eastern Washington and northern Idaho or in eastern British Columbia. This river system probably passed near or over the Chelan block of northwestern Washington and may have reached the sea in the vicinity of the present-day Olympic Mountains. The Cascade volcanic arc is considered to be the source for the young P_0 peaks. Eocene reset terranes in the Cascade Mountains and in the Omineca belt probably served as sources for the static P_1 and P_2 peaks. The P_3 peak is loosely attributed to a variety of Late Cretaceous plutonic terrains, with the most likely option being the eastern Cordillera muscovite-bearing plutons.

TECTONIC IMPLICATIONS FOR THE OSC

Geology and Structure of the OSC

The age data presented here have several important implications for the geology and regional structure of the OSC. First, the concentric distribution of FT ages clearly indicates a domal structure for uplift of the Olympic Mountains. Our reset samples define an area about 30 km across (inner dashed line in fig. 5) that coincides with the central and most deeply exhumed part of the Olympic Mountains. Mount Olympus, the highest summit in the Olympic Mountains (2427 m), lies within the reset area on its west side. Maximum metamorphic grade is also attained in this area (Brandon and Calderwood, 1990).

Outside this central area, χ^2 ages from unreset samples become progressively older with increasing distance from the reset area (fig. 5). Unreset samples from just outside the perimeter of the central reset area have χ^2 ages of 27 to 19 Ma, indicating Late Oligocene and Early Miocene depositional ages. At a greater distance, the χ^2 ages are clustered between 48 to 32 Ma indicating Middle Eocene to Early Oligocene depositional ages. We are, of course, assuming that the χ^2 age is a reasonable proxy for the depositional age of the sandstone.

The domal structure of the OSC is also apparent in the apatite FT dating of Roden, Brandon, and Miller (1990). The outer dashed line in figure 5 encloses all apatite localities that cooled during uplift of the Olympic Mountains (apatite ages less than 12 Ma).

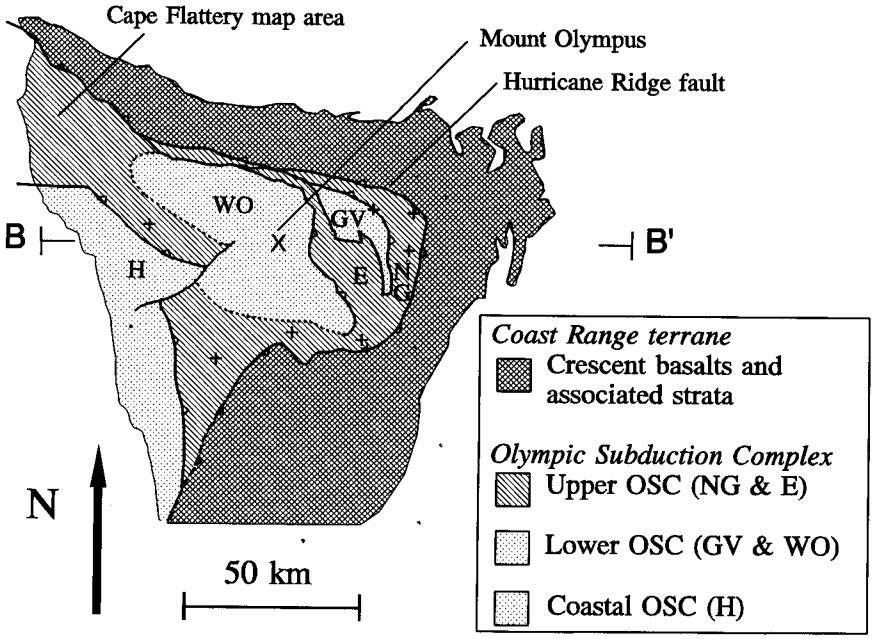

Fig. 15. Revised geologic map for the Olympic subduction complex. B-B′ marks the location of the cross section in figure 16. We propose that the OSC consists of three structural units: upper OSC, lower OSC, and coastal OSC. The legend shows a cross-reference between our units and those of Tabor and Cady (1978b), which are abbreviated as follows: NG = Needles-Gray Wolf assemblage, E = Elwha assemblage, GV = Grand Valley assemblage, WO = Western Olympic assemblage, and H = Hoh assemblage. The *upper OSC* consists of Middle Eocene through Lower Oligocene clastic rocks and minor slices of Lower and (?)Middle Eocene pillow basalt. This unit includes all our sandstones that yielded relatively old χ^2 ages (48–32 Ma; localities marked with a "+" symbol on the map), plus the Sooes and Ozette terranes of Snavely and others (1986a), which are exposed in the Cape Flattery map area. Microfossils from clastic rocks in the Sooes and Ozette terranes indicate an Eocene and possibly Oligocene age (Snavely and others, 1986a, b), making them coeval with our older χ^2 ages. The *lower OSC* is dominated by younger clastic rocks, Late Oligocene and Early Miocene in age (χ^2 ages of 27–19 Ma); pillow basalts are notably absent. The *coastal OSC* consists of Lower Miocene and possibly lowermost Middle Miocene clastic rocks with minor blocks of Eocene pillow basalt.

In light of these data, we propose a revised structural interpretation of the OSC (figs. 15 and 16). This interpretation is based primarily on the recognition of three structural units summarized below.

Upper OSC.—The upper OSC is considered to form the structurally highest part of the OSC. It is distinguished by the presence of numerous large lenses of pillow basalt and relatively old clastic rocks. The Needles-Gray Wolf assemblage of Tabor and Cady (1978b) represents a prime example of this structural unit. The pillow basalts are Early to (?)Middle Eocene in age based on fossiliferous limestone interbeds (Rau, 1975; Tabor and Cady, 1978b; Snavely and others, 1986, Snavely, Rau, and Hafley, 1986; P. Snavely, 1989, written communication; W. Rau, 1989,

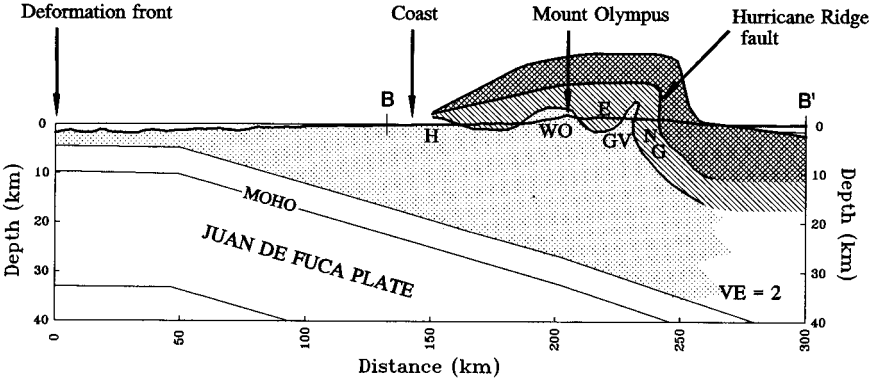

Fig. 16. Cross section along B-B′ in figure 15 showing our interpretation of the regional-scale structure of the OSC. Patterns and abbreviations are identified in figure 15. Structure of the Juan de Fuca plate is from Brandon and Calderwood (1990). Note that the geology projected above the present-day land surface (heavy line) has been removed over the last 12 my by uplift and erosion as discussed in Brandon and Calderwood (1990). The main new features of our interpretation are the recognition of a domal culmination in the central part of the Olympic Mountains and the inferred continuity at depth between the coastal OSC (labeled "H" for Hoh assemblage) and the lower OSC (labeled "WO" and "GV" for Western Olympic and Grand Valley assemblages).

1990, written communication). The clastic rocks are Middle Eocene to Early Oligocene in age. Those unreset samples with χ^2 ages in this age range (48–32 Ma) are all attributed to the upper OSC (locations marked by "+" symbols in fig. 15).

In cross section, we show the upper OSC as arching over the Mount Olympus area. To the east, the upper OSC includes the Needles-Gray Wolf assemblage and Elwha assemblage of Tabor and Cady (1978b). To the west, it includes the western half of the Western Olympic assemblage (Tabor and Cady, 1978b) and the Sooes and Ozette terranes, which are located in the Cape Flattery map area of Snavely and others (1986) (fig. 15). Microfossils indicate an Eocene and possibly Oligocene age for the clastic rocks in the Sooes and Ozette terranes (Snavely and others, 1986, Snavely, Rau, and Hafley, 1986), making them coeval with our χ^2 ages for sandstones of the upper OSC.

Based on stratigraphy, fossil ages, and chemical composition, the pillow basalts of the upper OSC appear to be identical to pillow basalts of the lower member of the Crescent Formation (Applegate and Brandon, 1989; M. T. Brandon, unpublished data), which makes up the base of the Coast Range terrane. In a number of cases, it can be shown that the basalt lenses in the upper OSC are fault bounded along their stratigraphically lower side and depositionally overlain by clastic rocks on their upper side (Tabor and Cady, 1978b; Applegate and Brandon, 1989). This relationship is taken as evidence that some, if not all, of the clastic rocks of the upper OSC were originally deposited on a basaltic basement similar to

the lower Crescent. Subsequent thrust faulting has resulted in an imbricated sequence of slices, many of which contain both basaltic basement and sedimentary cover.

Based on these observations, we infer that the upper OSC originated as part of the Coast Range terrane. We speculate that when subduction was initiated in the Olympics, a western extension of the Coast Range terrane was sliced off and underthrust to the east. This left a relatively coherent upper plate, which we now refer to as the Coast Range terrane, and a subjacent, more disrupted slab of Coast Range rocks, which we now identify as the upper OSC (see fig. 27 in Tabor and Cady, 1978a, for a similar interpretation). The underthrusting and imbrication of the upper OSC must postdate, at least in part, the youngest rocks that it contains. At present, the youngest ages are the χ^2 ages for clastic rocks of the Needles-Gray Wolf assemblage, which range from 39 to 33 Ma (table 5). Thus, we conclude that imbrication and underthrusting of the upper OSC occurred at sometime after ~33 Ma.

Lower OSC.—The lower OSC is exposed in the central and most deeply exhumed part of the Olympic uplift and is inferred to underlie structurally the upper OSC. The lower OSC is distinguished by the general absence of pillow basalts and the presence of clastic rocks with relatively young χ^2 ages, Late Oligocene and Early Miocene (27-19 Ma). This unit includes the eastern half of the Western Olympic assemblage and all the Grand Valley assemblage of Tabor and Cady (1978b). We envision that the lower OSC was formed by subduction underplating beneath the upper OSC, as discussed in Brandon and Calderwood (1990). In this sense, the lower OSC represents the true accretionary wedge, in that it was formed by transfer of material across the active plate boundary, whereas the upper OSC was formed by within-plate shortening of the leading edge of the overriding plate.

Coastal OSC.—The Coastal OSC is equivalent to the Hoh assemblage (Rau, 1975, 1979; Tabor and Cady, 1978b) which is exposed along the west coast of the Olympic Peninsula. The Hoh consists of imbricated slices of coherent turbidites and subordinate mudstone-rich mélanges. Microfossils from the Hoh indicate that most of the unit is restricted to an age of Early Miocene and possibly early Middle Miocene as well. Blocks of Eocene pillow basalt are also present. Once again, these blocks appear to be derived from the overlying Coast Range terrane based on chemistry and age (M. T. Brandon, unpublished data). Rau (1975, 1979) and Orange (1990) argue that the Hoh was formed by subduction accretion and local diaprism. These processes alone cannot account for the blocks derived from the Coast Range terrane. For this unit, we propose that downslope mass wasting was responsible for transporting the basalt blocks from the overlying Coast Range terrane down to the trench, where the blocks and associated sediments were subsequently added to the accretionary wedge. This interpretation would account for the large contrast in age between the pillow basalt blocks and the clastic sediments of the Hoh.

An interesting result of our FT dating is the discovery that clastic rocks of the lower OSC and the Hoh assemblage have similar depositional ages. We propose that the lower OSC, at least in part, is structurally and stratigraphically equivalent to the Hoh, and that these two units are connected in the subsurface beneath the western exposures of the upper OSC (fig. 16). In this interpretation, the Hoh and the lower OSC would represent different parts of a more extensive and contiguous Miocene accretionary unit. Differences in metamorphic grade are attributed to increasing temperature and pressure within the deeper, more landward part of the accretionary wedge. The Hoh contains widespread laumontite indicative of zeolite-facies metamorphism (Stewart, 1974) which suggests that it belongs to the shallower and more frontal part of the accretionary wedge. The occurrence of prehnite and pumpellyite in the lower OSC indicates a deeper accretionary setting for those rocks (Tabor and Cady, 1978b; Brandon and Calderwood, 1990).

Age and Conditions of Metamorphism

The FT ages for unreset and reset samples from the lower OSC provide tight brackets for the age of metamorphism of that unit. Metamorphism must postdate the χ^2 ages from unreset samples which are as young as 19 Ma and predate cooling ages from the reset samples which are about 14 Ma. These timing constraints agree closely with K-Ar ages that Tabor (1972) obtained for his most highly recrystallized samples, which are fine-grained mica phyllites from the Elwha assemblage, all of which are from locations within the reset area defined by our zircon samples (fig. 5). Tabor (1972) determined 10 K-Ar ages for 4 samples. When recalculated using modern isotopic constants, these ages have a mean of 17.9 Ma and a range of 16.6 to 20.4 Ma. Our interpretation is that these ages record the time of metamorphic recrystallization for this part of the OSC.

Tabor (1972) reports 56 other K-Ar ages for lower-grade, less-recrystallized rocks from the northeastern part of the OSC. Those ages varied widely, from 232 to 28 Ma (recalculated using modern isotopic constants). Note this range is similar to the range in FT grain ages for our unreset OSC samples, 389 to 14 Ma (tables 4 and 5). Thus, we see no reason to interpret these particular K-Ar ages as anything other than incompletely reset detrital ages.

The simple model of stepwise heating described in table 1 can be used to constrain the maximum temperatures experienced by our unreset and reset samples. The inference is that our unreset samples were never subjected to temperatures in excess of $Tz_{10\%}$, and our reset samples must have to be temperatures greater than $Tz_{90\%}$. To determine the correct values of $Tz_{10\%}$ and $Tz_{90\%}$, we need to specify the duration of heating, a difficult task in the absence of a specific time-temperature history. The duration of heating for our samples is probably in the range 3 to 25 my which indicates that $Tz_{10\%} \geq 175°C$ and $Tz_{90\%} \leq 250°C$ (table 1). A more specific result can be determined by using a maximum

duration of heating based on the difference between the time of accretion of the samples, as constrained by χ^2 ages, and the time of cooling to temperatures below about 115°C, as indicated by apatite FT ages. In our discussion above, we concluded that the upper OSC was underthrust beneath the Coast Range terrane after about 33 Ma and the lower OSC was added to the base of the accretionary wedge after about 27 to 19 Ma. Apatite FT ages indicate that all our zircon localities cooled below about 115°C at various times between 12 to 3.5 Ma (Roden, Brandon, and Miller, 1990; fig. 5). Thus, we estimate that the duration of heating was less than 20 my for the upper OSC and less than 15 to 7 my for the lower OSC. These time estimates indicate that: (1) the unreset samples never saw temperatures in excess of about 175° to 185°C, and (2) the reset samples were subjected to temperatures in excess of about 240° to 245°C.

The reset area is thought to represent the most deeply exhumed part of the OSC. The estimated peak temperature for the reset samples (> 240°-245°C) is used here to constrain the depth of structural burial for this area. Peak metamorphism for rocks of the reset area occurred between 19 to 14 Ma, as discussed above, and therefore predated uplift and erosion of the OSC, which began at about 12 Ma (Brandon and Calderwood, 1990). Based on this relationship, we argue that the surface heat flow in the vicinity of the Olympic Mountains at the time of metamorphism of the reset area can be approximated by the present surface heat flow in other areas where the Cascadia forearc has not been uplifted or deeply eroded.

In a compilation of thermal data for Washington, Blackwell, Steele, and Kelley (1985) report that the surface heat flow for the Coast Ranges of western Washington, exclusive of the Olympic Mountains, is 39.8 ± 3.2 mW m^{-2} (±2 standard error, N = 32). If we assume that heat flow is one dimensional and steady state, then the depth d(T) to a specific isotherm T can be calculated using the following relationship:

$$d(T) = (T - T_s)\frac{q_s}{k} \qquad (2)$$

where T_s is the average annual surface temperature, q_s is the surface heat flow, and k is the average thermal conductivity. The average thermal conductivity for the section that used to overlie the reset area (fig. 16) is estimated to be 2.05 ± 0.06 mW m^{-1} K^{-1} (average and ±2 standard error uncertainty are estimated by assuming a section composed of 45 percent basalt, 27.5 percent sandstone, and 27.5 percent mudstone and by calculating a weighted harmonic mean using compiled thermal conductivity data from Oxburgh, 1980; and Oxburgh and Wilson, 1989). Other relevant parameters are T_s = 8° ± 2°C and T = 245° ± 6°C (all estimated uncertainties are ±2 standard error; estimate for T_s is discussed in "Reset OSC Samples"). The average thermal gradient (q_s/k) is calculated to be 19.4° ± 1.7° C/km. The maximum depth of structural burial must be greater than d(245°C) = 12.2 ± 1.1 km. The absence of lawsonite in these rocks (see Introduction) indicates that the depth of structural burial

was probably not significantly greater than 12 km (the reaction: laumontite = lawsonite + quartz is estimated to occur at a depth of about 11 km; see Brandon and Calderwood, 1990).

Rate of Wedge Thickening

The available age data can be used to estimate the growth rate of the OSC. More specifically, we are interested in the rate of thickening of the accretionary wedge in the vicinity of Mount Olympus. Regional constraints discussed in the Introduction indicate that Cascadia subduction was initiated at ~36 Ma. The upper OSC was underthrust beneath the Coast Range terrane at some time after 33 Ma. The deepest part of the lower OSC was accreted at ~17 Ma (between χ^2 age of 19 Ma and the FT cooling age of 14 Ma) at a depth of ~12 km. Thus, over the interval 36 to 17 Ma, the wedge in the vicinity of Mount Olympus was thickened by ~12 km at an average rate of 0.6 km/my.

In the Mount Olympus area, the upper 12 km of the wedge was removed by erosion during late Cenozoic uplift of the Olympic Mountains. However, an additional 30 km of accreted materials (fig. 16) has been added beneath Mount Olympus since ~17 Ma. Geophysical evidence summarized in Brandon and Calderwood (1990) indicates that most, if not all, of the underlying wedge is composed of sedimentary rocks. If we assume that these sedimentary rocks were added to the wedge by underplating, then the wedge must have thickened by 30 km over the last 17 Ma, which indicates an average thickening rate of 1.75 km/my.

Thickening of the wedge is driven by two processes: underplating at the base of the wedge and deformation within the wedge. Pavlis and Bruhn (1983) argue that the lower part of a large accretionary wedge should be dominated by ductile flow. We suggest that the increased rate of wedge thickening over the last 17 my may be due to the fact that as the wedge grew, a greater portion of it would have lain below the brittle-ductile transition. Faster rates of strain in this lower, more ductile region might account for the increase in the rate of wedge thickening with time.

CONCLUDING REMARKS

The FT dating method is an effective tool for resolving questions about the age, internal structure, and tectonic evolution of sandstone-bearing subduction complexes. The apatite and zircon grains in accreted sandstones can be viewed as tracers that record the timing of critical thermal and tectonic events along a variety of displacement paths through the accretionary wedge. Zircon FT ages from unreset samples provide information about the depositional age and provenance of the accreted sediments. For trench-fill turbidites, the depositional age closely coincides with the start of the subduction/accretion process. Zircon and apatite ages from reset samples can be used to constrain the timing of metamorphism and the rate of cooling of the accreted sediments. This information provides an indirect measure of the average vertical velocity

of the accreted sediments relative to a site of initial accretion along the subduction zone decollement.

Our data from the Olympic Mountains indicate that, during the late Cenozoic, the residence time in the wedge for deeply accreted sediments has been surprisingly short. Late Oligocene and Early Miocene samples (χ^2 ages = 27 to 19 Ma) were subducted and accreted at depths of ~12 km. They moved upward from this site of initial accretion as indicated by zircon FT cooling ages of 14 Ma from adjacent reset samples. The metamorphic interior of the wedge has been exposed as a result of erosional denudation over the last 12 my following uplift of the modern Olympic Mountains. Average rates of erosion are estimated at ~1 km/my. Thus, the Olympic Mountains provide a useful example of how continued underplating, within-wedge ductile deformation, and erosion of the surface of the wedge can lead to the formation and subsequent exhumation of metamorphic rocks within a subduction zone setting.

ACKNOWLEDGMENTS

This project has benefitted greatly by the assistance of many individuals. Most samples were obtained from the rugged backcountry of the Olympic National Park. We are indebted to those who helped us in the field: David Applegate, Arthur Calderwood, Dan Coffey, Jon Einarsen, Jeff Feehan, Martha Goldstyne, Miriam Schoenbaum, and Harold Tobin. They toiled long and hard under heavy loads and with remarkably good cheer. Packers Kit Neeman and David Johnson provided valuable assistance with moving supplies and rocks in the low country. The National Park Service in Port Angeles, Washington, granted us permission to work in Olympic National Park and provided support with backcountry logistics. In this respect, we are particularly grateful to John Aho and Richard Hanson. Dick Stewart and Ray Wells kindly provided additional samples for our study (ZD6 and C4, respectively). David Applegate, Arthur Calderwood, Linda Neshyba, and Miriam Schoenbaum helped with various aspects of the mineral separations. C. W. Naeser assisted us with the neutron fluence measurements. K. Kelly and D. C. Engebretson kindly provided estimates of Cascadia convergence velocities. The paper was substantially improved as a result of critical reviews and comments by Mark Cloos, John Garver, Rowland Tabor, and Sean Willett. The research was funded by the National Science Foundation (EAR-8707442, EAR-9005777 to Brandon, and EAR-8816512 to Vance), Washington State Division of Geology and Earth Resources, ARCO, and Yale University.

APPENDIX I

This appendix contains locality descriptions for our zircon FT samples. The following format is used: laboratory number (field number, latitude, longitude), followed by the locality description. The prefix for the field number identifies the geologist who collected the sample (unless noted otherwise): "V" for J. A. Vance, "ARC" for A. R. Calderwood and M. T. Brandon, and "8" for M. T. Brandon. The laboratory number includes a prefix of Ç for the Eocene basin samples, F for the Fish Canyon tuff reference, ZD for an unreset OSC

sample, and ZR for a reset OSC sample. A note is included for those OSC samples that have also yielded apatite FT ages (apatite ages are indicated by the prefix "AR," followed by the laboratory number for the sample). The apatite results will be the subject of another paper.

C1 (V351, 47° 20.9′, −121° 59.1′) Fluvial sandstone from the upper part of the undivided Puget Group. Collected from a large open pit quarry 1.5 km south of Ravensdale Lake, near Ravensdale, Washington. This locality lies about 6 km north of the Green River gorge section of the Puget Group, which was dated by Turner and others (1983) using plagioclase K-Ar and apatite FT methods. The Ravensdale locality probably lies near the top of the Puget Group, whereas the good K-Ar ages of Turner and others (1983) were collected from the middle of the Puget Group, at about 1025 to 1540 m below the top of the unit.

C2 (V331, 46° 40.9′, −123° 02.2′) Fossiliferous, shallow marine sandstone from the Skookumchuck Formation near Centralia, Washington. Collected south of Centralia from the large borrow pit on the east side of the highway near Yardbird's Store. Walsh and others (1987, p. 13) provide stratigraphic details for the Skookumchuck. The unit has yielded foraminifera referable to the late Narizian stage and several isotopic ages that indicate an age of about 40 Ma (see C5 below). The Skookumchuck is stratigraphically equivalent to the upper Cowlitz Formation and overlies the Stillwater Member of the Cowlitz Formation from which sample C3 was collected.

C3 (V450, 46° 23.8′, −123° 02.9′) Marine sandstone from the Stillwater Member of the Cowlitz Formation, collected 3 km north of Ryderwood, Washington, on the road along the lower part of Owen Creek. See Walsh and others (1987, p. 11) for stratigraphic details. The unit has yielded foraminifera referable to the Narizian stage, which approximately corresponds to the interval 48 to 37.5 Ma. This unit stratigraphically underlies the Skookumchuck Formation and therefore should be older than sample C2 above.

C4 (V403, 45° 42.48′, −123° 20.01′) Sandstone from the Cowlitz Formation. Collected by Ray Wells from an outcrop about 3.5 km west of Timber, Oregon, in Reeher Forest Park. In Washington, the Cowlitz Formation is assigned to the upper Narizian (Walsh and others, 1987, p. 11). The Narizian stage approximately corresponds to the interval 48 to 37.5 Ma; the age of the upper/middle Narizian boundary is, at present, poorly resolved.

C5 (V335, approximate location: 46° 43′, −122° 58′) Volcanic ash from the Skookumchuck Formation. Collected from the Centralia coal mine. Triplehorn, Turner, and Frizzell (1980) report an average of 40 Ma for 6 K-Ar feldspar ages from ash beds at the coal mine.

F1 Volcanic zircon from the Fish Canyon tuff, a widely used reference sample, which has a well determined K-Ar age of 27.9 ± 0.7 (±2s) (Hurford and Green, 1983).

ZD38 (ARC88-16, 47° 50.80′, −124° 12.15′) Sandstone from unit Two of the Western Olympic assemblage (Tabor and Cady, 1978b). Collected southeast of Forks on logging road H3200 at 508 m (1665 ft). (From same sample as AR38.)

ZD22 (8782-2, 47° 33.38′, −123° 40.05′) Sandstone from unit Tur (Tabor and Cady, 1978b). Collected 2.9 km south on the road from the North Fork Ranger Station from an outcrop on the west side of a road at 155 m (510 ft). Unit Tur represents an undifferentiated part of the OSC which we tentatively include with the Western Olympic assemblage.

ZD44 (ARC88-22, 47° 29.08′, −123° 57.55′) Sandstone from unit Tur (Tabor and Cady, 1978b). Collected on USFS Road #2460 west of Quinault Lake at 183 m (600 ft). Unit Tur represents an undifferentiated part of the OSC which we tentatively include with the Western Olympic assemblage.

ZD50 (8892-1, 47° 52.55′, −123° 41.60′) Sandstone from unit Twog ("green sandstone") of the Western Olympic assemblage (Tabor and Cady, 1978b). Collected by D. Coffey from an outcrop on the south side of the Hoh River bridge at the confluence of Glacier Creek and Hoh River. Elevation is 408 m (1340 ft).

ZD6 (V312, 47° 47.61′, −123° 45.44′) Sandstone from unit Two of the Western Olympic assemblage (Tabor and Cady, 1978b). Collected by R. J. Stewart from summit of Mount Tom at about 2148 m (7048 ft).

ZD49 (8889-2, 47° 47.48′, −123° 17.47′) Sandstone from unit Tgst of the Grand Valley assemblage (Tabor and Cady, 1978b). Collected by D. Coffey from the summit of Wellesley Peak at 2060 m (6758 ft). (From same sample as AR49.)

ZD2 (86L-2, 47° 54.93′, −123° 22.61′) Sandstone collected at Hurricane Ridge in the vicinity of the Gray Wolf fault at 1920 m (6300 ft). The Gray Wolf fault separates the Grand Valley assemblage to the west from the Needles-Gray Wolf assemblage to the east (Tabor, Yeats, and Sorensen, 1972). The contact is not located well enough in the sample area to distinguish which unit was sampled. In the text, we conclude that the sample probably corresponds to the Needles-Gray Wolf assemblage (unit Tnm of Tabor and Cady, 1978b). (From same sample as AR2.)

ZD7 (V441, 47° 46.12′, −123° 11.62′) Sandstone of unit Tnm of the Needles-Gray Wolf assemblage (Tabor and Cady, 1978b). Collected along the trail to Sunnybrook Meadows at 1600 m (5250 ft). Tabor and Cady (1978b) show a large fold in this area.

ZD33 (ARC88-11, 47° 52.60′, −123° 08.70′) Sandstone from unit Tnm of the Needles-Gray Wolf assemblage (Tabor and Cady, 1978b). Collected 0.5 km west of the Hurricane Ridge fault on an old logging road west of USFS Road #2825 at 939 m (3080 ft).

ZD4 (V240, 47° 32.58′, −123° 22.36′) Sandstone from unit Tsc of Tabor and Cady (1978b), probably a southern continuation of the Needles-Gray Wolf assemblage. Collected from the trail along the North Fork of the Skokomish River, just north of the southern fault zone at 442 m (1450 ft).

ZD5 (V241, 47° 30.42′, −123° 21.77′) Sandstone from a unit that Tabor and Cady (1978b) describe as the "basaltic facies" of the Blue Mountain unit (Tbmb) (see Tabor, 1982, for further details). Collected on Road #2347, N of Elk Creek and W of Staircase Ranger Station, at the approximate elevation of 976 m (3200 ft). Vance and Brandon returned to this locality during the summer of 1990. We did not find a stratigraphic relationship between the sampled unit and nearby exposures of red limestone and pillow basalt, which belong to the lower Crescent Formation. Furthermore, the sandstone is not basaltic but instead is composed mainly of quartz and plagioclase with minor plutonic and volcanic lithic clasts, biotite, and rare muscovite. The heavy mineral fraction contains abundant epidote and garnet. Map patterns shown in Tabor (1982) suggest that the dated sandstone unit may be structurally interleaved with the lower Crescent Formation. An assignment to the Blue Mountain unit is not compelling. We tentatively include this locality with unit Tsc of Tabor and Cady (1978b) which has been mapped to within 2 km of the sample locality. Unit Tsc is probably a southern continuation of the Needles-Gray Wolf assemblage.

ZR17 (87727-1, 47° 47.34′, −123° 38.09′) Well bedded sandstone from unit Twog ("green sandstone") of the Western Olympic assemblage (Tabor and Cady, 1978b). Collected at the base of Humes Glacier at 1439 m (4720 ft). (From same sample as AR17.)

ZR9 (87716-2, 47° 46.73′, −123° 35.70′) Well bedded sandstone from unit Twog ("green sandstone") of the Western Olympic assemblage (Tabor and Cady, 1978b). Collected from the area east of the Queets Glacier and northeast of peak 5819 at 1665 m (5460 ft).

ZR46 (8887-1, 47° 49.34′, −123° 25.94′) Sandstone from unit Tgs of the Grand Valley assemblage (Tabor and Cady, 1978b). Collected near the trail west of Hayden Pass at 945 m (3100 ft). (From same sample as AR46.)

ZR48 (8889-1, 47° 47.66′, −123° 21.68′) Well bedded sandstone from unit Tess of the Elwha assemblage (Tabor and Cady, 1978b). Collected at 1982 m (6500 ft) on Mount

Fromme from strata depositionally overlying Eocene basalts exposed there. (From same sample as AR48.)

References

Applegate, J. D. R. and Brandon, M. T., 1989, An upper plate origin for basalt blocks in the Cenozoic subduction complex of the Olympic Mountains, northwest Washington State: Geological Society of America/Abstracts with Programs, v. 21, p. 51.

Armentrout, J. M., 1981, Correlation and ages of Cenozoic chronostratigraphic units in Oregon and Washington, *in* Armentrout, J. M., editor, Pacific Northwest Cenozoic Biostratigraphy; Geological Society of America Special Paper 184, p. 137–148.

Armstrong, R. L., 1974, Geochronometry of the Eocene volcanic-plutonic episode in Idaho: Northwest Geology, v. 3, p. 1–15.

———— 1979, Cenozoic igneous history of the U.S. Cordillera from latitude 42° to 49° North, *in* Smith, R. B., and Eaton, G. P., editors, Cenozoic Tectonics and Regional Geophysics of the Western Cordillera: Geological Society of America Memoir 152, p. 265–282.

———— 1988, Mesozoic and early Cenozoic magmatic evolution of the Canadian Cordillera: Geological Society of America Special Paper 218, p. 55–91.

Armstrong, R. L., Taubeneck, W. H., and Hales, P. O., 1977, Rb-Sr and K-Ar geochronometry of Mesozoic granitic rocks and their strontium-isotopic composition: Geological Society of America Bulletin, v. 84, p. 1375–1392.

Armstrong, R. L., and Ward, P., 1991, Evolving geographic patterns of Cenozoic magmatism in the North American Cordillera. The temporal and spatial association of magmatism and metamorphic core complexes: Journal of Geophysical Research, v. 96, p. 13201–13224.

Babcock, R. S., and Misch, P., 1988, Evolution of the crystalline core of the North Cascades Range, *in* Ernst, W. G., editor, Metamorphism and Crustal Evolution of the Western United States, Rubey v. 7: Englewood Cliffs, New Jersey, Prentice-Hall, p. 214–232.

Baldwin, S. L., Harrison, T. M., and Burke, K., 1986, Fission-track evidence for the source of accreted sandstones, Barbados: Tectonics, v. 5, p. 457–468.

Blackwell, D. D., Steele, J. L., and Kelley, S. A., 1985, Heat flow and geothermal studies in the State of Washington: Washington Department of Natural Resources, Division of Geology and Earth Resources, Open-File Report 85–6, 77 p.

Brandon, M. T., 1989a, Deformational styles in a sequence of olistostromal mélanges, Pacific Rim Complex, western Vancouver Island, Canada: Geological Society of America Bulletin, v. 101, p. 1520–1542.

———— 1989b, Origin of igneous rocks associated with mélanges of the Pacific Rim Complex, western Vancouver Island, Canada: Tectonics, v. 8, p. 1115–1136.

Brandon, M. T., and Calderwood, A. R., 1990, High-pressure metamorphism and uplift of the Olympic subduction complex: Geology, v. 18, p. 1252–1255.

Brandon, M. T., Cowan, D. S., and Vance, J. A., 1988, The Late Cretaceous San Juan Thrust System, San Juan Islands, Washington: Geological Society of America Special Paper 221, 81 p. and 1 plate.

Brandon, M. T., and Vance, J. A., 1992, Zircon fission-track ages for the Olympic subduction complex and adjacent Eocene basins, western Washington State: Washington State Division of Geology and Earth Resources Open File Report 92-6, in press.

Cady, W. M., 1975, Tectonic setting of the Tertiary volcanic rocks of the Olympic Peninsula, Washington: United States Geological Survey Journal of Research, v. 3, p. 573–582.

Cady, W. M., MacLeod, N. S., and Addicott, W. O., 1963, Summary of investigations, Washington: United States Geological Survey Professional Paper 475-A, p. A96.

Carlson, D. H., Fleck, R., Moye, F. J., and Fox, K. F., 1991, Geology, geochemistry, and isotopic character of the Colville Igneous Complex, northeastern Washington: Journal of Geophysical Research, v. 96, p. 13313–13333.

Carpenter, B. S., and Reimer, G. M., 1974, Calibrated glass standards for fission-track use: National Bureau of Standards Special Publication, number 260-49, 17 p.

Cerveny, P. F., Naeser, N. D., Zeitler, P. K., Naeser, C. W. and Johnson, N. M., 1988, History of uplift and relief of the Himalaya during the past 18 million years: Evidence from fission-track ages of detrital zircons from sandstones of the Siwalik group, *in* Kleinspehn, K. L., and Paola, C., editors, New Perspectives in Basin Analysis: New York, New York, Springer-Verlag, p. 43–61.

Chase, R. B., Bickford, M. E., and Tripp, S. E., 1978, Rb-Sr and U-Pb isotopic studies of the northeastern Idaho batholith and border zone: Geological Society of America Bulletin, v. 89, p. 1325–1334.

Clowes, R. M., Brandon, M. T., Green, A. G., Yorath, C. J., Sutherland Brown, A., Kanasewich, E. R., and Spencer, C., 1987, LITHOPROBE—southern Vancouver Island: Cenozoic subduction complex imaged by deep seismic reflections: Canadian Journal of Earth Sciences, v. 24, p. 31–51.

Cowan, D. S., 1982, Geologic evidence for post-40 m.y.b.p. large-scale northwestward displacement of part of southeastern Alaska: Geology, v. 10, p. 309–313.

Criss, R. E., Lanphere, M. A., and Taylor, H. P., Jr., 1982, Effects of regional uplift, deformation, meteoric-hydrothermal metamorphism on K-Ar ages of biotites in the southern half of the Idaho batholith: Journal of Geophysical Research, v. 87, p. 7029–7046.

Curray, J. R., Moore, D. G., Lawver, L. A., Emmel, F. J. Raitt, R. W., Henry, M., and Kieckhefer, R., 1979, Tectonics of the Andaman Sea and Burma: American Association of Petroleum Geologists, Memoir 29, p. 189–198.

Davis, A. S., and Plafker, G., 1986, Eocene basalts from the Yakutat terrane: Evidence for the origin of an accreting terrane in southern Alaska: Geology, v. 14, p. 963–966.

Davis, E. E., and Karsten, J. L., 1986, On the cause of the asymmetric distribution of seamounts about the Juan de Fuca ridge: ridge-crest migration over a heterogeneous asthenosphere: Earth and Planetary Science Letters, v. 79, p. 385–396.

Deer, W. A., Howie, R. A., and Zussman, J., 1982, Rock-Forming Minerals, v. 1A: Orthosilicates: London, Longman, 919 p.

Desmarais, N. R., ms, 1983, Geology and geochronology of the Chief Joseph plutonic-metamorphic complex, Idaho-Montana: Ph.D. dissertation, University of Washington, Seattle, Washington, 150 p.

Dodson, M. H., 1976, Kinetic processes and thermal history of slowly cooling solids: Nature, v. 259, p. 551–553.

———— 1979, Theory of cooling ages, *in* Jäger, E., Hunziker, J. C., Lectures in Isotope Geology: Berlin, Germany, Springer-Verlag, p. 194–202.

Duncan, R. A., 1982, A captured island chain in the Coast Range of Oregon and Washington: Journal of Geophysical Research, v. 87, p. 10827–10837.

Einarsen, J. M., ms., 1987, The petrography and tectonic significance of the Blue Mountain unit, Olympic Peninsula, Washington: M. S. thesis, Western Washington University, Bellingham, Washington, 175 p.

Engebretson, D. C., Gordon, R. G., and Cox, A., 1985, Relative motions between oceanic and continental plates in the Pacific basin: Geological Society of America Special Paper 206, 59 p.

England, P., and Wells, R. E., 1991, Neogene rotations and quasicontinuous deformation of the Pacific Northwest continental margin: Geology, v. 19, p. 978–981.

Ewing, T. E., 1980, Paleogene tectonic evolution of the Pacific Northwest: Journal of Geology, v. 88, p. 619–638.

Fairchild, L. H., and Cowan, D. S., 1982, Structure, petrology, and tectonic history of the Leech River complex northwest of Victoria, Vancouver Island: Canadian Journal of Earth Sciences, v. 19, p. 1817–1835.

Finn, C., 1990, Geophysical constraints on Washington convergent margin structure: Journal of Geophysical Research, v. 95, p. 19533–19546.

Fleischer, R. L., Price, P. B., and Walker, R. M., 1965, Effects of temperature, pressure, and ionization of the formation and stability of fission tracks in minerals and glasses: Journal of Geophysical Research, v. 70, p. 1497–1502.

Fox, Jr., K. F., Rinehart, C. D., Engels, J. C., and Stern, T. W., 1976, Age of emplacement of the Okanogan gneiss dome, north-central Washington: Geological Society of America Bulletin, v. 87, p. 1217–1224.

Galbraith, R. F., 1981, On statistical models for fission-track counts: Journal of Mathematical Geology, v. 13, p. 471–478.

Galbraith, R. F., and Green, P. F., 1990, Estimating the component ages in a finite mixture: Nuclear Tracks and Radiation Measurements, v. 17, p. 197–206.

Gleadow, A. J. W., 1981, Fission-track dating methods: what are the real alternatives?: Nuclear Tracks and Radiation Measurements, v. 5, p. 3–14.

Green, P. F., 1981, A new look at statistics in fission-track dating: Nuclear Tracks and Radiation Measurements, v. 5, p. 77–86.

———— 1985, Comparison of zeta calibration baselines for fission-track dating of apatite, zircon, and sphene: Chemical Geology, Isotope Geoscience Section, v. 58, p. 1–22.

Green, P. F., Duddy, I. R., Gleadow, A. J. W., and Tingate, P. R., 1985, Fission track annealing in apatite: Track length measurements and the form of the Arrhenius plot: Nuclear Tracks and Radiation Measurements, v. 10, p. 323–328.

Green, P. F., Duddy, I. R., Gleadow, A. J. W., and Lovering, J. F., 1989, Apatite fission-track analysis as a paleotemperature indicator for hydrocarbon exploration, *in* Naeser, N. D., and McCulloh, T. H., editors, Thermal History of Sedimentary Basins: New York, New York, Springer-Verlag, p. 181–195.

Green, P. F., and Hurford, A. J., 1984, Thermal neutron dosimetry for fission track dating: Nuclear Tracks and Radiation Measurements, v. 9, p. 231–241.

Harland, W. B., Armstrong, R. L., Cox, A. V., Craig, L. E., Smith, A. G., and Smith, D. G., 1990, A geologic time scale 1989: Cambridge, Cambridge University Press, 263 p.

Haugerud, R. A., Van Der Heyden, P., Tabor, R. W., Stacey, R. W., and Zartman, R. E., 1991, Late Cretaceous and early Tertiary plutonism and deformation in the Skagit Gneiss Complex, North Cascade Range, Washington and British Columbia: Geological Society of America Bulletin, v. 103, p. 1297–1307.

Heller, P. L., Peterman, Z. E., O'Neil, J. R., and Shafiqullah, M., 1985, Isotopic provenance of sandstones from the Eocene Tyee Formation, Oregon Coast Range: Geological Society of America Bulletin, v. 96, p. 770–780.

Heller, P. L., and Ryberg, P. T., 1983, Sedimentary record of subduction to forearc transition in the rotated Eocene basin of western Oregon: Geology, v. 11, p. 380–383.

Heller, P. L., Tabor, R. W., O'Neil, J. R., Pevear, D. R., Shafiquillah, M., and Winslow, N. S., 1992, Isotopic provenance of Paleogene sandstones from the accretionary core of the Olympic Mountains, Washington: Geological Society of America Bulletin, v. 104, p. 140–153.

Heller, P. L., Tabor, R. W., and Suczek, C. A., 1987, Paleogeographic evolution of the United States Pacific Northwest during Paleogene time: Canadian Journal of Earth Sciences, v. 24, p. 1652–1667.

Hurford, A. J., 1986, Cooling and uplift patterns in the Lepontine Alps, south central Switzerland, and an age of vertical movement on the Insubric fault line: Contributions of Mineralogy and Petrology, v. 92, p. 413–427.

Hurford, A. J., Fitch, F. J., and Clarke, A., 1984, Resolution of the age structure of the detrital zircon populations of two Lower Cretaceous sandstones from the Weald of England by fission track dating: Geological Magazine, v. 121, p. 269–277.

Hurford, A. J., and Green, P. F., 1983, The zeta age calibration of fission-track dating: Isotope Geoscience, v. 1, p. 285–317.

Hyndman, D. W., 1983, The Idaho batholith and associated plutons, Idaho and western Montana: Geological Society of America Memoir 159, p. 213–240.

Hyndman, D. W., Alt, D., Sears, J. W., 1988, Post-Archean metamorphic and tectonic evolution of western Montana and northern Idaho, *in* Ernst, W. G., editor, Metamorphism and Crustal Evolution of the Western United States. Rubey, v. 7: Englewood Cliffs, New Jersey, Prentice Hall, Incorporated, p. 332–361.

Irving, E., and Brandon, M. T., 1990, Paleomagnetism of the Flores volcanics, Vancouver Island, in place by Eocene time: Canadian Journal of Earth Sciences, v. 27, p. 811–817.

Irving, E., and Wynne, P. J., 1990, Palaeomagnetic evidence bearing on the evolution of the Canadian Cordillera: Philosophical Transactions of the Royal Society of London A, v. 331, p. 487–509.

James, K., and Durrani, S. A., 1986, The effect of crystal composition on fission-track annealing and closure temperatures in geologic minerals: implications for the cooling rates of terrestrial and extraterrestrial rocks: Nuclear Tracks and Radiation Measurements, v. 11, p. 277–282.

Jarrard, R. D., 1986, Relations among subduction parameters: Reviews of Geophysics, v. 24, p. 217–284.

Johnson, S. Y., 1984, Evidence for a margin-truncating transcurrent fault (pre-Late Eocene) in western Washington: Geology, v. 12, p. 538–541.

———— 1985, Eocene strike-slip faulting and nonmarine basin formation in Washington, *in* Biddle, K. T., and Christie-Blicke, N., editors, Strike-Slip Deformation, Basin Formation, and Sedimentation: Society of Economic Paleontologists and Mineralogists, Special Publication 37, p. 283–302.

Kasuya, M., and Naeser, C. W., 1988, The effect of α-damage on fission-track annealing in zircon: Nuclear Tracks and Radiation Measurements, v. 14, p. 477–480.

Keach, R. W., II, Oliver, J. E., Brown, L. D., and Kaufman, S., 1989, Cenozoic active margin and shallow Cascades structure: COCORP results from western Oregon: Geological Society of America Bulletin, v. 101, p. 783–794.

Kincer, J. B., 1941, Climate and weather data for the United States, *in* Climate and Man, Yearbook of Agriculture: Washington, D. C., United States Government Printing Office, p. 685–1228.

Kowallis, B. J., Heaton, J. S., and Bringhurst, K., 1986, Fission-track dating of volcanically derived sedimentary rocks: Geology, v. 14, p. 19–22.
Krishnaswami, S., Lal, D., and Prabhu, N., 1974, Characteristics of fission tracks in zircon: applications to geochronology and cosmology: Earth and Planetary Science Letters, v. 22, p. 51–59.
Lewis, R. S., and Kiilsgaard, T. H., 1991, Eocene plutonic rocks in south central Idaho: Journal of Geophysical Research, v. 96, p. 13295–13311.
Lewis, T. J., Bentkowski, W. H., Davis, E. E., Hyndman, R. D., Souther, J. G., and Wright, J. A., 1988, Subduction of the Juan de Fuca plate: thermal consequences: Journal of Geophysical Research, v. 93, p. 15207–15225.
Lonsdale, P., 1988, Paleogene history of the Kula plate: offshore evidence and onshore implications: Geological Society of America Bulletin, v. 100, p. 733–754.
Liu, T. K., 1982, Tectonic implication of fission-track ages from the Central Range, Taiwan: Proceedings of the Geological Society of China, number 25, p. 22–37.
———— 1988, Fission-track dating of the Hsuehshan Range: thermal record due to arc-continent collision in Taiwan: Acta Geologica Taiwanica, Science Reports of the National Taiwan University, number 26, p. 279–290.
Massey, N. W. D., 1986, The Metchosin Igneous Complex, southern Vancouver Island: ophiolite stratigraphy developed in an emergent island setting: Geology, v. 14, p. 602–605.
McLachlan, G. J., and Basford, K. E., 1988, Mixture models: New York, New York, Marcel Dekker, Incorporated, 253 p.
Medford, G. A., 1975, K-Ar and fission-track geochronometry of an Eocene thermal event in the Kettle River (west half) map area, southern British Columbia: Canadian Journal of Earth Sciences, v. 12, p. 836–843.
Miller, C. F., and Bradfish, L. J., 1980, An inner Cordilleran belt of muscovite-bearing plutons: Geology, v. 8, p. 412–416.
Miller, F. K., and Engels, J. C., 1975, Distribution and trends of discordant ages of plutonic rocks of northeastern Washington and northern Idaho: Geological Society of America Bulletin, v. 86, p. 517–528.
Miller, R. B., and Bowring, S. A., 1990, Structure and chronology of the Oval Peak batholith and adjacent rocks: Implications for the Ross Lake fault zone, North Cascades, Washington: Geological Society of America Bulletin, v. 102, p. 1361–1377.
Monger, J. W. H., Price, R. A., Tempelman-Kluit, D. J., 1982, Tectonic accretion and the origin of two major metamorphic and plutonic welts in the Canadian Cordillera: Geology, v. 10, p. 70–75.
Moore, J. C., Byrne, T., Plumley, P. W., Reid, M., Gibbons, H., and Coe, R. S., 1983, Paleogene evolution of the Kodiak Islands, Alaska: consequences of ridge-trench interaction in a more southerly latitude: Tectonics, v. 2, p. 265–293.
Moye, F. J., and Johnson, K. M., 1989, Is the "Challis Arc" really an arc?: Geological Society of America, Abstracts with Programs, v. 21, no. 5, p. 119.
Naeser, N. D., Naeser, C. W., and McCulloh, T. H., 1989, The application of fission-track dating to the depositional and thermal history of rocks in sedimentary basins, *in* Naeser, N. D., and McCulloh, T. H., editors, Thermal History of Sedimentary Basins: New York, New York, Springer-Verlag, p. 157–180.
Naeser, N. D., Zeitler, P. K., Naeser, C. W., and Cerveny, P. F., 1987, Provenance studies by fission-track dating—etching and counting procedures: Nuclear Tracks and Radiation Measurements, v. 13, p. 121–126.
Norman, M. D., and Mertzman, S. A., 1991, Petrogenesis of Challis volcanics from central and southwestern Idaho: trace element and Pb isotopic evidence: Journal of Geophysical Research, v. 96, p. 13279–13293.
Orange, D. L., 1990, Criteria helpful in recognizing shear-zone and diapiric mélanges: examples from the Hoh accretionary complex, Olympic Peninsula, Washington: Geological Society of America Bulletin, v. 102, p. 935–951.
Parrish, R. R., 1983, Cenozoic thermal evolution and tectonics of the Coast Mountains of British Columbia 1. Fission-track dating, apparent uplift rates, and patterns of uplift: Tectonics, v. 2, p. 601–631.
Parrish, R. R., Carr, S. D., and Parkinson, D. L., 1988, Eocene extensional tectonics and geochronology of the southern Omineca belt, British Columbia and Washington: Tectonics, v. 7, p. 181–212.
Pavlis, T. L. and Bruhn, R. L., 1983, Deep-seated flow as a mechanism for the uplift of broad forearc ridges and its role in the exposure of high P/T metamorphic terranes: Tectonics, v. 2, p. 473–497.

Potts, P. J., 1987, A Handbook of Silicate Rock Analysis: New York, New York, Chapman and Hall, 622 p.

Priest, G. R., 1990, Volcanic and tectonic evolution of the Cascade volcanic arc, Central Oregon: Journal of Geophysical Research, v. 95, p. 19583–19599.

Prothero, D. R., and Armentrout, J. M., 1985, Magnetostratigraphic correlation of the Lincoln Creek Formation, Washington: implications for the age of the Eocene/Oligocene boundary: Geology, v. 13, p. 208–211.

Rau, W. W., 1975, Geologic map of the Destruction Island and Taholah quadrangles, Washington: Washington Department of Natural Resources, Geology and Earth Resources Division, Geologic Map GM-13, 1 sheet, scale 1:62,500.

———— 1979, Geologic map in the vicinity of the Lower Bogachiel and Hoh River Valleys, and the Washington Coast: Washington Department of Natural Resources, Geology and Earth Resources Division, Geologic Map GM-24, 1 sheet, scale 1:62,500.

———— 1981, Pacific Northwest Tertiary benthic foraminiferal biostratigraphic framework—An overview: Geological Society of America Special Paper 184, p. 67–84.

Renne, P. R., Becker, T. A., and Swapp, S. M., 1990, $^{40}Ar/^{39}Ar$ laser-probe dating of detrital micas from the Montgomery Creek Formation, northern California: Clues to provenance, tectonics, and weathering processes: Geology, v. 18, p. 563–566.

Roberts, J. H., Gold, R., and Armani, R. J., 1968, Spontaneous fission decay constant of ^{238}U: Physics Review, v. 174, p. 1482–1484.

Robinson, P. T., Brem, G. F., and McKee, E. H., 1984, John Day Formation of Oregon: A distal record of early Cascade volcanism: Geology, v. 12, p. 229–232.

Roden, M. K., Brandon, M. T., and Miller, D. S., 1990, Apatite fission-track thermochronology of the Olympics subduction complex, Washington: Geological Society of America Abstracts with Programs, v. 22, p. A324.

Rusmore, M. E., and Cowan, D. S., 1985, Jurassic-Cretaceous rock units along the southern edge of the Wrangellia terrane on Vancouver Island: Canadian Journal of Earth Sciences, v. 22, p. 1223–1232.

Sevigny, J. H., Parrish, R. R., Donelick, R. A., and Ghent, E. D., 1990, Northern Monashee Mountains, Omineca Crystalline Belt, British Columbia: timing of metamorphism, anatexis, and tectonic denudation: Geology, v. 18, p. 103–106.

Sevigny, J. H., Parrish, R. R., and Ghent, E. D., 1989, Petrogenesis of peraluminous granites, Monashee Mountains, southeastern Canadian Cordillera: Journal of Petrology, v. 30, p. 557–581.

Seward, D., and Rhoades, D. A., 1986, A clustering technique for fission-track dating of fully to partially annealed minerals and other non-unique populations: Nuclear Tracks and Radiation Measurements, v. 11, p. 259–268.

Sherrod, D. R., and Smith, J. G., 1989, Preliminary map of upper Eocene to Holocene volcanic and related rocks of the Cascade Range, Oregon: United States Geological Survey Open-File Report 89-14, 1 sheet, scale 1:500,000, and 20 p. text.

Silberling, N. J., Jones, D. L., Blake, Jr., M. C., and Howell, D. G., 1987. Lithotectonic terrane map of the western conterminous United States: United States Geological Survey, Miscellaneous Field Studies Map MF-1874-C, 1 sheet, scale 1:2,500,000, and 20 p. text.

Smith, J. G., 1989, Geologic map of upper Eocene to Holocene volcanic and related rocks in the Cascade Range, Washington: United States Geological Survey Open-File Report 89-311, 1 sheet, scale 1:500,000, and 61 p. text.

Snavely, P. D., Jr., 1987, Tertiary geologic framework, neotectonics, and petroleum potential of the Oregon-Washington continental margin, *in* Scholl, D. W., Grantz, A., and Vedder, J. G. editors, Geology and Resource Potential of the Continental Margin of Western North America and Adjacent Ocean Basins-Beaufort Sea to Baja California: Circum-Pacific Council for Energy and Mineral Resources, Earth Science Series, v. 6, p. 305–335.

Snavely, P. D., Jr., and MacLeod, N. S., 1974, Yachats Basalt—An upper Eocene differentiated volcanic sequence in the Oregon Coast Range: United States Geological Survey Journal of Research, v. 2, p. 395–403.

Snavely, P. D., Jr., MacLeod, N. S., Niem, A. R., and Minasian, D. L., 1986, Geologic map of Cape Flattery area, northwestern Olympic Peninsula, Washington: United States Geologic Survey Open-File Report 86-344B, 1 sheet, scale 1:48,000.

Snavely, P. D., Jr., Rau, W. W., and Hafley, D. J., 1986, Tertiary Foraminiferal localities in the Cape Flattery area, northwestern Olympic Peninsula, Washington: United States Geological Survey Open-File Report 86-344A, 18 p.

Stewart, R. J., 1974, Zeolite facies metamorphism of sandstone in the western Olympic Peninsula, Washington: Geological Society of America Bulletin, v. 85, p. 1139–1142.

Sweetkind, D. S., and Blackwell, D. D., 1989, Fission-track evidence of the Cenozoic thermal history of the Idaho batholith: Tectonophysics, v. 157, p. 241–250.

Tabor, R. W., 1972, Age of the Olympic metamorphism, Washington: K-Ar dating of low-grade metamorphic rocks: Geological Society of America Bulletin, v. 83, p. 1805–1816.

———— 1982, Geologic map of the Wonder Mountain Roadless Area, Mason County, Washington: United States Geological Survey Miscellaneous Field Studies Map MF-1418-A, 1 sheet, scale 1:62,500.

Tabor, R. W. and Cady, W. M., 1978a, The structure of the Olympic Mountains, Washington—analysis of a subduction zone: United States Geological Survey Professional Paper 1033, 38 p.

———— 1978b, Geologic map of the Olympic Peninsula: United States Geological Survey Map I-994, 2 sheets, scale 1:125,000.

Tabor, R. W., Frizzell, V. A., Jr., Whetten, J. T., Waitt, R. B., Swanson, D. A., Byerly, G. R., Booth, D. B., Hetherington, M. J., and Zartman, R. E., 1987, Geologic map of the Chelan 30-minute by 60-minute quadrangle, Washington: United States Geological Survey Miscellaneous Investigations Map I-1661, 1 sheet, scale 1:100,000, and 33 p. text.

Tabor, R. W., Haugerud, R. H., Brown, E. H., Babcock, R. S., and Miller, R. S., 1989, Accreted terranes of the North Cascades Range, Washington: International Geological Congress, 28th Field Trip Guidebook T307, 62 p.

Tabor, R. W., Yeats, R. S. and Sorensen, M. L., 1972, Geologic map of the Mount Angeles Quadrangle, Clallam and Jefferson Counties, Washington: United States Geological Survey Map GQ-958, 1 sheet, scale 1:62500.

Tagami, T., Ito, H., and Nishimura, S., 1990, Thermal annealing characteristics of spontaneous fission tracks in zircon: Chemical Geology, Isotope Geoscience Section, v. 80, p. 159–169.

Triplehorn, D. M., Turner, D. L., and Frizzell, V. A., Jr., 1980, Stratigraphic significance of radiometric ages of Eocene coals in western Washington, *in* Carter, L. M., editor, Proceedings of the Fourth Symposium on the Geology of Rocky Mountain Coal: Colorado Geological Survey Resources Series 10, p. 87.

Turner, D. L., Frizzell, V. A., Triplehorn, D. M., Naeser, C. W., 1983, Radiometric dating of ash partings in coal of the Eocene Puget Group, Washington: Implications for paleobotanical stages: Geology, v. 11, p. 527–531.

Underwood, M. B., Bachman, S. B., and Schweller, W. J., 1980, Sedimentary processes and facies associations within trench and trench-slope settings, *in* Field, M. E., Bouma, A. H., and Colburn, I., editors, Quaternary Depositional Environments on the Pacific Continental Margin: Society of Economic Paleontologists and Mineralogists, Pacific Section, p. 211–229.

Vance, J. A., Walker, N. W., and Mattinson, J. M., 1986, U/Pb ages of early Cascade plutons in Washington State: Geological Society of America Abstracts with Programs, v. 18, no. 2, p. 194.

Wagner, G. A., 1981, Fission-track ages and their geologic interpretation: Nuclear Tracks and Radiation Measurements, v. 5, p. 15–25.

Walsh, T. J., Korosec, M. A., Phillips, W. M., Logan, R. L., and Schasse, H. W., 1987, Geologic map of Washington-southwest quadrant: Washington Division of Geology and Earth Resources Geologic Map GM-34, 2 sheets, scale 1:250,000, and 28 p. text.

Wells, R. E., Engebretson, D. C., Snavely, P. D., Jr., and Coe, R. S., 1984, Cenozoic plate motions and the volcano-tectonic evolution of western Oregon and Washington: Tectonics, v. 3, p. 275–294.

Wells, R. E., and Heller, P. L., 1988, The relative contribution of accretion, shear, and extension to Cenozoic tectonic rotation in the Pacific Northwest: Geological Society of America Bulletin, v. 100, p. 325–338.

Zaun, P. E., and Wagner, G. A., 1985, Fission-track stability in zircons under geological conditions: Nuclear Tracks and Radiation Measurements, v. 10, p. 303–307.

Zeitler, P. K., Duddy, I. R., Gleadow, A. J. W., Green, P. F., and Hurford, A. J., 1985, Comment on "zircon and sphene as fission-track geochronometer and geothermometer: a reappraisal" by K. D. Bal, N. Lal, and K. K. Nagpaul: Contributions to Mineralogy and Petrology, v. 91, p. 305–306.